UNITED STATES
DEPARTMENT OF THE INTERIOR
GEOLOGICAL SURVEY

GEOLOGIC STUDIES OF THE POINT CONCEPTION DEEP STRATIGRAPHIC TEST WELL OCS-CAL 78-164 NO. 1 OUTER CONTINENTAL SHELF SOUTHERN CALIFORNIA, UNITED STATES

Edited by

Harry E. Cook

Open-File Report
79-1218

Menlo Park, California
July 1979

ERRATA SHEET FOR

Open-File Report
79-1218

GEOLOGIC STUDIES OF THE POINT CONCEPTION
DEEP STRATIGRAPHIC TEST WELL
OCS-CAL 78-164 NO. 1
OUTER CONTINENTAL SHELF
SOUTHERN CALIFORNIA, UNITED STATES

Edited by

Harry E. Cook

Page 3, line 3 should read "southwest" instead of "southeast"

Page 60, line 37 should read "Po Basin of Italy" instead of "P Basin of Italy"

Page 64, line 23 should read "(Fig. 2 of" instead of "(Fig. 1b of"

Page 65, 4th line from the bottom should read "lowest part of the Foxen Mudstone, which is described in the"

Page 69, lines 6 through 15 should read:

Porosities of sandstone units that occur above 5,700 ft fall within the higher porosity region of envelop A (Fig. 2). The range of porosities for these upper sandstone units may be predicted from the range of sandstone porosities that occur over the same burial depths in the Los Angeles and Ventura basins where normal marine clastic deposits have undergone similar burial histories (no unloading). However, if true, this conclusion may be due to a fortuitous set of circumstances (McCulloh, pers. commun.). The unusually high geothermal gradient (McCulloh and Beyer, this report) may have tended to accelerate porosity-reducing diagenesis (Maxwell, 1964), while the presence of abundant hydrocarbons in the upper part of the section (Claypool, this report) may have impeded porosity-reducing diagenesis (Lowry, 1956).

TABLE OF CONTENTS

GEOLOGIC STUDIES OF THE POINT CONCEPTION DEEP STRATIGRAPHIC TEST WELL OCS-CAL 78-164 NO. 1 OUTER CONTINENTAL SHLEF SOUTHERN CALIFORNIA, UNITED STATES

Harry E Cook, Editor
U.S. Geological Survey
Menlo Park California

SUMMARY

1. The Point Conception OCS-Cal 78-164 No. 1 well penetrated 9,106 ft (drilled depth 10,571 ft) of sedimentary rocks in the offshore southern California borderland. The age of the sediment was determined by examination of planktic and benthic foraminifers, radiolarians, diatoms, and coccoliths. Based on coccoliths, the section is Cenozoic in age down to a drilled depth of about 10,000 ft. At this depth an unconformity is inferred to exist between Miocene and Lower Cretaceous or uppermost Jurassic strata. From about 10,000 ft to the base of the well at 10,571 ft, the sediment contains Mesozoic coccoliths. On the basis of benthic foraminifera no unconformity was found at the 10,000 ft level. Instead, Miocene benthic foraminifera occur from about 8,300 to 10,571 ft with no evidence for pre-Miocene sediment. Other fossil groups were not age diagnostic below a drilled depth of about 4,500 ft. However, other types of data also suggest an unconformity occurs at about 10,000 ft. These data are derived from sonic and density logs, seismic reflection profiles, dipmeter values, and sediment changes.

2. Significant shows of hydrocarbons occurred between 2,900 and 5,800 ft. The sediment down to a depth of about 4,400 ft is mainly mudstone, siltstone, and sandstone. Siliceous mudstone is abundant from 4,400 to 5,450 ft. From 5,450 to 7,400 ft porcellanite, chert, and minor amounts of dolomite dominate the section. Siltstone, mudstone, sandstone, and conglomerate occur in the interval from 7,400 to 9,735 ft. From 9,735 ft to the base of the hole the section consists of sheared and polished mudstone and siltstone.

3. By analogy with several outcrop areas on land, the well section most closely resembles sediment exposed in the Tranquillon Mountain area. There lower Miocene beds overlap Oligocene, Eocene, and Upper Cretaceous formations onto Lower(?) Cretaceous strata.

4. The U.S.G.S. ran a CDP multichannel acoustic reflection profile 1.8 mi southeast of the Point Conception well. Some of the high amplitude reflectors in this profile approximate the boundaries of major rock units identified by changes in electric log parameters, lithology, sonic velocity, and paleontologic ages. This acoustic profile is divided into eight seismic-stratigraphic units.

5. The present geothermal gradient in the Point Conception well is 48°C/km. This is an exceptionally high gradient and is comparable to temperature gradients from the largest oil fields in the Santa Maria Basin and the Wilmington oil field in the Los Angeles Basin. Temperatures occur in this well that are higher than those at equivalent depths in most of the Santa Barbara Channel, Ventura Basin, and large parts of the Los Angeles and San Joaquin Basins. The geothermal gradient in the Point Conception well is consistent with temperatures high enough for the generation of petroleum at depths reached in this well.

6. Organic geochemical studies coupled with data on vitrinite reflectance data indicate the organic matter from the Point Conception well is dominantly of a type which has excellent oil-generating capacity. The organic matter in the Cenozoic sediment is immature to marginally mature in terms of the degree of thermochemical transformation usually required for abundant petroleum generation. However, the concentration of extractable hydrocarbons is exceptionally high, and these extractable hydrocarbons have characteristics in common with crude oils from the nearby Santa Maria Basin. This and other geochemical data suggest that the organic matter in these rocks may yield significant amounts of hydrocarbons at early stages of thermochemical transformation.

7. Log calculations indicate that the section down to 5,400 ft is strongly undercompacted, with mean porosity values in the range from 44.4 to 33.8 percent. Strata between 5,400 and 9,450 ft have calculated density log porosity values from 29.8 to 9.3 percent. Porosity values from a core at 9,529 to 9,549 ft range from 15.8 to 17.9 percent. Porosity values calculated from the density log through the interval 9,451 to 9,979 ft have a mean value of 10 percent. Burial consolidation and cementation by carbonate and phyllosilicate minerals may account for much of the progressive loss of porosity with increasing depth.

8. Petroleum in most California oil fields, both onshore and offshore, occurs in sandstone reservoirs with intergranular porosity. However, in a few places, interconnected fractures in diagenetically altered siliceous "shale" form the reservoirs. Two such places are the nearby Santa Maria Basin onshore and the Santa Barbara Channel offshore. The Santa Maria Valley oil field is an almost purely stratigraphic trap in which fracture porosity in the Monterey Shale has created large reservoirs. Whether such fractures occur in the Point Conception well is not known. However, fracture porosity in purely diagenetic or structural-diagenetic combination traps may prove to be a key element in the discovery of oil in the area surrounding this well.

9. A number of geologic parameters are favorable for the discovery of petroleum in this area--high geothermal gradients, a thick section of richly organic-prone source rocks, strata thousands of feet thick composed in large part of orginally biogenic opaline silica, and a deformational history that has produced broad folds and some large faults.

INTRODUCTION

The Point Conception well is classified as an Offshore Deep Stratigraphic Test and is designated the OCS-Cal 78-164 No. 1. This well was drilled about 10 mi southeast of Point Arguello (lat. 34°28'56.6"N, long. 120°47'0"W) in 1,428 ft of water. Drilling continued to a total depth of 10,571 ft below the Kelly Bushing. This is the second deep stratigraphic test that has been drilled on the offshore southern California borderland. The first one (OCS-CAL 75-70 No. 1) was drilled in 1975 on Cortes Bank, a few hundred miles southeast of the Point Conception well.

Point Conception well was located off-structure but adjacent to the area offered for leasing on June 29, 1979, as part of OCS Lease Sale No. 48. Although it was drilled off-structure, significant shows of oil and gas were noted at various intervals between a drilled depth of 2,900 ft and 5,800 ft. The granting of Federal leases within 50 mi of the Point Conception well has made possible the publication of data on this well within 60 days after such leasing.

This report is divided into separately authored sections on geological, geophysical, geochemical, and paleontological topics. Most of these topics are still being studied, but because the Point Conception well has such immediate interest, publication of these preliminary results and interpretations is warranted. Later this Open-File Report will be reissued as a Survey Circular.

All depth references in this report are drilled depths below the Kelly Bushing, which is 37 ft above mean sea level. Water depth is 1,428 ft, thus the sea floor begins at a drilled depth of 1,465 ft.

ACKNOWLEDGMENTS

The editor has attempted to assemble topics that would meet the interests of both the petroleum industry and academic community. He is most grateful to the authors for their cooperation and willingness to participate in this study. Technical assistance in sample preparation, analyses, drafting, and data compilation was provided by L. Bailey, J. Blank, W. Chamberlain, J. Joyce, L. Krystinik, M. Randall, and P. Swenson. H. Cullins, W. Roberts, V. Stephens, F. Webster, and K. Yenne were very helpful in supplying data from this well. The editor appreciates very much the clerical help of Terry Coit who assisted in numerous phases of this report.

WELL DATA

R. B. Tudor
U.S. Geological Survey
Los Angeles, California

A. Summary of Well Data

1. Operator:

   a) Exploration Services Company Inc.

2. Participants

   a) Aminoil U.S.A., Inc.
   b) Amoco Production Co.
   c) Chevron, U.S.A., Inc.
   d) Continental Oil Co.
   e) Exxon Co., U.S.A.
   f) Getty Oil Co.
   g) Gulf Oil Co.
   h) Marathon Oil Co.
   i) Mobil Oil Corp.
   j) Oxy Petroleum, Inc.
   k) Phillips Petroleum Co.
   l) Shell Oil Co.
   m) Superior Oil Co.
   n) Union Oil Co. of California

3. Principal Contractor:

   a) Global Marine, Inc., Glomar Atlantic #1 Drilling Vessel

4. Support Contractors and Services:

a)	C&C Fisheries, Inc.	Electric Marvel Standby Boat
b)	Global Marine, Inc.	Glomar Atlantic
c)	Halliburton Services	Cement, Chemicals
d)	Leppaluoto Offshore Marine	M/V Harold T Crewboat
e)	Magcobar	Drilling Fluids
f)	Offshore Crane and Serivce Co., Inc.	Crane Service
g)	Rotor Aids, Inc.	Helicopter Services
h)	Western Boat Operators, Inc.	MV Ocean Tarpon. Supply Boat

5. GeoScience Contractors and Services:

a)	Anderson, Warren and Associates	Consulting Micropaleontology Sampling Processing
b)	General Oceanographics	Shallow Seismic Profiles
c)	Core Laboratories, Inc.	Core Analysis
d)	Dresser Olympic Operations	Deep Seismic Profiles
e)	Exploration Logging	Mud Logging
f)	GeoChem Laboratories	Geochemical Analysis
g)	Glomar Atlantic	Weather Surveys
h)	Intersea Research Corp.	Geophysical Geological Studies Wave Rider Buoy Data
i)	Marathon Research	Thin Sections
j)	Navigation Services, Inc.	Offshore Surveyors
k)	Oceanographic Services, Inc.	Meteorology Survey
l)	Schlumberger Offshore	Well logging, Formation Testing
m)	SSC-Birdwell Division	Velocity-Surveying

6. Lease Designation: Unleased

7. Well No: OCS-CAL 78-164, No. 1

8. Location: California Coordinate System--Lambert Zone 5

Surface	X = 1,165,502 ft Y = 369,005 ft	At Surface	X = 704,838 m Y = 3,817,706 m	UTM Zone 10

Block N796 E28 UTM

Offshore Tract 463

(OCS Sale No. 53)

Surface: Longitude $120^{\circ}47'0"$
Latitude $34^{\circ}28'56.6"$

9. Classification: Offshore Deep Stratigraphic Test

10. Elevation: RKB-37 ft

11. Water Depth: 1,428 ft

12. Spud Date: October 7, 1978

13. Date T.D. Reached: December 9, 1978

14. Completion Date: December 18, 1978

15. Status: Plugged and Abandoned

16. Total Depth: 10,571 ft RKB

17. Plug-Back Depth: 1,527 ft RKB

B. Operational Data

1. Mud Program

The drilling fluid used in the mud program for the initial 175 ft of drilled hole below the ocean floor (1,640 RKB) was salt water. From this point to total depth of 10,571 ft TKB a Gel Water mud was used.

2. Hole Dimensions:

A 36-inch hole was drilled to a depth of 175 ft below the ocean floor (1,640 RKB), thence a 26-in. hole to 532 ft below the ocean floor (1,997 RKB), a 17 1/2-in. hole from 532 ft to 1,550 feet (3,105 ft RKB), a 12 1/4-in. hole from 1,550 ft to 3,998 ft (5,463 RKB), and an 8 1/2-in. hole to total depth of 9,106 ft below the ocean floor (10,571 RKB).

3. Casing Report

Casing	Depth Set	Hole Size	Cementing Record
30"	1618'	36"	700 SX Class H (2% $CaCl_2$ seawater)
20"	1995'	26"	1090 SX Cl. H (2% $CaCl_2$ seawater)
13 3/8"	2991'	17 1/2"	840 SX Cl. H (2 1/2% gel water)
9 5/8"	5440'	12 1/4"	940 SX Cl. G (2 1/2% gel water)

4. Open Hole Test - None

5. Cores:

One conventional core was taken from 9,529 ft to 9,549 ft, and 20 feet was recovered. One junk basket core was taken from 7,066 ft to 7,068 ft and 1 ft was recovered. Nine sidewall cores were taken from 3,064, 3,199, 3,650, 5,054, 10,222, 10,310, 10,318, and 10,253 ft.

Number Recovered and Analyzed - 9

5. Geochemical Analysis:

Analysis of Mud, Ditch, and Core Samples from 2,000 ft to 10,571 ft.

Number of Samples: 58
Number Analyzed: 58

6. Surveys: from 1,962 ft to 10,571 ft Total Depth.

Wireline Services: Operator-Schlumberger Electric Logs:
Dual Induction-Laterolog 2"=100' and 5"=100' (2 separate logs)
Compensated Neutron-Formation Density 5" (1 log)
Computer Processed Log 5" (1 log)
Formation Factor 5" (1 log)
Dip Meter 2"=100' (2 separate logs) Tadpol Plot
Borehole Compensated Sonic Log 2" and 5" (2 logs)
Long Spaced 8'-10' Sonic Log 5" (1 log)
Cement Bond Log Variable Density 5" (1 log)
BHC Sonic -- Variable Density 5" (1 log)
Continuous Dipmeter 5" Run 1 and Run 2 (2 logs)
Mudlog--Lithology 2"
Temperature Data Log 1"
Drilling Pressure Log 1"
Pressure Analysis Log 1"
Direction Survey - Single Shot only
Repeat Formation Tester None

The well was drilled as a vertical hole, but due to the rapid rate of penetration some deviation occurred. A Single Shot Directional Survey was run. The bottom survey was taken at 10,571 ft total depth. The hole angle was $8^{o}45'S\ 72^{o}W$.

C. Sample and Circulation Data

1. Ditch Sample Program

From	To	Sample Interval	Total Samples
2,000 ft	10,571 ft	30 ft	286

2. Circulations
N.A.

3. Lost Circulations
3,085-4,500 ft, at intervals

D. Plugging Program

1. Cement plugs were placed at the following depths:

#1 5900 - 5700'
#2 5440 - 5390'
#3 1665 - 1527'

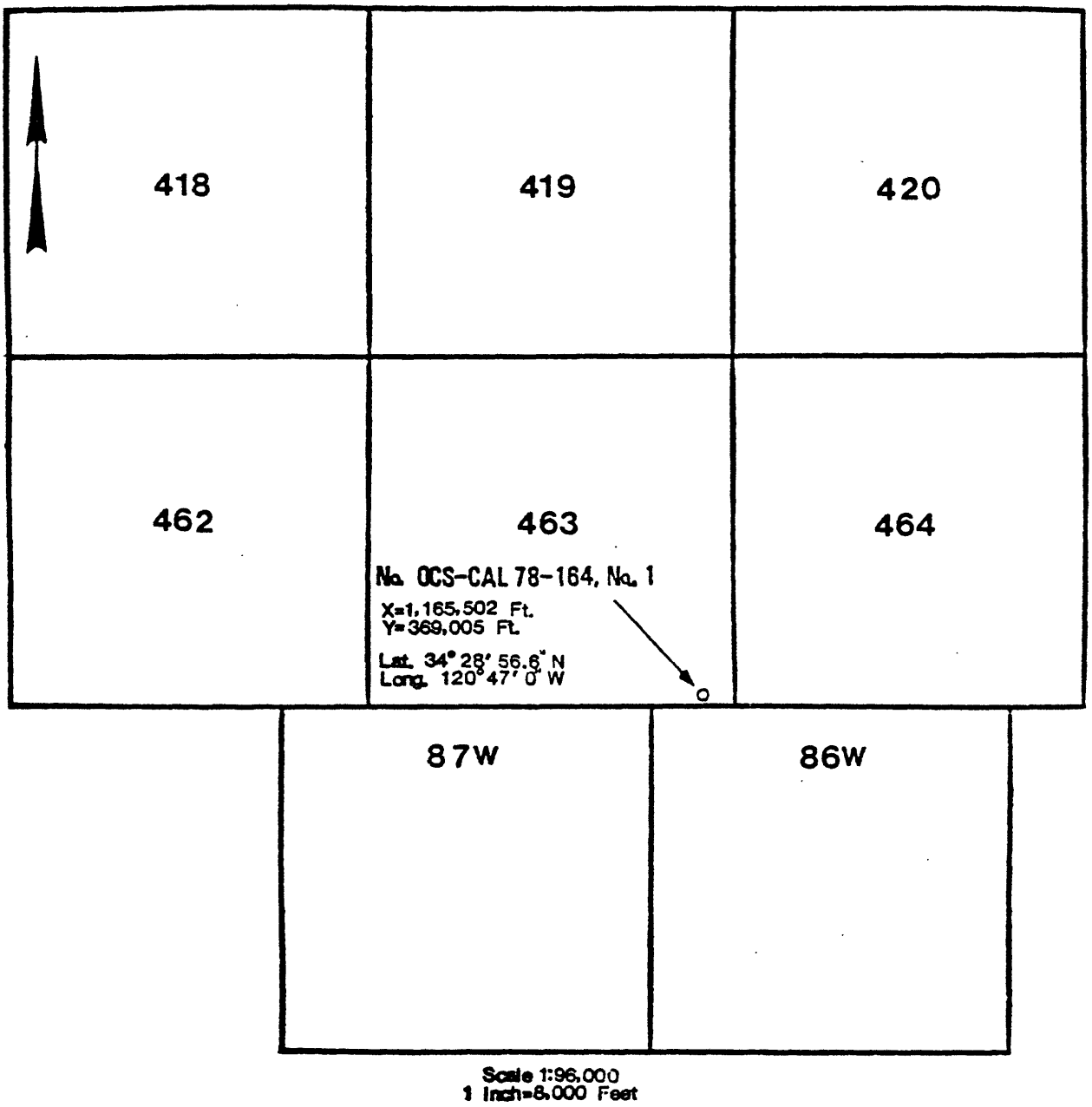

Location plat showing the projected surface position of the OCS-CAL 78-164 No. 1 well.

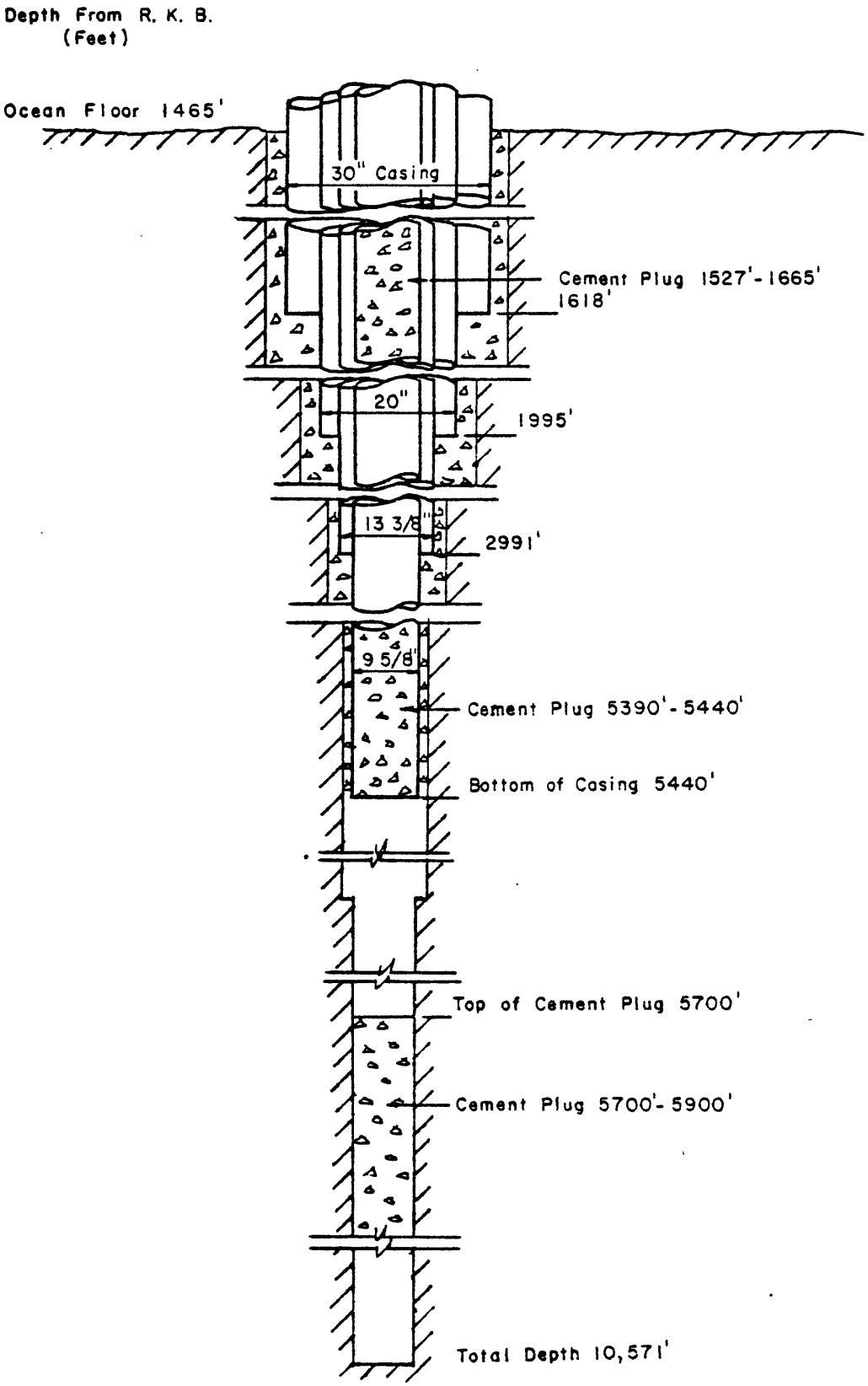

Schematic diagram showing relative position of casing strings, cement displacement, and plugging and abandonment program

GEOLOGIC SETTING

D. S. McCulloch, J. G. Vedder, H. C. Wagner, and R. H. Brune
U.S. Geological Survey
Menlo Park California

INTRODUCTION

Placement of cooperative offshore stratigraphic test well OCS Cal 78-164 No. 1 into one of the traditionally used structural and geomorphic provinces of southern California is problematical. Although the well site is directly west of the Transverse Ranges province as depicted by Jahns (1954), the structural grain offshore has closer affinities to that of the southern Coast Ranges province (von Huene, 1969; Howell, McCulloch, and Vedder, 1978; Willingham, 1979). The well is near the north edge of the Arguello plateau (von Huene, 1969) on the slope incised by tributaries of the Arguello Canyon system. All well depths refer to drilled depths beginning at the derrick floor. Thus, the sea floor is at a drilled depth of 1,465 ft.

In order to compare the section drilled in Well OCS-Cal 78-164 No. 1 with possibly correlative sections elsewhere, four well-known onshore areas have been selected for brief descriptions of stratigraphy and structure. In addition, interpretations of offshore geophysical data are used to supplement the onshore geologic information and to infer correlations with the well section. The onshore areas include the western Santa Maria basin, the Santa Ynez Mountains near Point Arguello and Tranquillon Mountain, the Point Conception-Cañada de Santa Anita area, and San Miguel Island. The sub-seafloor interpretations are derived from a U.S.G.S. CDP multichannel acoustic-reflection profile that transects the area near the well (Fig. 1a).

Because stratigraphic names differ from place to place among the selected onshore areas and because such names connote chronostratigraphic units to some geologists, we do not use formal nomenclature for the well section. Application of names to parts of the well section in which correlation is uncertain or unknown would be misleading and possibly incorrect. Even though correlation of some stratigraphic sequences in the well is fairly certain, names are used only for comparison with their onshore counterparts.

Santa Maria Basin

In the western Santa Maria basin, the exposed sedimentary section has a maximum thickness of about 10,000 ft (3,050 m); and the subsurface section about 27,000 ft (8,250 m) (Woodring and Bramlette, 1950). Basement rocks at Point Sal include a Jurassic ophiolite about 160 m.y. old and

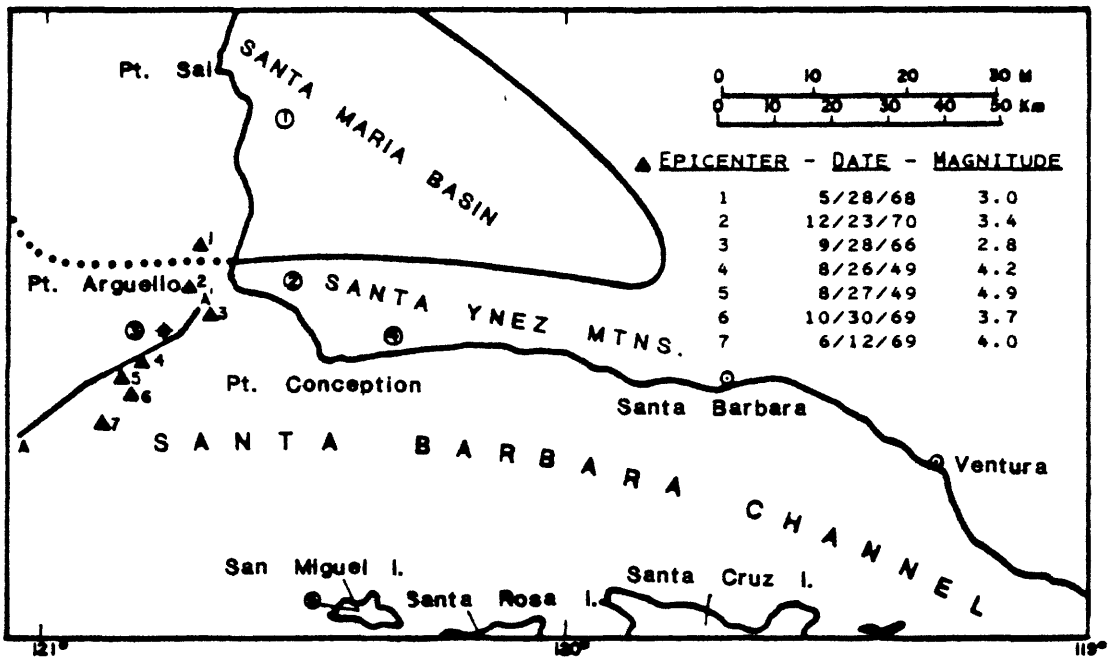

Figure 1a. Locality map showing Pt. Conception well (10 mi SW of Pt. Arguello) in relation to seismic-reflection profile (A-A'). Circled numbers refer to stratigraphic columns shown in Figure 1b.

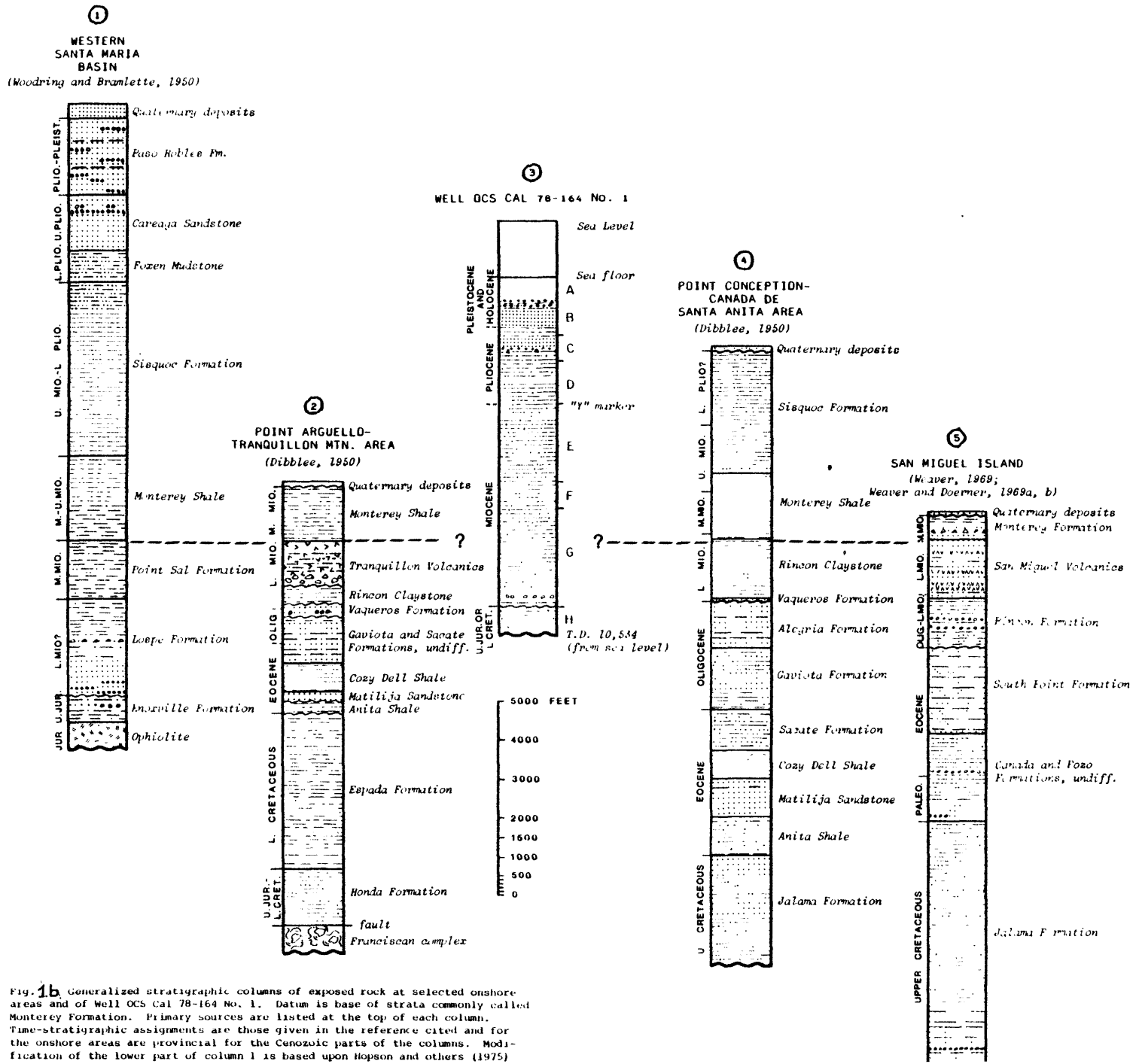

Fig. 16 Generalized stratigraphic columns of exposed rock at selected onshore areas and of Well OCS Cal 78-164 No. 1. Datum is base of strata commonly called Monterey Formation. Primary sources are listed at the top of each column. Time-stratigraphic assignments are those given in the reference cited and for the onshore areas are provincial for the Cenozoic parts of the columns. Modification of the lower part of column 1 is based upon Hopson and others (1975)

overlying beds of late Kimmeridgian(?) and Tithonian (Late Jurassic) age (Hopson and others, 1975). Farther east, Franciscan rocks constitute the basement. Upper Cretaceous, Paleocene and Eocene rocks are not known in the onshore part of the basin southwest of the Santa Maria River-Foxen Canyon-Little Pine fault zone. The nonmarine Lospe Formation probably accumulated in Oligocene(?) and early Miocene(?) time during the initial phase of basin development. Marine formations of Miocene and Pliocene age have a composite maximum thickness of 11,500 to 15,000 ft (3,500 to 4,575 m) and are overlain by a nonmarine section as much as 4,500 ft (1,375 m) thick (Krammes and Curran, 1959; Crawford, 1971). Column 1, Figure 1b shows the stratigraphic succession of these rocks; their offshore counterparts are described briefly by Hoskins and Griffiths (1971), McCulloch and others (1977), and Howell, McCulloch, and Vedder (1978).

The major structural features of the Santa Maria district trend west-northwest, parallel to the basin trough. Minor west-trending folds and faults, however, transect the pattern of the larger scale features. Open folds and narrow, closely spaced, and asymmetric folds with vergence both northward and southward are characteristic of the basin structures (Woodring and Bramlette, 1950; Crawford, 1971). Many of the folds began to form near the end of the Miocene and presumably culminated in the Pleistocene. Faults, both exposed and in the subsurface, commonly trend northwest. Dip slip as well as strike slip has been attributed to them, and various tectonic interpretations have been proposed including regional compression, pull-apart structure with rotation, and sinistral wrench faulting (Dibblee, 1978; Hall, 1978; Sylvester and Darrow, 1979). Many of the central basin faults cut late Pliocene and Quaternary rocks.

Point Arguello-Tranquillon Mountain Area

The Point Arguello-Tranquillon Mountain area is geologically atypical of the bulk of the western Santa Ynez Mountains. Unconformities characterize the stratigraphic sequence, which is nearly 12,000 ft (3,650 m) thick; and a large accumulation of Miocene volcanic rocks interrupts the sedimentary succession. Franciscan melange north of Cañada Honda Creek is faulted against Dibblee's (1950) type Honda Formation at the few places where the contact is exposed. Fossils recently collected from the Honda Formation have been assigned to the Tithonian, Valanginian, and Hauterivian to Barremian Stages (Late Jurassic and Early Cretaceous age) (D. L. Jones, oral commun., 1979). Interbedded sandstone and siltstone of Dibblee's (1950) type Espada Formation conformably overlie the Honda; the Type Espada, in turn, is unconformably overlain by the Oligocene and early Miocene Vaqueros Formation and Rincon Claystone (Col. 2, Fig. 1b). Noteworthy in this area are the absence of surface exposures of Upper Cretaceous rocks, absence of nonmarine Oligocene beds, a major unconformity at the base of the Oligocene-lower Miocene section, and a relatively thick conglomeratic section of the Vaqueros Formation. As much as 1,200 ft (365 m) of rhyolitic flow and tephra in the lower part of the Miocene section are centered around Tranquillon Mountain.

The Tranquillon Mountain area has undergone several episodes of struc-

tural deformation since deposition of the Espada Formation. This activity resulted in complete erosion of the Upper Cretaceous Jalama Formation except in the subsurface section near Sudden. Faults and folds as old as Oligocene and unconformities at the base and top of the Anita Shale and Vaqueros Formation and at the base of the Tranquillon Volcanics attest to the episodic deformation throughout the Tertiary (Dibblee, 1950). The dominant structural feature is anticlinal with smaller folds superimposed. In general, folds trend west-northwest and northwest and are relatively broad, particularly in the pre-middle Miocene rocks. Faults trend east to northeast and have dip-slip separation, except for the Cañada Honda fault along which left-slip separation, as well as dip-slip component, south side up, is indicated by en echelon folds and stratigraphic relatiions (Dibblee, 1950).

Point Conception-Cañada de Santa Anita Area

The homoclinal sequence exposed along the coastal belt from Point Conception to Cañada de Santa Anita is representative of the rocks that constitute the crest and south flank of the Santa Ynez Mountains as far east as Santa Barbara. This uninterpreted succession of marine sedimentary rocks ranges in age from Late Cretaceous to late Miocene and is about 15,500 ft (4,725 m) thick. The named stratigraphic units, their thickness, and general lithologic character, are shown in column 4, Figure 1b. Presumably the Upper Cretaceous Jalama Formation is underlain in the subsurface by rocks equivalent to the Espada, Honda, and Franciscan rocks in the vicinity of Tranquillon Mountain. Strata younger than the Sisquoc Formation were penetrated by wells in the Santa Ynez Unit on the Outer Continental Shelf (OCS) about 5 miles (8 km) offshore. This young sub-seafloor section includes Pliocene, Pleistocene, and Holocene sediments (commonly called Repetto, Pico, Santa Barbara, San Pedro, and Saugus Formations) that have a composite thickness of about 10,000 ft (3,050 m) (Vedder and others, 1976).

The coastal belt between Point Conception and Cañada de Santa Anita is structurally simple. With the exception of a syncline in Miocene strata of the Point Conception area, the beds are homoclinal and strike parallel to the shoreline. North of the ridge crest and bordering Jalama Creek, the east-trending Pacifico fault marks the north edge of the homocline. According to Dibblee (1978), the fault is traceable for about 10 miles (16 km), the south side is up with stratigraphic separation of about 5,000 ft (1,525 m), and a left-slip component is indicated by adjacent folds. Although Dibblee did not map the fault through folded Monterey Shale in the seacliff near the mouth of Jalama Canyon, a fault labeled the Pacifico fault extends about 1.5 miles (2.4 km) offshore on Plate II, Appendix 2.5, of a report by Earth Sciences Associates (1975).

San Miguel Island

Notwithstanding the fact that it lies nearly 40 miles (65 km) southeast of the well site, San Miguel Island has a stratigraphc sequence that warrants comparison with the well section. Weaver (1969) and Weaver and Doerner (1969a, b) report nearly 15,000 ft (4,575 m) of Upper Cretaceous

and Tertiary section of which 6,325 ft (1,928 m) of interbedded sandstone and shale are assigned to the Jalama Formation and from which Turonian, Campanian, and Maestrichtian (Late Cretaceous) microfossils are recorded. The overlying lower and middle Tertiary section consists of interbedded sandstone, siltstone, and minor conglomerate of Paleocene, Eocene and Oligocene age and basaltic to dacitic volcanic rocks, volcaniclastic beds, and siliceous shale of Miocene age (Col. 5, Fig. 1b). Rocks similar to those exposed on the island underlie the insular platform to the northwest.

Weaver and Doerner's (1969a, b) geologic map of San Miguel Island shows that the principal structural feature is a faulted homocline that strikes west-northwest. A northwest-trending syncline, which is fault truncated along its southwestern flank, disrupts the homocline in the easternmost part of the island. The dominant set of faults, some of which have large amounts of dip-slip separation, generally are nearly vertical and strike northwest. A set of minor faults, chiefly along the south-central coast of the island, strikes north to northeast.

Relation of Offshore Geology to the Well Site

The following discussion is based largely upon interpretation of a CDP multichannel acoustic-reflection profile that passes approximately 1.8 miles (2.9 km) southeast of the well (Fig. 1a). The data were collected by the U.S. Geological Survey R/V S.P. LEE using a 24-channel, 2400-meter streamer and a 2.2 liter air gun array. The profile is shown (Fig. 2) after the data were stacked, deconvolved and migrated. Lithologic, biostratigrahic, electrical resistance, and sonic data from the well have been integrated into the profile by projection parallel to the regional structure and by approximately maintaining a constant water depth (0.6 sec).

Many of the seismic reflectors in the profile produce distinctive high amplitude signals; others occur within packets defined by the geometry of the packet. Some of the high amplitude reflectors and packet boundaries appear to approximate the boundaries of major rock units identified by changes in electric log characteristics, lithology, and sonic velocity and paleontologic ages from ditch and core samples. A line drawing of the acoustic reflection profile shows the reflector positions and packet boundaries (Fig. 2). To facilitate descriptions of the acoustic profile and discussion of possible correlations, the interpreted acoustic profile is divided into seismic-stratigraphic units A through H.

At the intercept of projection of the well to the profile, the base of unit A is marked by a high amplitude reflector at a depth of 0.10 sec below the sea floor. High resolution acoustic profiles (3.5 kHz) suggests that deposits of Holocene age are only about 0.05 sec thick, and therefore unit A or the 24-channel profile may include sediments of both Pleistocene and Holocene age.

Unit B is a packet of contiuous reflectors that maintains a relatively constant thickness seaward from the projected position of the well. This unit appears to lie disconformably on the deformed underlying unit C.

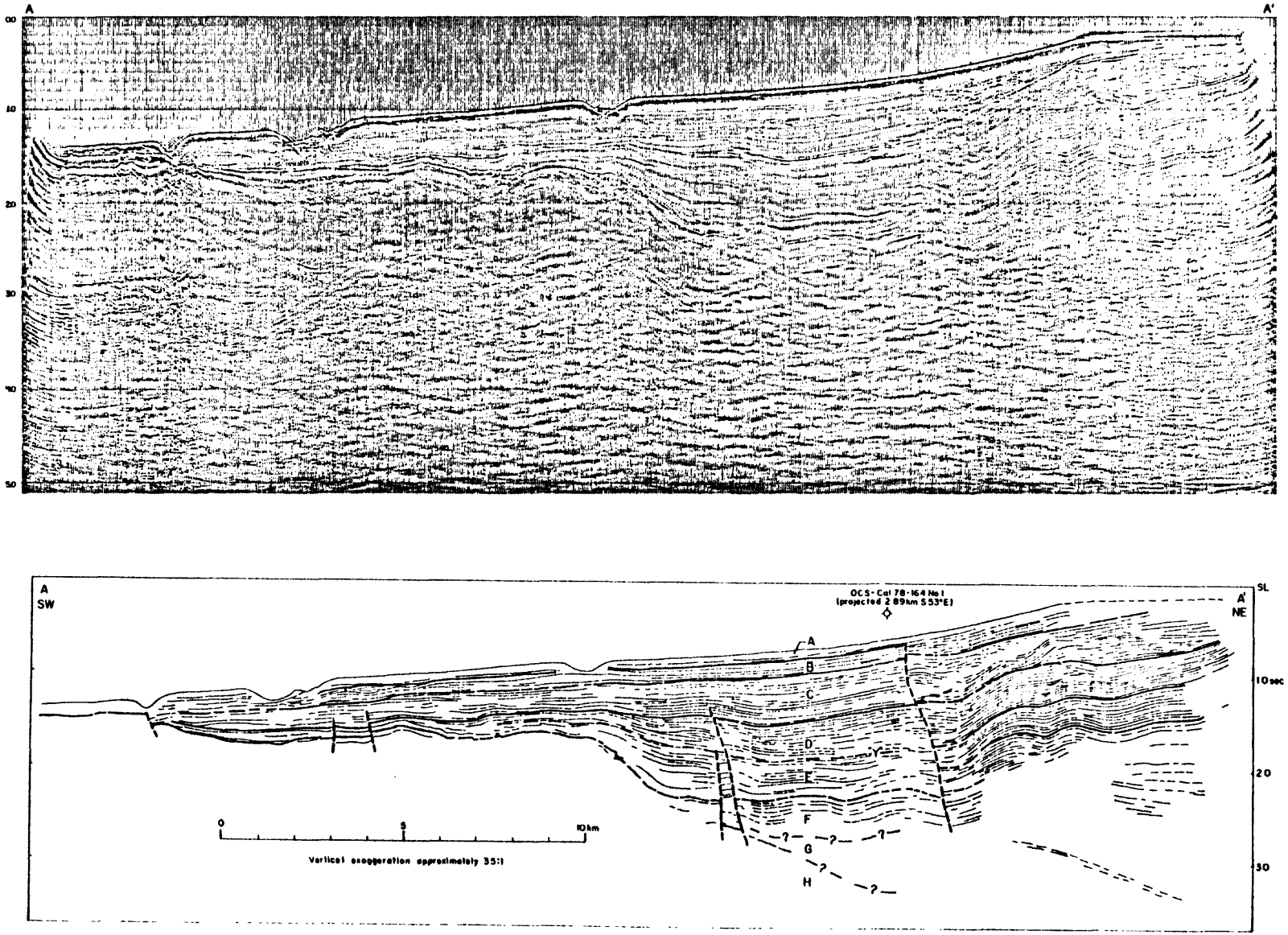

Figure 2. Multichannel seismic reflection profile (above) and line drawing of profile (below). Line of profile shown on Figure 1a.

Conglomerate beds in the well between 2,000 and 2,200 ft (610 and 671 m) appear to be part of unit B (Fig. 1b). The conglomerates contain Quaternary shell fragments and a large proportion of the clasts are rhyolitic volcanic rocks that may have been derived from the Tranquillon Volcanics of Dibblee (1950). In the well, Wheelerian, Venturian, Repettian, Delmontian and Mohnian Formainifera imply a middle Miocene to late Pliocene age for this; however, the probable ages of reflecting units lower in the section suggest, as do other paleontologic data, that this unit is younger and that both the Pliocene and Miocene Foraminifera are redeposited, possibly from the same erosional high that contributed the volcanic detritus to the conglomerate.

The upper reflectors in unit C are discontinuous, and on nonmigrated seismic profiles produce numerous hyperbolic reflectors that suggest the presence of discrete point-surface features. This boundary presumably marks the change from the predominantely silty claystone of unit B to conglomerate and silty sandstone of unit C. The change occurs at a depth of about 3,040 ft (927 m) in the well (approximately 0.26 sec below the seafloor in the profile). Reflectors are increasingly persistent downward in unit C, possibly as a result of downward fining and the sporadic occurrence of calcareous beds. The base of unit C is defined by a high amplitude reflector at a depth approximately 0.75 sec below the seafloor and 3,700 ft (1,128 m) in the well. At about this depth in the well, there is an abrupt increase in sonic velocity following an initial high amplitude positive velocity spike. At this same depth, the lithology log shows a change from the sand beds to calcareous sandstone and shale beds. In the profile, the base of unit C rests disconformably on unit D, and the unit thins westward over an acoustic-basement high by loss of section at its base. Clasts in the conglomerate include fragments of chert and tuff probably derived from the Monterey Formation. The presence of abundant chert fragments is typical of the Careaga Sandstone in the Santa Maria basin (Woodring and Bramlette, 1950). Thus, unit C may be the offshore equivalent of the Careaga Sandstone. As with unit B above, there is the possibility of redeposition in this unit. Onshore, the Careaga Sandstone is late Pliocene in age; however, possible Delmontian Stage Formainifera were identified in cuttings between 3,070 and 3,100 ft (936 and 945 m).

The base of unit D is equated with the electric log "Y" marker (Fig. 1b), which is used by some geologists to define a boundary that they believe separates strata equivalent to the Foxen Mudstone from the Sisquoc Formation beneath the Santa Barbara Channel (Frank Webster, oral commun., 1979). On the seismic profile, this boundary is drawn parallel to the bedding at an acoustic depth of 1.19 sec (equivalent to 4,740 ft [1,445 m] in the well). Unit D thins westward over the acoustic basement high, and the reflectors suggest that there is a disconformity within the unit. In the well, the "Y" marker occurs in a calcareous siltstone section, but the lithologic log does not indicate a change at this depth. Onshore, the Foxen Mudstone is assigned a middle(?) to late Pliocene age in the Santa Maria district (Woodring and Bramlette, 1950), and David Bukry (this report) identifies Pliocene nannofossils from the upper part of this interval. As in the overlying units, there is possible redeposition of

older Foraminifera, for late Mohnian to Delmontian Foraminifera occur between 3,600 and 4,200 ft (1,097 and 1,280 m) (R. E. Arnal, oral commun., 1979).

Unit E, which also thins westward over the acoustic basement high, is defined at its base by a high amplitude reflector at a depth of 1.63 sec below the sea floor at the intercept of the projected well section and the profile. At a depth of 6,700 ft (2,042 m) in the well, the uppermost chert beds were drilled and the sonic velocity increased. Prominent reflectors within this unit may represent a sandstone zone that is characterized by a high impedance contrast in the well (Beyer, this report). Although, the calcareous shale and siltstone that constitute this unit contain few fossils, the stratigraphic position of this unit between the "Y" marker and first occurrence of chert suggest that is may be partly equivalent to the Sisquoc Formation, which is assigned a late Miocene to early Pliocene age in the Santa Maria basin (Woodring and Bramlette, 1950).

Unit F is bounded at the top by the uppermost of several well-defined seismic reflectors. The unit boundaries are close to those of the chert sequence at approximately 6,760 and 7,412 ft (2,060 and 2,259 m) in the well (1.63 and 2.07 sec below the seafloor on the profile). This unit appears to be confined to the eastern side of the acoustic basement high, and to onlap its eastern flank. On the basis of its chert content and bedding character this part of the well section is tentatively correlated with the chert-rich sequences of the Monterey Shale of middle to late Miocene age. In the well, the chert sequence contains nondiagnostic fossils or is barren.

Unit G, at the projected well position, lies below the lowermost well-defined reflector of unit F and above an east-dipping reflector which, when extended down dip to the projected well section, intersects it at a depth of about 9,990 ft (3,018 m) (approximately 1.7 sec below the seafloor of the profile), where the well sequence changes from predominantly siltstone to sandstone. Within unit G, poorly defined reflectors do not clearly indicate bedding or structural relations to the acoustic basement. In the well, two foraminiferal stages are represented by Luisian and Relizian assemblages from sample intervals 8,200 to 9,280 ft (2,449 to 2,829 m) and 9,280 to 9,310 ft (2,829 to 2,838 m) respectively (R. E. Arnal, oral commun., 1979). The unit also contains sparse, poorly preserved Cretaceous fossils that probably were redeposited. Sparse nannofossils indicate an early to middle Miocene age to a depth of 9,820 ft (2,993 m) (Bukry, this report). The cored interval of pebbly sandstone in the well (9,529 to 9,559 ft [2,904 to 2,914 m]) presumably falls within unit G.

The lowermost beds in the well (below 9,970 ft [3,039 m]) are composed of sandstone and shale that contain nannofossils of Late Jurassic to Early Cretaceous age (Bukry, this report). These rocks are not evident on the acoustic profile, but a suggestion of eastward dips at the projected well site and to the east seems to warrent the designation of unit H. Eastward dips also are indicated in the dipmeter survey of the well below 10,100 ft (3,085 m); above this, in the interval 9,370 to 9,600 ft (2,256 to 2,926 m)

the dips are northward (Prensky, this report). These rocks probably thicken northeastward from the well and may be equivalent to the Espada Formation in the Point Arguello-Tranquillon Mountain area. No reflector separates these inferred strata from the acoustic basement southwest of the projected well, but the apparent lack of bedding in this basement high suggests that it may be composed of Franciscan rocks, which have a similar acoustic signature and are thought to form structural highs in the offshore Santa Maria basin (Page and others, 1979).

Well OCS-Cal 78-164 No. 1 was drilled in a basin that is bounded on the west by a north-northwest trending structural high (Hoskins and Griffiths, 1971). Although not well defined on the acoustic profiles, the floor of the basin probably is a deformed, pre-Miocene erosion surface cut across Franciscan(?) rocks and the Espada Formation(?). The oldest paleontologically dated Tertiary deposit on the basin floor is early to middle Miocene; thus, a large part of the thick Upper Cretaceous and Paleogene section that is preserved in the Santa Barbara Channel region either was not deposited at the well site or was completely eroded. Removal by erosion seems most likely because Eocene rocks occur on the Santa Lucia Bank structural high along the western edge of the offshore Santa Maria basin, and erosional remnants inferred to be of Eocene age are reported to lie unconformably below Miocene rocks in the offshore Santa Maria basin (Hoskins and Griffiths, 1971).

The structural feature that forms the flank of the basin southwest of the drill site began to obstruct the accumulation of sediments (units F and G) by early to middle Miocene time. It was not until late Miocene or early Pliocene time (unit E) that basin sediments overlapped the structural high. The thinning and upwarping of units E, D, and possible C, indicate that uplift continued to affect basin sedimentation until late Pliocene time. Since that time, sediment appears to have passed over the structural high with only slight deformation. At the well site and to the west, the profile shows that units are gently folded within the basin and the folding decreases upward. This geometry suggests that compression persisted througout the structural development of this young Tertiary basin.

Southwest of the projection of the well, several east-dipping, small faults displace reflectors on the profile. In general, these small faults appear not to have affected rocks in the upper part of unit C (upper Pliocene?). A nearly vertical fault directly northeast of the projected position of the well, however, cuts younger rocks (unit B), and high resolution acoustic-reflection profiles (Fig. 3), suggest that it may break beds close to the seafloor. The change in acoustic reflectors across this young fault makes it difficult to match seismic-stratigraphic units, but a high amplitude reflector at the base of unit B appears to indicate a component of reverse slip with the ast side up. Young reverse faults are to be expected in this area, for an east-west compressive component is reflected by young folding and reverse faulting in the offshore Santa Maria basin (McCulloch and others, 1977; Page and others, 1979). Gawthrop (1975, Fig. 4) indicates several epicenters in the vicinity of the well (Fig. 1a).

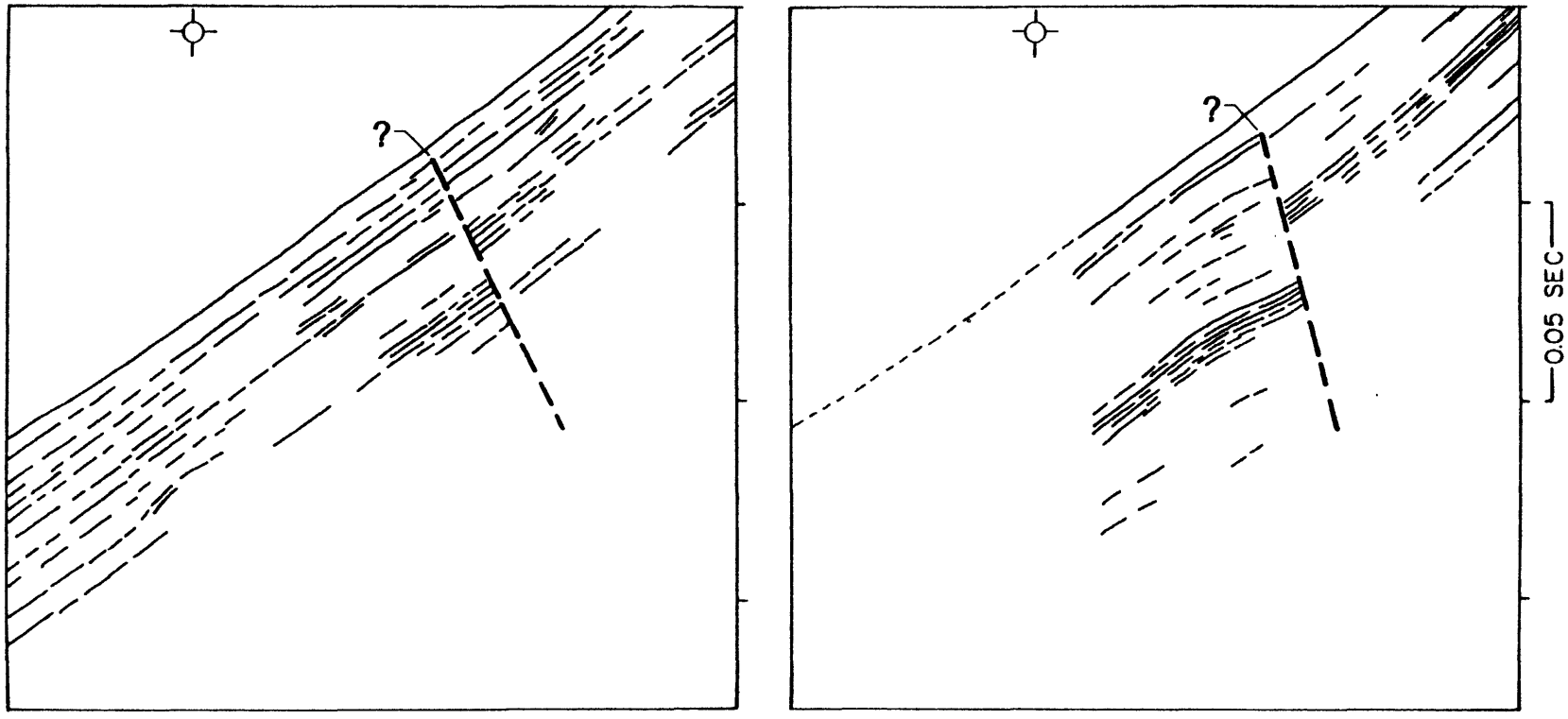

Figure 3. Interpretation of high resolution seismic reflection profiles (3.5 kHz to left, uniboom to right) showing probably offset of seismic reflectors along the fault northeast of Well OCS Cal 78-164 No. 1.

East of the young reverse fault, folding decreases upward as it does to the west, but fold amplitudes are generally greater to the east. Movement on the fault may have reduced compressive stress to the west, or the juxtaposed rocks may have been folded elsewhere and been displaced against the basin by strike slip. Lateral movement is suggested by the marked difference in acoustic character of reflectors on opposite sides of the fault, and packets bounded by high amplitude reflectors do not appear to match. Therefore, seismic-stratigraphic correlations across the fault are uncertain. Movements on the east side of the fault may have had a vertical component that displaced the more folded units upward. The basement rocks probably are increasingly shallow east of the well; free-air gravity data (Beyer and others, 1974) indicate that the basin edge slopes upward to the northeast, and Upper Jurassic to Lower Cretaceous rocks are exposed in the Point Arguello-Tranquillon Mountain area.

In several respects, the fault east of the well is analogous to the Hosgri fault (Wagner, 1974) that bounds the east margin of the offshore Santa Maria basin. At the well site and to the north, faults within the basins to the west die off in rocks of Pliocene age (Page and others, 1979). Both the fault east of the well and the Hosgri fault are seismically active and have young, probably Holocene displacement with a component of high-angle reverse movement. Both faults lie along the eastern side of young Tertiary basins; basement is known to have been displaced upward along the east side of the Hosgri fault, and this relation also is possible along the fault east of the well.

Summary of the Well Section

Details of the composition, physical properties, and ages of the rocks drilled in OCS-Cal 78-164 No. 1 well are given in succeeding parts of this report. In general, the well section consists of Cenozoic and late Mesozoic sedimentary rocks, chiefly siltstone and sandstone (Col. 3, Fig. 1b). By analogy with outcrop areas, the well section most closely resembles that exposed in the vicinity of Tranquillon Mountain, where lower Miocene beds overlap Oligocene, Eocene, and Upper Cretaceous formations onto Lower(?) Cretaceous strata.

A paleontologic discontinuity between Miocene and Lower Cretaceous or Upper Jurassic strata occurs below 9,970 ft (3,039 m). This discontinuity and a change in amount and direction of dip on the dipmeter survey between 9,650 and 10,100 ft (2,941 and 3,078 m) (Prensky, this report) suggest a major unconformity at approximately 9,900 ft (3,018 m). Within the Cenozoic section, gaps in the fossil record after Oligocene time, if present, have not been recognized because processed samples from much of the drilled interval 4,000 to 6,000 ft (1,219 to 1,829 m) were barren or contained nondiagnostic or poorly preserved assemblages. Noteworthy are the absence in the Miocene section of volcanogenic rocks related to the Tranquillon Volcanics and strata that are equivalent to the Rincon Claystone. Paleogene strata also are absent. Unusual coarse clastic rocks in the lowermost part of the Miocene section in the well are unlike any known to us from the mainland. These conglomeratic sandstone beds were cored between 9,529 and

9,549 ft (2,904 and 2,911 m) and contain mineral and lithic detritus that suggest either dual source terranes of granitic and ophiolitic(?) rocks or the recycling of one or both types of clasts from older sedimentary formations. Possibly they are related to the Vaqueros Formation in the Point Arguello area. Volcanic clasts in these conglomeratic sandstone beds are sparse and unlike the Tranquillon Volcanics. In the Pliocene and Pleistocene sections, however, rhyolitic debris and tuffaceous shale clasts are common suggesting erosion of both the Tranquillon Volcanics and the Monterey Shale.

Episodic uplift and erosion throughout much of late Cenozoic time disrupted the sedimentary succession in the Point Arguello-Tranquillon Mountain area and in the vicinity of the well. In contrast, the uninterrupted Tertiary section exposed east of Point Conception was deposited in a relatively inactive tectonic environment.

Although the thickness of the section exposed at San Miguel Island is comparable to that drilled in the well, the rocks are significantly different. On the island, the beds of the Monterey Formation are largely volcanogenic and coarser grained than are strata typical of the formation, particularly in the lower part (Weaver and Doerner, 1969b). Basaltic volcanic and volcaniclastic rocks constitute more than one-third of the late Cenozoic section on the island, and Paleocene and Eocene rocks make up more than one-half of the Tetiary section. The entire 6,000 ft (1,830 m) of Cretaceous rocks on the island is younger (Turonian to Maestrichtian) than any of the Upper Jurassic to Lower Cretaceous sections in the well, and the Paleogene conglomerates on the island contain metavolcanic clasts unlike any in the well.

In conclusion, it is difficult either to correlate the well directly with known outcrop sections or to confidently reconstruct its relation to the regional structural framework. Uncertainties in rock ages and inconclusive paleontologic correlations, as well as the lack of conventional cores that would have aided identification of depositional environments, hinder such interpretations. The occurrence in the bottom of the well of Upper Jurassic and Lower Cretaceous strata similar to the Espada Formation(?) suggests that early in its history the well site was contiguous with the terrane that underlies the western Santa Ynez Mountains. Uplift and erosion in early Tertiary time resemble conditions in the southern part of the offshore Santa Maria basin, where erosional remnants of Eocene rocks rest on a basement of probable Franciscan Complex and are separated from early to middle Miocene sedimentary rocks by a major unconformity. No comparable unconformity is present beneath the western Santa Barbara Channel, where there is an unbroken succession of early Tertiary marine sediments (Curran and others, 1971). This episode of Tertiary deformation formed the basin at the well site as well as the offshore Santa Maria basin and other shallow-shelf basins to the north. The late Cenozoic section in the well reflects the presence of a nearby topographically high and structurally complex area that shed both lithic and fossil detritus into the basin in which the well was drilled. Since early Tertiary time, the style of deformation of the basin offshore from Point Arguello seems to have been similar to that of the offshore Santa Maria basin.

REFERENCES CITED

Beyer, L. A., Pisciotto, K. A., and Sasnett, N. B., 1974, Free-air gravity map of the California continental borderland, in Vedder and others, eds., Preliminary report on the geology of the continental borderland of southern California: U.S. Geological Survey Miscellaneous Field Studies Map MF-624.

Crawford, F. D., 1971, Petroleum potential of Santa Maria province, California, in Cram, I. H., ed., Future petroleum provinces of the United States--their geology and potential: American Association of Petroleum Geologists Memoir 15, v. 1, p. 316-328.

Curran, J. F., Halle, K. B., and Herron, R. F., 1971, Geology, oil fields, and future petroleum potential of the Santa Barbara Channel area, California, in Cram, I. H., ed., Future petroleum provinces of the United States--their geology and potential: American Association of Petroleum Geologists Memoir 15,v. 1, p. 192-211.

Dibblee, T. W., Jr., 1950, Geology of southwestern Santa Barbara County, California--Point Arguello, Lompoc, Point Conception, Los Olivos, and Gaviota quadrangles: California Department of Natural Resources, Division of Mines Bulletin 150, 95 p.

_____ 1978, Analysis of geologic-seismic hazards to Point Conception LNG terminal site: Santa Barbara County, Department of Public Works, 72 p.

Earth Science Associates, Inc., 1975, Additional geologic and seismological studies 1975, in Final safety analysis report, units 1 and 2, Diablo Canyon site: Prepared for Pacific Gas and Electric Company; submitted to U.S. Nuclear Regulatory Commission, Docket Nos. 50-275 and 50-323, app. 2.5E.

Gawthrop, W. H., 1975, Seismicity of the central California Coastal Region: U.S. Geological Survey Open-File Report 75-134, 87 p.

Hall, C. A., Jr., 1978, Origin and development of the Lompoc-Santa Maria pull-apart basin and its relation to the San Simeon-Hosgri strike-slip fault, western California: California Division of Mines and Geology Special Report 137, p. 25-31.

Hopson, C. A., Franco, C. J., Passagno, E. A., Jr., and Mattinson, J. M., 1975, Preliminary report and geologic guide to the Jurassic ophiolite near Point Sal, southern California coast: Field Trip Guidebook No. 5, Geological Society America, Cordilleran Section, Los Angeles, California, March 1975.

Hoskins, E. G., and Griffiths, S. R., 1971, Hydrocarbon potential of northern and central California offshore, in Cram, I. H., ed., Future petroleum provinces of the United States--their geology and potential American Association of Petroleum Geologists Memoir 15, v. 1, p. 212-228.

Howell, D. G., McCulloch, D. S., and Vedder, J. G., 1978, General geology, petroleum appraisal, and nature of environmental hazards, eastern Pacific shelf, latitude 28° to 38° north: U.S. Geological Survey Circular 786, 29 p.

Jahns, R. H., 1954, Investigations and problems of southern California geology, in Jahns, R. H., ed., Geology of southern California: California Division of Mines Bulletin 170, chapter 1, p. 5-29.

Krammes, K. F., and Curran, J. F., chairman, and others, 1959, Correlation section across the Santa Marie basin from Cretaceous outcrop in Santa Ynez Mountains northerly to Franciscan outcrop north of Santa Maria River, California: American Association of Petroleum Geologists, Pacific Section, Correlation Section 12.

McCulloch, D. S., Clarke, S. H., Jr., Field, M. E., Scott, E. W., and Utter, P. M., 1977, A summary report on the regional geology, petroleum potential, and environmental geology of the southern proposed Lease Sale 53, central and northern California Outer Continental Shelf: U.S. Geological Survey Open-file Report 77-593, 57 p.

Page, B. M., Wagner, H. C., McCulloch, D. S., Silver, E. A., and Spotts, J. H., 1979, Geologic cross section of the continental margin off San Luis Obispo, the Southern Coast Ranges, and the San Joaquin Valley, California: Geological Society of America Map and Chart Series, MC-28G, 1:250,000.

Sylvester, A. G., and Darrow, A. C., 1979, Structure and neotectonics of the western Santa Ynez fault system in southern California: Tectonophysics, v. 52, p. 389-405.

Vedder, J. G., Greeene, H. G., Scott, E. W., and Taylor, J. C., and others, 1976, A summary report of the regional geology, petroleum potential, environmental geology, and technology for exploration and development in the area of proposed Lease Sale 42, California Continental Borderland: U.S. Geological Survey Open-file Report 76-787, 43 p.

van de Kamp, P. C., Harper, J. D., Conniff, J. J., and Morris, D. A., 1974, Facies relations in the Eocene-Oligocene in the Santa Ynez Mountains, California: Journal of the Geological Society of London, v. 130, o. 545-565.

von Huene, Roland, 1969, Geologic structure between the Murray fracture zone and the Transverse Ranges: Marine Geology, v. 7, p. 475-499.

Wagner, H. C., 1974, Marine geology between Cape San Martin and Point Sal, south-central California offshore. A preliminary report: U.S. Geological Survey Open-file Report 74-252, 17 p.

Weaver, D. W., 1969, The Cretaceous rocks, in Weaver, D. W., and others, eds., Geology of the northern Channel Islands: American Association of Petroleum Geologists Pacific Section and Society of Economic Paleontologists and Mineralogists Special Publication, p. 14-15.

Weaver, D. W., and Doerner, D. P., 1969a, Lower Tertiary stratigraphy, San Miguel and Santa Rosa Islands, in Weaver, D. W., and others, eds., Geology of the northern Channel Islands: American Association of Petroleum Geologists Pacific Section and Society of Economic Paleontologists and Mineralogistis Special Publication, p. 30-46.

_____ 1969b, Mid-Tertiary stratigraphy, San Miguel Island, in Weaver, D. W., and others, eds., Geology of the northern Channel Islands: American Association of Petroleum Geologists Pacific Section and Society of Economic Paleontologists and Mineralogists Special Publication, p. 80-83.

Willingham, C. R., 1979, The structural character of the western termination of the Transverse Range province, California: Geological Society of America, Cordilleran Section, Abstracts with Programs, v. 11, no. 3, p. 135.

Woodring, W. P., and Bramlette, M. N., 1950, [1951], Geology and paleontology of the Santa Maria district, California: U.S. Geological Survey Professional Paper 222, 185 p.

IMPLICATIONS FOR PETROLEUM APPRAISAL

Thane H. McCulloh
U.S. Geological Survey
Seattle, Washington

SUMMARY

Facts and interpretations developed as a consequence of the Point Conception OCS-Cal 78-164 No. 1 well provide important corroborative testimony regarding the petroleum potential of the OCS region extending from Point Arguello on the north to the southwest edge of the Santa Barbara Channel. The data and interpretations that suggest a substantial petroleum potential exists are: (1) The notable hydrocarbon shows that were reported during the drilling of this off-structure test (Menard, 1978); (2) the high geothermal gradient inferred from temperatures measured in the well; (3) organic geochemical analyses of well samples; (4) organic petrographic analyses of those same samples; (5) lithologic and stratigraphic information gained by studying the well samples and geophysical well logs; (6) consideration of the stratigraphic, lithologic, and geochemical data in relation to regional stratigraphic and structural patterns. Each of these topics is developed more fully below and the implications of each for petroleum occurrence are discussed.

SHOWS OF OIL AND GAS

With the exception of the following quotes all depths in this paper represent drilled depths beginning at the derrick floor. Thus, the sea floor starts at a drilled depth of 1,465 ft (derrick floor 37 ft above sea level plus water depth of 1,428 ft). "Indications of oil and gas were noted in drilling mud and cuttings at various intervals from about 1,850 ft to 4,000 ft below the ocean floor." "While it is unusual to come up with shows in a deep stratigraphic test located off-structure, no conclusions about commercial discoveries in the adjacent proposed sale areas can be drawn until the areas are leased and direct on-structure exploratory drilling occurs." These statements, quoted from a news release issued on November 1, 1978, over the name of the Director of the U.S. Geological Survey, provide a fair summary of the principal facts and interpretations of most of the hydrocarbon shows encountered during drilling of this well. A few details and some discussion are warranted.

The shallowest "show" recorded on the mud log occurred at a depth of about 2,900 ft. The show was of gas without indications of crude oil or heavier hydrocarbons and originated from a clayey interval. The shallowest indication of migratory hydrocarbons heavier than methane occurred at about 3,355 ft. These hydrocarbons consisted of chromatographically analyzed ethane, propane and butane accompanied by traces of petroliferous sands in

the drill cuttings. Shows of both gas and more-or-less tarry oil are abundant to general from 3,410 ft to about 5,850 ft. Minor indications of tarry oil and heavy paraffin homologs were recorded throughout the deeper Miocene strata to a depth of about 9,400 ft.

Compositional details about the oil shows are lacking. No production tests were conducted and samples were not collected for analysis. Many of the shows of both gas and oil were from siltstone, mudstone, or calcareous shale as determined from induction electric log, the mud-log lithologic notes, and sample lithologies. The hydrocarbons which occur in such fine-grained strata are either indigenous products or have migrated from deeper sources. These fine-grained sediments would be regarded by most petroleum geologists as lacking the permeability to serve as petroleum reservoirs.

In any event, the shows of oil and gas that occurred during drilling of this well attest eloquently to the presence of effective petroleum source rocks at or near the well site.

SUBSURFACE TEMPERATURES

Release of petroleum from source rocks is primarily a response to thermochemical changes induced by geothermal heating during burial. An exceptionally high geothermal gradient, such as that in the Pt. Conception well (McCulloh and Beyer, this report), enable release of petroleum at shallow burial depths.

Heat, generated mainly from decay of radiogenic elements in the earth's crust and mantle, flows continuously outward toward the land surface or seafloor. The change in temperature with depth, the geothermal gradient, depends not only on the outward flow of heat, which is variable, but also on the thermal conductivity of rocks. In addition, this gradient is influenced by local thermal disturbances (temporal) or distortions (areal) imposed at the outer surface, and on heat transfer induced by physical movement of fluids through porous and permeable rocks. Thus, the geothermal gradient can be extremely variable from place to place (and through extended time), and is not predictable in any simple way.

Heating of the sediment and aqueous pore solutions triggers or facilitates thermochemical reactions among those inorganic and organic phases that were stable only at low temperatures and fluid pressures. Particularly susceptible to burial heating are the unstable (Hunt, 1975) complex organic compounds derived from living organisms.

The temperatures reached and the duration of heating are principal controlling factors in the generation of petroleum from "sedimentary organic matter." Because the rates of such reactions increase exponentially with rising temperature, a modest temperature shift results in a very large shift in the rate of petroleum generation. Thus, even though the reactions probably <u>begin</u> at a temperature and time reached shortly after deposition (Erdman, 1975), the ". . . threshold of <u>intense</u> oil generation . . ." seems to be fairly sharply defined for a particular type

of source organic matter (Albrecht, 1969, Connan, 1974). This fact has contributed to the concept of the "liquid-window" in petroleum generation (Pusey, 1973, p. 195).

Expert opinions about the threshold temperature that must be exceeded for important oil generation to occur in petroleum source rocks span a surprisingly wide range. This temperature range is about 60°C for geologically old rocks and about 150°C for very young rocks (Phillipi, 1965; Wassojewitsh et al., 1969). In the Pt. Conception well an average temperature gradient of 0.048°C per meter has been calculated (McCulloh and Beyer, this report). The geothermal gradient normally varies between 0.008°C and 0.40°C per meter on land, but is somewhat higher in deep-sea sedimenhts (Verhoogen et al., 1970). In accordance with this gradient, 60°C is exceeded at a depth of about 3,715 ft below the sea floor (5,180 ft drilled depth), about 1,825 ft deeper than the first show of oil recorded on the mud log; 150°C would be encountered deeper then the bottom of the hole.

Cornelius (1975, fig. 1 and pg. 33-35), following others, suggests that the threshold temperature for the beginning of important oil generation is higher in geologically very young rocks than in rocks buried for long periods of time--that time as well as temperature influences the release of mobile hydrocarbons from source strata. In the Pt. Conception well, rocks as young as Neogene have temperatures in the range between 100° and 150°C. These temperatures are suggested by Cornelius as thresholds for the "oil window." 100°C is exceeded in this well at a drilled depth of about 7,935 ft (6,470 ft below the sea floor). This temperature is within a predominantly calcareous fine-grained section of Miocene strata through which presumably indigenous heavy tarry oil were reported.

No evidence exists to suggest that temperatures in this well have ever been higher. Similarly, there is only scanty and equivocal evidence to suggest that the present high geothermal gradient is a late development. Instead, all available evidence appears to suggest that the Santa Maria basin, westernmost Santa Ynez Mountains and the western Santa Barbara Channel are all parts of a region characterized by persistent high geothermal gradients (and possibly by high heat flow). In any case, an exceptionally high geothermal gradient is inferred to exist in this well. These subsurface temperatures exceed most estimates of the threshold temperatures needed for important generation of petroleum from "oil-prone" source materials in very young rocks. These thresholds are exceeded within the Neogene strata and are generally consistent with the interpretation that the deeper shows of oil are indigenous (rather than migrated).

IMPLICATIONS OF ORGANIC GEOCHEMICAL CHARACTERISTICS

Information available about the organic geochemical characteristics of the strata penetrated in this well is sparse but adequate. Details regarding the results of organic geochemical analyses of drill cuttings are reported by Claypool et al (this report). In summary, the Neogene samples are somewhat above average in total organic content; the organic matter is

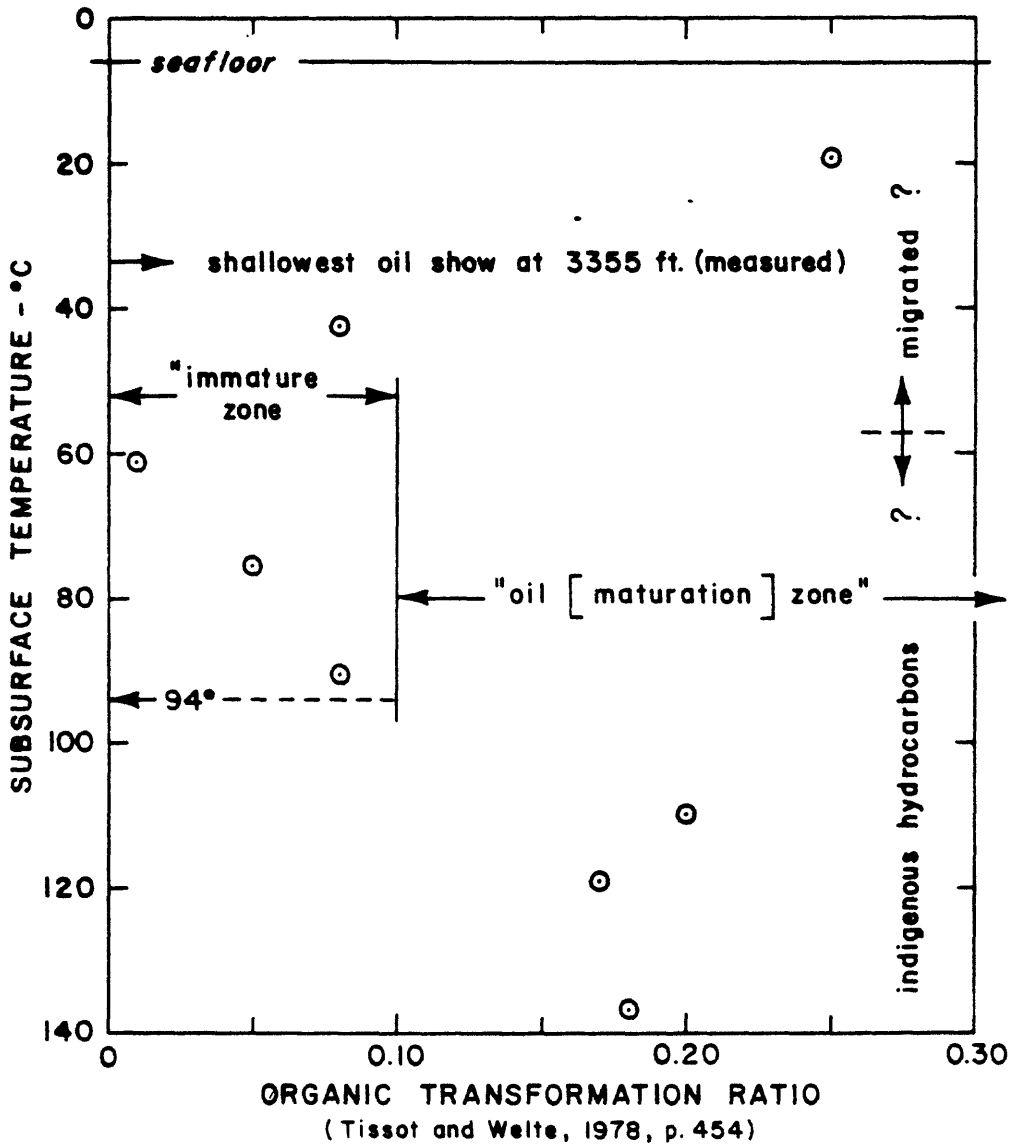

Figure 1. Transformation ratio versus present temperature in Pt. Conception OCS-Cal 78-164 No. 1 well.

dominantly hydrogen-rich "sapropelic" kerogen of excellent oil-generating capabilities. Most of the rocks analyzed are thus classified as potential source rocks for petroleum. One sample representative of the Mesozoic section in the bottom of the well is mature but dominated by gas-prone "humic" organic matter.

Analytical measures of thermochemical maturity of the cutting samples are interpreted on balance as indicating that the rocks at 7,090 ft and deeper are "mature" from an oil generation view point, and that most of the shallower samples are immature to marginally mature (Claypool et al., this report). The extractable hydrocarbon compositions of the submature to mature samples at depths from 5,000 to 10,000 ft show many distinctive characteristics in common with some crude oils from the Santa Maria basin onshore to the northeast of the site. Taylor (1976, p. 25) suggests that organic matter in Miocene strata, of the carbonate-rich type characteristic of the Monterey Shale, may have " . . . a composition which yields a heavy oil at an early stage of diagenesis."

The deepest sample analyzed (10,303 to 10,571 ft) exhibits an atomic H/C ratio (0.86) indicative of a dominance of hydrogen-poor "humic" organic matter rather than greatly advanced thermal maturity. Nearly all of the shallower samples exhibit multiple organic geochemical properties indicative of organic matter rich in hydrogen and derived in substantial part from aquatic algae.

One index of the degree to which organic matter of potential source rocks has moved toward thermal "maturity" is the trend of the organic "transformation ratio" (Tissot and Welte, 1978, p. 453-454) relative to depth and temperature. "Transformation ratio" is defined as the ratio of that part of the total organic content that has alredy (naturally) formed hyrocarbons to the total (natural plus potential) hydrocarbon yield that a sample is capable of generating. One measure of the "transformation ratio" is obtained by quantitative laboratory pyrolysis (Claypool and Reed, 1976; Espitalie et al., 1977). The amount of hydrocarbons naturally present in a rock and volatilized at low tempertures are separately measured from the amount generated by pyrolysis of the solvent-insoluble kerogen at temperatures higher than 250°C. The ratio of the first quantity to the sum of both is a measure of the "transformation ratio." If no hydrocarbons have migrated out of or into the rock analyzed, the ratio should increase steadily with increasing depth and temperature. A ratio of 0.1 is considered indicative of the threshold of important oil generation (Tissot and Welte, 1978, fig. V.1.16).

"Transformation ratios" are reported by Claypool et al (this report) for the eight composite samples analyzed from this well. The ratios are related in Figure 1 to the inferred subsurface temperature pertaining to the midpoint depth for each composite sample. A clear trend from very low to moderate ratio values is defined by the six deeper sample points, suggestive of the expectable steady increase with rising temperature. The intercept of the approximate trend with the 0.1 ratio line appears to occur at a temperture of about 94°C. This temperature is in reasonable accord

with both the shows of oil reported on the mud log and some estimates of the temperature threshold of the "oil window" in young source strata. The portion of the section colder (shallower) than 94°C (7,520 ft drilled depth) is presumed to be "immature" to "marginally mature" even for these unusually oil-prone source rocks.

The transformation ratios of the two shallowest samples are anomalous and suggest a separate trend. Nonindigenous (migrated) hydrocarbons probably account for this reversal trend at temperatures less than 60°C.

A transformation ratio of 0.4 is considered to mark the upper limit for important oil generation (Tissot and Welte, 1978, fig. V.1.16). The highest ratio obtained for the Pt. Conception well (0.25) is far below that upper limiting value. This suggests that lateral equivalents of the deeper Neogene section would probably remain capable of generating petroleum at burial depths many thousands of feet greater than those encountered in this well.

The organic geochemical characteristics of the cuttings samples analyzed from this well indicate that source rocks are prsent that contain total organic contents characterized by excellent oil-generating qualities. Extractable hydrocarbon contents and geochemical thermal maturity indices suggest that such source rocks are within the oil maturation zone in the well at depths of 7,500 ft (94°C) and more, and that those at shallower depths are immature to marginally mature. Shows of oil between 3,355 ft and 5,000 ft (or more) presumably rsult from hydrocarbons that migrated into their present positions from hotter and deeper sources. This occurred even though many of the shows were from strata which display well logging responses implying rocks too impermeable to serve as reservoir beds.

ORGANIC PETROGRAPHIC CHARACTERISTICS AND THEIR IMPLICATIONS

Measurements of the optical reflectance of vitrinite (and other identifiable plant fragments) that were concentrated from the eight composite cuttings samples from this well are reported elsewhere (Bostick, this report). Although fewer measurements were made than one would wish, these results are very interesting because they are in part so anomalous. When interpreted in other than conventional terms, they appear to carry extremely important implications regarding the petroleum potential of the source strata.

The microscopically determined optical reflectance of vitrinite has been widely used by coal petrographers to measure the degree of low-rank thermal alteration resulting from more-or-less deep burial (Teichmüller and Teichmüller, 1966; Bostick, 1974; Castaño and Sparks, 1974). The threshold for generation of oil in commercially important amounts is indicated by vitrinite reflectance values of 0.55 to 0.65 percent (Cornelius, 1975, fig. 1; Hood et al., 1975; Dow, 1978, fig. 2). Reflectance values lower than 0.5 percent are generally viewed as indicative of temperatures too low or thermal exposure times too short for important generation of petroleum hydrocarbons.

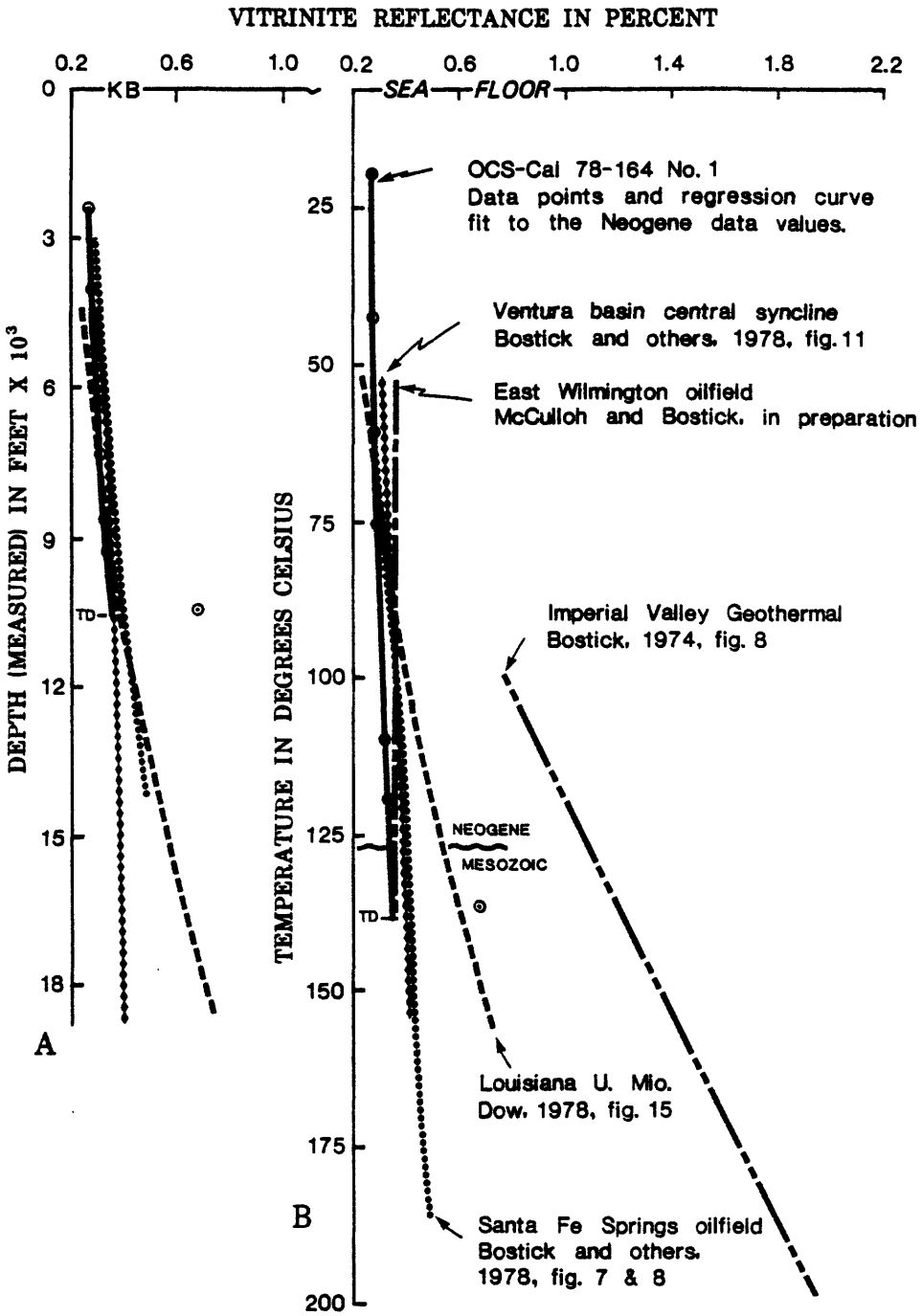

Fig. 2 (A) Vitrinite reflectance - depth gradient for the COST well 78-164 and comparative data from selected California and Louisiana sites.

Fig. 2 (B) Vitrinite reflectance - temperature gradient for the COST well 78-164 with selected comparative data.

Viewed in conventional terms, the vitrinite reflectance data reported from this well are anomalous. If the bottommost sample is excluded (because it is from Mesozoic strata beneath a major regional unconformity), the lowest and highest mean reflectance values reported for the Neogene samples are 0.28 and 0.34 percent. These are from seven composite cuttings samples representing 8,270 ft of section and span a present temperature range from 19 to 199°C. The age of the oldest Neogene rock sampled probably approaches 17 m.y. Much of the section is older than rocks elsewhere that show higher reflectance values at greater depths but equivalent temperatures (Dow, 1978, fig. 15). Although exact details of the thermal history are not known, the short effective burial time cannot be sufficiently influential to explain vitrinite reflectance values that show so little variation over such a depth range. Even where the rocks and the temperatures indicate that the threshold of the oil window has been passed, the mean reflectance of vitrinite does not exceed 0.34 percent.

The vitrinite reflectance values are compared in Figure 2 with like data from four other selected localities where rapid (and continuing) deposition of geologically young strata practically guarantees that present burial depths have not been exceeded. A straight line has been fit by linear regression analysis to the reflectance and mean depth values for the samples from the Neogene part of the Pt. Conception well. Analogous trend lines are shown for each of the other localities. This comparison shows there is no simple satisfactory standard depth gradient of vitrinite reflectance. Figure 2 also shows the anomalous nature of the Pt. Conception data compared with vitrinite in Gulf Coast sediment, and the strong similarity between this trend and the trends for the Wilmington and Santa Fe Springs oil fields, California (Bostick et al., 1979). The same sets of data shown in Figure 2a have been plotted in Figure 2b as vitrinite reflectance gradients with respect to present burial temperatures, thereby normalized for differences in geothermal gradients among the five localities. Although the normalizing procedure changes the relative positions among the five data sets, the anomalous trend of the data is not rectified. The explanation for the anomalous trend does not lie in the present thermal conditions or the burial history of the rocks. The 94°C temperature threshold for important oil generation (Fig. 1) corresponds with a vitrinite reflectance percentage of 0.32 (uncertainty range of 0.28 to 0.37).

Optical reflectance of vitrinite has been plotted against "transformation ratio" for all eight analyzed Pt. Conception well samples (Fig. 3). The deepest (Mesozoic) sample in the well, not unexpectedly, plots apart from all the other samples. The latter show only slight systematic interdependence between these two organic parameters. A clear trend with respect to both depth and temperature has already been shown for the "transformation ratios," a trend that can be rationalized in terms of other indicators of source-rock maturation, including temperature. From Figure 3, the conclusion is self-evident that the vitrinite reflectance values from this well bear little relationship to the depth or temperature at which oil-prone organic matter has crossed the threshold into the oil maturation zone.

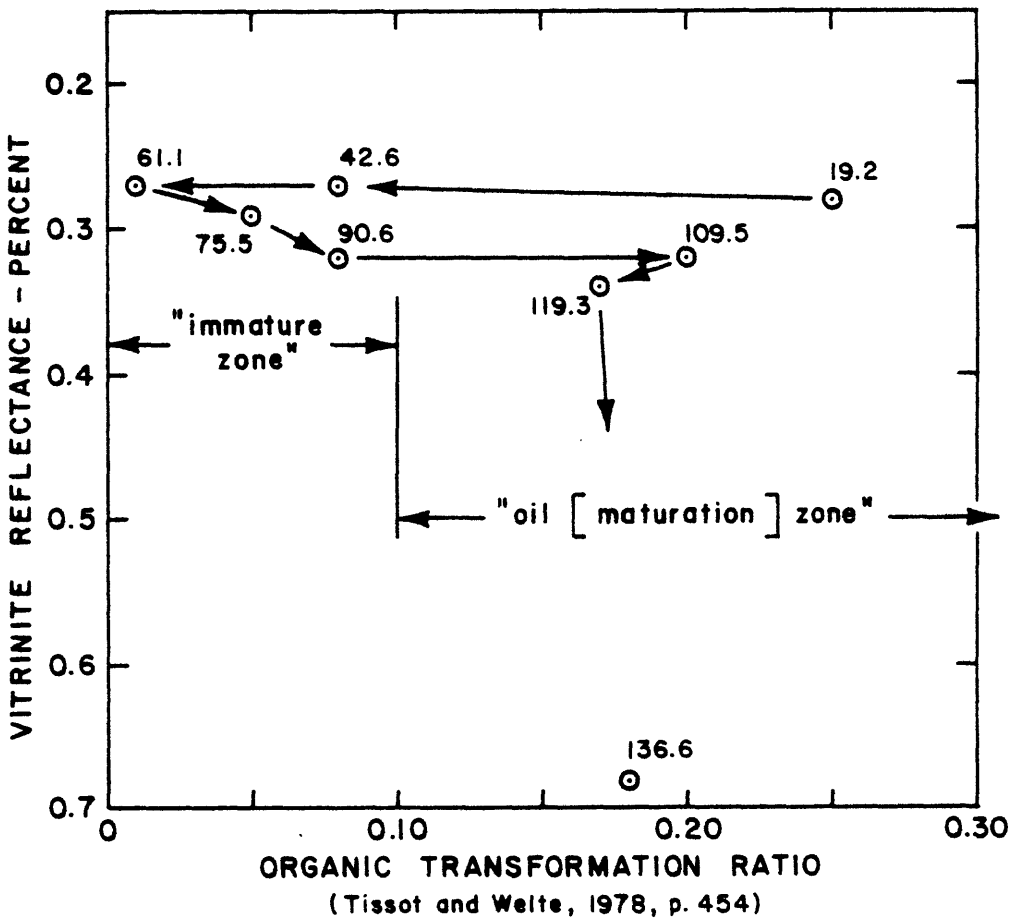

Figure 3. Plot of optical reflectance of vitrinite against organic transformation ratio. Small numbers beside points indicate present subsurface temperatures at the mean sample depths. Pt. Conception OCS-Cal 78-164 No. 1 well.

The unusual characteristics of the vitrinite from the Pt. Conception well are not unique. Anomalously low reflectance of vitrinite occurs in other geologically young potential source rocks that contain (or have generated) oil and that are at temperatures high enough to have entered the "oil window." Such occurrences prompt advancement of three alternative explanatory hypotheses. (1) The thermochemical reactions that cause the elevation of optical reflectance in hydrogen-poor vitrinite may be relatively ineffective in the presence of immature petroleum released from intimately associated hydrogen-rich organic matter. (2) Some adsorption or reaction mechanism may permit immature petroleum (possibly strongly polar compounds) to suppress, retard, or conceal the changes in vitrinite that express themselves as elevated optical reflectance. (3) The physical changes in vitrinite which are manifested as differences in optical reflectance lag behind the chemical changes in the more reactive portions of the kerogen responsible for the release of most of the heavier compounds of petroleum; thus, the unusual nature of much of the organic matter has rsulted in oil generation at a temperature and time insufficient for attainment of vitrinite reflectance levels of 0.5 percent or more.

The author tends to favor hypothesis (1) but is quick to admit that compelling evidence in favor of one hypothesis or another is lacking. A fourth hypothesis, that high fluid pressures may have caused "pressure retardation" of the vitrinite alteration (McTavish, 1978), can be rejected. The section penetrated is characterized by normally pressured interstitial fluids (maximum pressure gradient to 10,000 ft is 0.514 psi per foot or less).

A satisfactory explanation for the occurrence of "immature" vitrinite in "marginally mature" source rocks of excellent oil-generating capabilities is not yet in hand. The empirical observation of such "anomalous" differences and similarities in reflectance-temperature gradients from one geologically similar environment to another invites consideration of the following possibility.

If the vitrinite in young rocks that have been affected by the presence of petroleum is different from that in comparable rocks that have been unaffected (or less affected) by oil-prone source products, then possibly such effects could be calibrated. Vitrinite reflectance profiles, normalized for independently assessed burial temperatures or paleotemperatures (and possibly for age differences) might then provide measures of the petroleum-richness of their regional surroundings. High reflectance values in rocks at some index temperature (such as 100°C or 125°C) would reflect an oil-poor or sterile environment. Conversely, low reflectance values in rocks at that index temperature would be indicative of surroundings rich in petroleum compounds. In such a scheme, the rocks from the Pt. Conception well would rank at the oil-rich extreme of the spectrum, along with rocks from such other petroliferous sites as East Wilmington oil field in the Los Angeles basin and Kettleman North Dome oil field in the San Joaquin Valley of California.

IMPLICATIONS OF LITHOLOGIC AND STRATIGRAPHIC DATA

The Pt. Conception well penetrated 8,005 ft of predominantly fine-grained clastic strata of Neogene age (Holocene to early middle Miocene). This is underlain by 265 ft of calcareous marine sandstone and pebble conglomerate containing nondiagnostic pelecypod shells (questionably early Miocene). The lower Miocene sediment unconformably overlies 836 ft of sandy siltstone and mudstone containing marine microfossils of Early Cretaceous to Late Jurassic in age (Bukry, this report). The only conspicuous depositional break or faunal hiatus is the regional unconformity at the base of the apparently continuous Neogene section.

Porosity of the sandstones and other lithologies is based mainly on estimations calculated from geophysical logs, questionable measurements made on a few sidewall cores, and reliable measurements made on one conventional core. Log calculations indicate that the section down to 5,400 ft is strongly undercompacted (Prensky, this report), with mean porosity values in the range from 44.4 to 33.8 percent (based on density log response and an assumed matrix density of 2.65 g/cc). Upper and middle Miocene strata between 5,400 and 9,450 ft yield calculated density log porosity values in the range from 29.8 to 9.3 percent (the lower values from predominantly limey siltstone). Measurements of porosity made on selected samples of sandstone from the conventional core recovered from between 9,529 and9,549 ft fall in the range between 15.8 and 17.9 percent, whereas values calculated from the density log through the interval 9,451 to 9,979 ft have a mean value of 10 percent. Burial consolidation, complicated to some extent by cementation (by diagenetic carbonate and, locally, minor phyllosilicate minerals), appears to account for the progressive loss of porosity with increasing depth.

Porosities of the more permeable sandstones are such that commercial petroleum production could probably result if enough petroleum-charged sandstone could be found in the region. Sandstones and fractured diagenetically altered siliceous rocks are the two lithologies most deserving attention from a reservoir potential view point.

The predominantly fine-grained and thinly bedded character of most of the Neogene section in this well is a noteworthy characteristic. Sandstone beds are few in number. This sandstone is mostly fine- to very fine-grained, and tends to occur in widely separated thin beds, especially below about 5,900 ft.

Above 5,900 ft a few thicker sandstone units interrupt this overall pattern and are associated with several of the most impressive "shows" of oil. Conglomeratic sandstone grading to silty sandstone and siltstone in the interval, 3,250 to 3,720 ft is the most impressive of these coarser units. This interval is mainly early Pleistocene in age, the lowermost portion possibly being Pliocene (Bukry, this report). The interval may be stratigraphically correlative with part of the Careaga Sandstone and the uppermost Foxen Mudstone of the onshore Santa Maria district (Woodring and

Bramlette, 1950, p. 36-49), long regarded as "Pliocene" in accordance with provincial standards.

The section below 5,900 ft is dominantly very fine-grained, notably calcareous, and virtually devoid of thick, coarse-grained sandstone. Regional patterns of sandstone distribution in rocks of equivalent age to the east and the north suggest that important amounts of coarse-grained facies are not likely to occur in most of the equivalent sectin in a large region surrounding this well. Possibly some local development of coarser-grained sandstone might occur in equivalent strata many miles to the south or southeast of the site.

An important exception to the overall tendency for the Neogene sediment to be fine-grained and without thick coarser clastic strata is the 235-ft thick sequence of conglomeratic sandstone penetrated between 9,450 and 9,735 ft. Although not satisfactorily dated paleontologically, the writer considers this unit to be a correlative of the Vaqueros Sandstone and conglomerate of the westernmost Santa Ynez Mountains (VanderHoof, 1956) where 75 ft of lower Miocene thick-bedded, locally conglomeratic sandstone has yielded rocks at least 150 million barrels of oil and large volumes gas . . . along the Santa Barbara coast," this coarse-grained interval penetrated (and partially cored) in the Pt. Conception well is of particular interest. If the correlation of these strata with the Vaqueros Formation is valid, rocks of equivalent facies will probably be present at the same horizon east and southeast of the Pt. Conception well, but may be absent or have an erratic distribution toward the north, south, and west.

No Paleogene strata were encountered in this well even though approximately 5,000 ft of marine clastic beds, predominantly "proximal turbidites" and "shallow marine" sandstone of Paleocene through Oligocene age, occur in the westernmost Santa Ynez Mountains between Upper Cretaceous beds below and lower Miocene Vaqueros Sandtone unconformably above (van de Kamp et al., 1974). More than 4,300 ft of equivalent strata were penetrated by an exploratory well at Cuarta Offshore oil field, approximately 10 mi east of Pt. Conception (and roughly 25 mi east of the Pt. Conception well). There oil-saturated sandstone occurs "in the Alegria, Gaviota, Sacate, and Cozy Dell formations . . ." (Cordova, 1972, p. 7) of late Eocene and Oligocene ages.

The disappearance of these extensively developed and locally petroliferous clastic units between Pt. Conception and the Pt. Conception test well probably results from post-depositional deformation, uplift, and early Miocene erosion. Data from seismic reflection profiles north and east of the Pt. Conception site suggest truncation of a pre-Neogene sequence that appears to thicken toward the east and northeast. The southwestern truncated edge of this sequence trends roughly southeast from an offshore point near Point Arguello. Seismic reflection data south and west of the Pt. Conception well suggest that the Paleogene sequence does not reappear in those directions within the area underlain by a thick Neogene cover.

Even though the clastic Paleogene strata were not encountered in this

well and therefore may not be present beneath much of the area south and southwest of this well and Point Arguello, they should not be disregarded in any assessment of the petroleum potential of this area. Because massive sandstone is abundant in portions of the Paleogene section, such rock could act as reservoirs. This sandstone could have primary porosity and permeability or secondary porosity and permeability resulting from weathering at the erosion surface represented by the overlying angular unconformity. The most likely possibilities for seeking such traps fall in the region east and southeast of the Pt. Conception test well.

Little can be said about the implications of this well regarding the petroleum potential of the Mesozoic sediment because so little of that section was penetrated. South of the northern San Joaquin Valley, Cretaceous and older rocks are notably nonproductive where they have been tested by drilling, even though tantalizing indications of both gas and oil have been encountered in several places. A low level of source-rock maturity is indicated for the single sample representing the Mesozoic rocks in this well (Claypool et al., this report; Bostick, this report). This suggests that those rocks have not undergone destructive alteration during deep burial or tectonism in spite of their long history. This implies that the entire younger Cretaceous section in this area may deserve consideration as retaining some potential for yielding commerical petroleum, particularly gas, even though some experts believe that Jurassic or Lower Cretaceous strata constitute "basement" (Feister and Hall, 1977, p. 39).

Primary intergranular porosity and associated permeability in uncemented sandtone provides the natural storage capacity and potential producibility required for commercial petroleum production from most California reservoirs, both onshore and offshore. In a few places, interconnected fractures in diagenetically altered siliceous "shales" provide the needed storage and fluid transmissibility (Regan and Hughes, 1949; Taylor, 1976, p. 12). Two such places are the Santa Maria basin onshore (Crawford, 1971) and the Santa Barbara Channel offshore (Curran et al., 1971, p. 202; U.S. Dept. of Interior, 1975; v. 1, p. II-32; Feister and Hall, 1977). "Miocene Monterey fractured shale has produced 75 percent of the oil . . ." produced through 1976 from the oil fields of the Santa Maria basin (Feister and Hall, 1977, p. 39), and much of the proven reserves in the Santa Ynez Unit of the western Santa Barbara Channel occur in stratigraphically equivalent fractured siliceous "shale" reservoirs. The pertinence of these very important occurrences to the findings in the Pt. Conception well should not be underestimated.

Although the underlying controls responsible for such fracture porosity in siliceous sedimentary rocks are not known in detail, it is clear that diagenetically controlled volume changes play a key role. The progressive change of diatomaceous opal-A to opal-CT and then to quartz in chert and porcelanite result from increasing tempertures associated with increasing burial depth (influenced secondarily by time and possibly other factors) (Mizutani, 1970; Murata et al., 1977). The mineral changes result in progressive volume contractions. Bulk-volume contractive fracture formation in relatively pure siliceous rocks can follow. The conversion of

opal-A to opal-CT is thought to occur over a temperture range from 25 to 56°C. The conversion range for opal-CT to quartz is 43° to 81°C (Pisciotto, 1979). Thus, fracture porosity develops at depths and temperatures only slightly shallower than the threshold for intense oil generation suggested by the organic geochemical data from this well. Some evidence exists that admixed detritial terrigenous sediment "retards" opal-CT formation (Isaacs, 1979).

Siliceous rocks containing opal-CT are present in this well (Hein et al., this report) from about 4,400 ft (nearly 50°C) to about 5,800 ft (more than 70°C). Siliceous strata are abundant deeper than 5,800 ft, but quartz is the dominant or only silica species at those levels. Fractured rock resulting from such mineralogical changes probably occurs within the range of opal-CT formation as well as at the transition from opal-CT to quartz. Whether such fractures occur in the Pt. Conception hole is not known at this time.

Reservoirs that produce oil from fractured siliceous rocks in California tend to be associated with anticlinal structures or plunging anticlinal noses, but purely stratigraphic accumulations can also occur. The Santa Maria Valley oil field onshore is an almost purely stratigraphic accumulation in which fracture porosity in the Monterey Shale has created resevoirs from which an estimated 140 million barrels of oil equivalent have already been produced (Taylor, 1976, p. 12).

Fracture porosity in purely diagenetic or structural-diagenetic combination traps may prove to be a key element in the discovery of oil in the region surrounding the Pt. Conception well. Several ingredients suggest that a purposeful search for petroleum in fractured siliceous Miocene strata might yield positive results. These include: high geothermal gradients, a thick section of richly organic oil-prone source rocks, formations thousands of feet thick composed in large part of orginally biogenic opaline silica, a fairly thick cover of superincumbent strata in portions of the region, and a deformational history that has produced broad folds and some large faults. Diagenetic traps may be found in the western part of the Santa Barbara Channel and in an extensive area west and northwest of the Pt. Conception site.

Questions that have or could be raised (McCulloch et al., 1977, p. 34) about the difficulties of producing oil from fractured siliceous shale resevoirs are not the proper subject matter of this report and therefore will not be addressed in detail. Changing economics (Aguilera and van Poollen, 1979) and evolving technologies (Demesy and Chardonneau, 1979) both may convert marginal or submarginal resources of immature, shallow, viscous and dense asphaltic crude oil into producible reserves. In this connection, it may not be inappropriate to recall that the discovery of the Santa Maria Valley field was confirmed as an important find by a well which had an initial production potential of 2,400 barrels per day of 16.4° gravity oil flowing from the Monterey Shale at a depth of 2,576 ft (Frame, 1938, p. 37).

REFERENCES CITED

Albrecht, P., and Ourisson, G., 1969, Diagenese des hydrocarbures satures dans une serie sedimentaire epaisse (Douala, Cameroun): Geochim. et Cosmochim. Acta, v. 33, p. 138-142.

Aguilera, Roberto, and van Poollen, H. K., 1979, Fractured shales present an attractive gas potential: Oil and Gas Journal, v. 77, no. 10, p. 167, 170, 172, 176, 178.

Bostick, N. H., 1974, Phytoclasts as indicators of thermal metamorphism, Franciscan assemblage and Great Valley sequence (Upper Mesozoic), California: Geological Society of America Special Paper 153, p. 1-17.

Bostick, N. H., Cashman, S. M., McCulloh, T. H., and Waddell, C. T., 1979, Gradients of vitrinite reflectance and present temperature in the Los Angeles and Ventura Basins, California, in Oltz, D. F., ed., A Symposium in Geochemistry: Low temperature metamorphism of kerogen and clay minerals: Society of Economic Paleontologists and Mineralogists, Pacific Section, Los Angeles, California, p. 65-96.

Castano, J. R., and Sparks, D. M., 1974, Interpretation of vitrinite reflectance measurements in sedimentary rocks and determination of burial history using vitrinite reflectance and authigenic minerals: Geological Society of America Special Paper 153, p. 31-52.

Claypool, G. E., and Reed, P. R., 1976, Thermal analysis technique for source-rock evaluation: quantitative estimate of organic richness and effects of lithologic variation: American Association of Petroleum Geologists Bulletin, v. 60, p. 608-612.

Connan, Jacques, 1974, Time-temperature relation in oil genesis: American Association of Petroleum Geologists Bulletin, v. 58, no. 12, p. 2516-2521.

Cordova, Simon, 1972, Cuarta offshore oil field: California Division of Oil and Gas, Summary of Operations, v. 58, no. 1, p. 5-13.

Cornelius, C. D., 1975, Geothermal aspects of hydrocarbon exploration in the North Sea area: Norges Geologiske Undersøkelse, Nr. 316, Bulletin 29, p. 29-67.

Crawford, F. D., 1971, Petroleum potential of Santa Maria Province, California, in Cram, I. H., ed., Future petroleum provinces of the United States--their geology and potential: American Association of Petroleum Geologists Memoir 15, p. 316-328.

Curran, J. F., Halle, K. B., and Herron, R. F., 1971, Geology, oil fields, and future petroleum potential of Santa Barbara Channel area, California, in Cram, I. H., ed., Future petroleum provinces of the United States--their geology and potential: American Association of Petroleum Geologists Memoir 15, p. 192-211.

Demesy, Jean-Paul, and Chardonneau, Joel, 1979, Rod pumping heavy, viscous oils offshore: World Oil, v. 188, no. 5, p. 177.

Dibblee, T. W., Jr., 1950, Geology of southwestern Santa Barbara County, California--Point Arguello, Lompoc, Point Conception, Los Olivos, and Gaviota quandrangles: California Division of Mines Bulletin 150, 95 p.

Dow, W. G., 1978, Petroleum source beds on continental slopes and rises: American Association of Petroleum Geologists Bulletin, v. 62, no. 9, p. 1584-1606.

Erdman, J. G., 1975, Relations controlling oil and gas generation in sedimentary basins: Ninth World Petroleum Congress, Proceedings, v. 2, p. 139-148.

Espitalie, J., Laporte, J. L., Madec, M., Marquis, F., Leplat, P., Paulet, J., and Boutefeu, A., 1977, Methode rapide de caracterisation es rockes meres, de leur potentiel petrolier et de leur degre d'evolution: Rev. Inst. Fr. Pet., v. 32, p. 23-42.

Feister, G. H., and Hall, E. A., 1976, Tomorrow's oil from southern California basins: American Association of Petroleum Geologists Miscellaneous Publication 24, 51st AAPG Pacific Section Meeting Selected Papers, p. 39-46.

Frame, R. G., 1938, Santa Maria Valley oil field: California Oil Fields (California Division of Oil and Gas), v. 24, no. 2, p. 27-47.

Hood, A., Gutjahr, C. C. M., and Heacock, R. L., 1975, Organic metamorphism and the generation of petroleum: American Association of Petroleum Geologists Bulletin, v. 59, no. 6, p. 986-996.

Hower, John, Eslinger, E. V., Hower, M. E., Perry, E. A., 1976, Mechanism of burial metamorphis of argillaceous sediment: 1 mineralogical and chemical evidence: Geological Society of America Bulletin, v. 87, p. 725-737.

Hunt, J. M., 1975, Is there a geochemical depth limit for hydrocarbons?: Petroleum Engineer International, v. 47, no. 3, p. 112, 116, 118, 120, 123-124.

Isaacs, C. M., 1979, Lateral diagenesis in Monterey Shale, Santa Barbara Coast, California: American Association of Petroleum Geologists Annual Meeting Program, p. 109.

Kubler, B., 1968, Evaluation quantitative du metamorphisme par la cristallinite de l'illite: Bull. Centre Rech. Pau-SNPA, v. 2, no. 2, p. 385-397.

Maxwell, J. C., 1964, Influence of depth, temperature and geologic age on porosity of quartzose sandstone: American Association of Petroleum Geologists Bulletin, v. 48, no. 5, p. 697-709.

McCulloch, D. S., Clarke, S. H., Jr., Field, M. E., Scott, E. W., and Utter, P. M., 1977, A summary report on the regional geology, petroleum potential, and environmental geology of the southern proposed Lease Sale 53, central and northern California Outer Continental Shelf: U.S. Geological Survey Open-File Report 77-593, 57 p.

McTavish, R. A., 1978, Pressure retardation of vitrinite diagenesis, offshore north-west Europe: Nature, v. 271, p. 648-650.

Menard, H. W., 1978, Stratigraphic test well yields oil and gas "shows" offshore California: U.S. Geological Survey New Release, 1 November 1978, 2 p.

Mizutani, Shinjiro, 1970, Silica minerals in the early stages of diagenesis: Sedimentology, v. 15, p. 419-436.

Murata, K. J., Friedman, Irving, and Gleason, J. D., 1977, Oxygen isotope relations between diagenetic silica minerals in Monterey Shale, Temblor Range, California: American Journal of Science, v. 277, p. 259-272.

Phillipi, G. T., 1965, On the depth, time and mechanism of petroleum generation: Geochim. et Cosmochim. Acta, v. 29, p. 1020-1049.

Pisciotto, K. A., 1979, Deduction of past geothermal gradients in Neogene siliceous rocks in Circum-Pacific region: American Association of Petroleum Geologists Annual Meeting, Program, p. 146.

Pusey, W. C., III, 1973, Paleotemperatures in the Gulf Coast using the ESR-Kerogen method: Gulf Coast Association of Geological Societies Trans., v. 23, p. 195-202.

Regan, L. T., Jr., and Hughes, A. W., 1949, Fractured reservoirs of Santa Maria district, California: American Association of Petroleum Geologists Bulletin, v. 33, no. 1, p. 32-51.

Taylor, J. C., 1976, Geological appraisal of the petroleum potential of offshore southern California: The Borderland compared to onshore coastal basins: U.S. Geological Survey Circular 730, 43 p.

Teichmuller, Marlies, and Teichmuller, Rolf, 1966, Geological causes of coalification, in Advances in chemistry series, 55, American Conference on coal science, 23-26 June 1964, University Park, Pennsylvania: Am. Chem. Soc., Washington, D.C., p. 133-155.

Tissot, B. P., and Welte, D. H., 1978, Petroleum formation and occurrence--a new approach to oil and gas exploration: New York, Springer-Verlag, 538 p.

U.S. Geological Survey, 1975, Oil and gas development in the Santa Barbara Channel Outer Continental Shelf off California: Draft Environmental Statement 75-35, v. 1, sec. 2, 207 p.

Van de Kamp, P. C., Harper, J. D., Conniff, J. J., and Morris, D. A., 1974, Facies relations in the Eocene-Oligocene in the Santa Ynez Mountains, California: Journal of Geological Society, London, v. 130, p. 545-565.

VanderHoof, V. L., 1956, Correlation chart, central California Coast Ranges: California Oil Fields (California Division of Oil and Gas), v. 42, no. 1, p. 43, 1 pl.

Verhoogen, J., Turner, F. J., Weiss, L. E., Wahrhaftig, C., and Fyfe, W. S., 1970, The earth, an introduction to physical geology: Holt, Rinehart, and Winston, Inc., 748 p.

Wassojewitsch, N. B., Kortchagina, J. I., Lopatin, N. W., Tschernyschew, W. W., and Tschernikow, K. A., 1969, Die Hauptphase der Erdolbildung: Zeitschrift angew. Geol., v. 15, p. 612-615.

Woodring, W. P., and Bramlette, M. N., 1950, Geology and paleontology of the Santa Maria District, California: U.S. Geological Survey Professional Paper 222, 185 p.

GEOTHERMAL GRADIENTS

T. H. McCulloh[1] and L. A. Beyer[2]
[1]U.S. Geological Survey
Seattle, Washington

[2]U.S. Geological Survey
Menlo Park, California

INTRODUCTION

In any study of burial diagenetic changes in sedimentary rocks, consideration of temperature and time--the thermal history--are of the utmost importance (Klemme, 1975). Elevated subsurface temperatures and prolonged geothermal heating are generally regarded as controlling influences for the generation of petroleum from sedimentary organic matter (Erdman, 1975). Geothermal heating also exerts a controlling influence on the diagenetic inorganic reactions between pore fluids and thermodynamically unstable mineral species (for example, Kubler, 1968,; Mizutani, 1970; Hower et al., 1976; Murata et al., 1977; Pisciotto, 1979); these reactions tend to reduce intergranular porosity and permeability as burial temperature or(and) time increase (Maxwell, 1964). The Pt. Conception well penetrated a thick section of geologically youthful strata which accumulated without important interruption. Thus, information about the present subsurface thermal gradient in this section is the first step toward understanding the thermal history, and thereby important controls on both organic and inorganic diagenetic reactions.

Only disequilibrium temperatures recorded during open-hole logging operations are available from the Pt. Conception well. These temperatures were measured by means of maximum-recording thermometers while the borehole was still recovering from the disturbing thermal effects associated with drilling and circulation of (cooling) drilling fluid. Thirteen separate temperatures were recorded in four depth groups at various times between 3.5 hours and 21 hours after cessation of circulation of drilling fluid. These erroneously low values are shown in Figure 1 (open dots) in relation to other data and interpretations.

ADJUSTMET OF DISEQUILIBRIUM TEMPERATURE MEASUREMENTS

A variety of analytical and empirical techniques have been devised to correct disequilibrium borehole temperatures to approximate equilibrium values. All of these techniques ultimately depend upon statistical comparisons betwen disequilibrium measurements and matching trustworthy data measured carefully in wells where thermal equilibrium has been reestablished (Jaml et al., 1969; Kehle, 1972; Joyner, 1975). A comparative

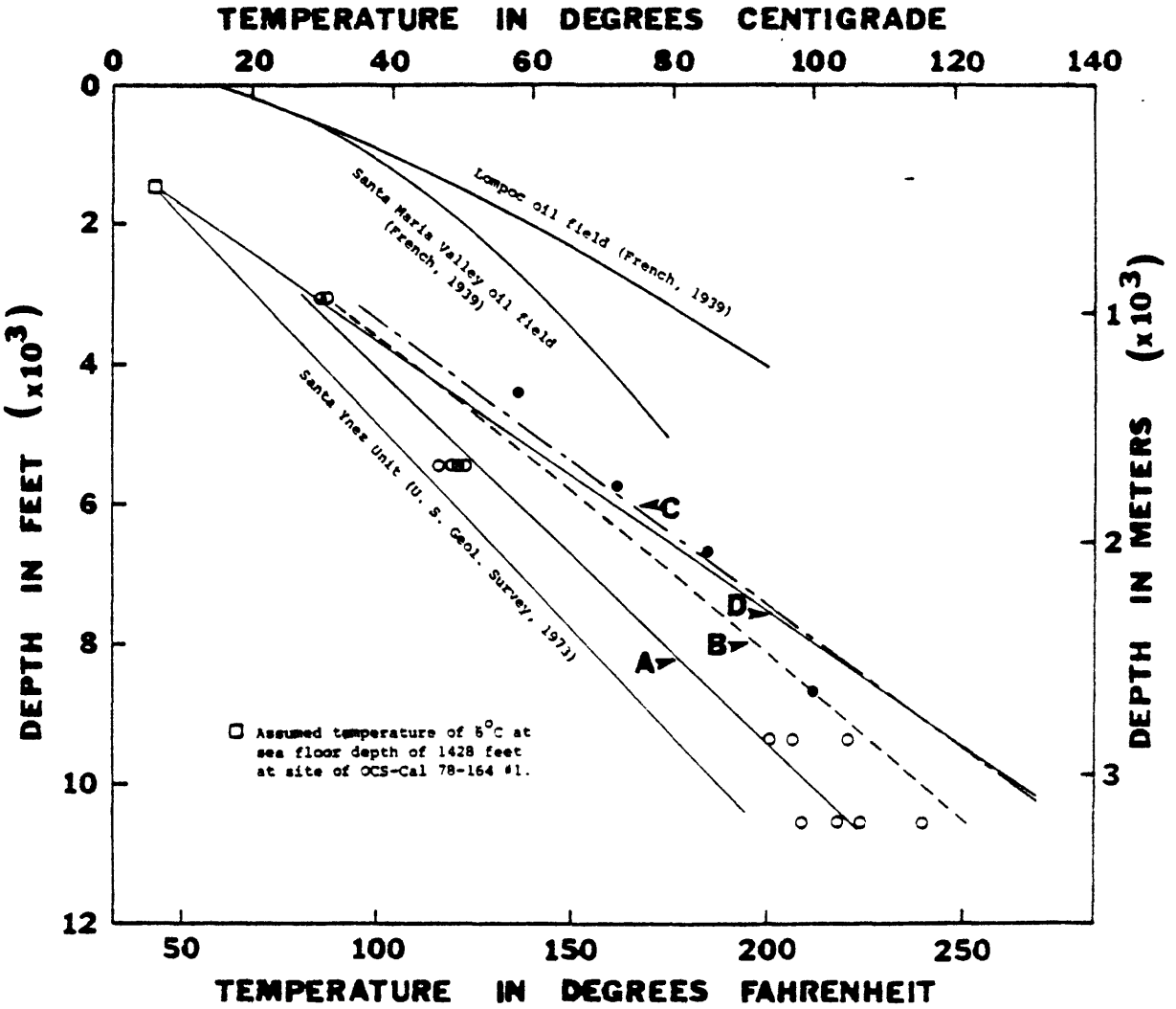

Figure 1. Basic data and interpretations pertaining to present subsurface thermal conditions at well OCS-Cal 78-164 No. 1 and comparative data from adjacent pertinent oil fields. Open circles = unadjusted temperatures taken from headings of well logs of OCS-Cal 78-164 No. 1. Line A is fitted by linear regression analysis to unadjusted temperature data. Line B is the adjusted temperature gradient based on the correction procedure of the AAPG Geothermal Survey of North America (Kehle et al., 1970; Kehle, 1972). Line C is the adjusted temperature gradient based on the correction procedure of Tanaka and Sato (1977). Line D is the adjusted average temperature gradient based on the procedure developed by the senior author. Published temperature profiles for the Lompoc and Santa Maria Valley oil fields and the published temperature gradient for the Santa Ynez Unit are also shown. Solid circles = four estimated temperature-depth values derived by Hein et al. (this report) from diagenetic mineral occurrence and phase data.

study of the various published correction procedures and the results of their application show that different approaches yield somewhat divergent results. This is especially true in regions where very high geothermal gradients prevail. These divergent results have prompted the senior author to assemble disequilibrium and equilibrium data from many widely different locations in California, Alaska, and south Texas, and to develop an empirical scheme for estimating the adjustments to be applied to disequilibrium data. The results of applying this approach to data from the Pt. Conception well are shown in Figure 1, together with results obtained by using two other established techniques described by Kehle (1972) and by Tanaka and Sato (1977). The procedures followed are briefly discussed below.

Pairs of depth and temperature values are tabulated from all available measurements and are then used to define a straight or simple curved line by means of linear regression analysis. Line A of Figure 1 is such a line fitted to the OCS-Cal 78-164 No. 1 disequilibrium temperature values. Depending upon the adjustment scheme used, a depth-dependent positive correction or percentage increase in temperture is applied to the line (Fig. 1).

The correction procedure of the AAPG Geothermal Survey of North America (Kehl et al., 1970; Kehle, 1972) was applied to the Pt. Conception well data. Line B of Figure 1 represents this correction. These AAPG correction procedures are based on data from wells in south Louisiana, an area of low geothermal gradients. The same AAPG procedure, used by the senior author, yields results that tend to be too cold by 10 to 20 percent when applied to data from wells in regions of unusually high geothermal gradients.

Line C of Figure 1 results from application of a correction procedure based on data from Japanese oil-producing basins (Tanaka and Sato, 1977). These investigators derived a multiplication factor of 1.31 with which to correct the thermal gradient defined by (disequilibrium) logging temperatures to the gradient defined by using temperatures measured during bottom hole pressure tests. This multiplication factor was changed only slightly from one area to another even though individual temperature gradients differed substantially from one field to another. Most of their data are from reservoirs of intermediate depths. Relationships at very shallow depths (<3,000 ft) and at large depths (>10,000 ft) are under-represented. It is at shallow and great depths where their procedure appears to yield deficient results.

Line D of Figure 1 is the average gradient (0.048°C per meter) resulting from application of the procedure developed by the senior author. This procedure has much in common with that of Tanaka and Sato (1977). A proportionality factor (based on empirical relationships) is used to determine the correction to be added to the linear regression line for depths between the sea floor and the drilled depth of 10,571 ft. Unlike the singular value of Tanaka and Sato, the proportionality factor is a variable that is proportional also to the magnitude of the disequilibrium

gradient. A smaller factor than 1.31 is used for low apparent gradients, and a somewhat larger factor than 1.31 is used for excessively high apparent gradients. The average overall gradient for the Pt. Conception well is determined by using 6°C at the sea floor together with the adjusted temperature value at the drilled depth of 10,571 ft.

DISCUSSION

The tectonic setting and geothermal conditions of the Pt. Conception well resemble more closely those of the Niigta basin in Japan than those of south Louisiana. Therefore, we believe the temperature correction procedure of Tanaka and Sato is more valid than the AAPG procedure, especially in the deeper part of the well. Note that the results based on the senior author's procedure are close to those of Tanaka and Sato (1977) at depths greater than about 6,000 ft, while better correspondence with the method of Kehle (1972) is evident at shallower depths.

For comparative purposes, Figure 1 also shows the temperature profiles from the Lompoc and Santa Maria Valley oil fields in the Santa Maria Basin (French, 1939), and the temperature gradient in the Santa Ynez Unit in the western Santa Barbara Basin (U.S. Geological Survey, 1973). In addition, four estimated temperature-depth values are shown in Figure 1 (solid dots) derived from diagenetic mineral first occurrences and phase data (Hein et al., this report). Considerable uncertainty accompanies these four mineral temperature estimates. They should be viewed only as general indicators of maximum possible temperatures during the thermal history of the rocks.

Regardless of the temperature correction procedure used, a temperature gradient of 0.48°C per meter inferred for the Pt. Conception well is high. Geothermal gradients normally vary between 0.008°C and 0.040°C per meter on land (Verhoogen et al., 1970). It is comparable to the temperature gradients known from the largest oil fields of the Santa Maria Basin and from the Wilmington oil field in the Los Angeles Basin. Higher temperatures occur in this well than have been reported at equivalent depths in most of the Santa Barbara Channel, Ventura Basin, and large portions of the Los Angeles and San Joaquin Basins. Temperatures high enough for maturation of source rocks and generation of petroleum occur within the range of depths penetrated in the well. There is no evidence that the temperatures now prevailing in the well were exceeded at any depth in the past. Furthermore, the present exceptionally high thermal gradient is considered to have been a lengthy duration; there is scant evidence to suggest otherwise.

REFERENCES CITED

Erdman, J. G., 1975, Relations controlling oil and gas generation in sedimentary basins: Ninth World Petroleum Congress, Proceedings, v. 2, p. 139-148.

French, R. W., 1939, Geothermal gradients in California oil wells, in Drilling and production practice, 1939: American Petroleum Institute, p. 653-658.

Hower, John, Eslinger, E. V., Hower, M. E., Perry, E. A., 1976, Mechanisms of burial metamorphism of argillaceous sediment: 1 mineralogical and chemical evidence: Geological Society of America Bulletin, v. 87, p. 725-737.

Jaml, Pedro, Dickey, P. A., and Tryggvason, Eysteinn, 1969, Subsurface temperature in south Louisiana: American Association of Petroleum Geologists Bulletin, v. 53, no. 10, p. 2141-2149.

Joyner, H. D., 1975, A correlation of electric-log-indicated reservoir temperature with actual reservoir temperature--southwest Louisiana: Journal of Petroleum Technology, p. 181-182.

Kehle, R. O., 1972, Geothermal survey of North America 1971 annual progress report: American Association of Petroleum Geologists Research Committee, unpublished duplicated report, 31 p.

Kehle, R. O., Schoeppel, R. J., and Deford, R. K., 1970, The AAPG geothermal survey of North America: Geothermics, Special Issue, 1970, p. 358-367.

Klemme, H. D., 1975, Geothermal gradients, heat flow and hydrocarbon recovery, in Fischer, A. G., and Judson, Sheldon, eds., Petroleum and global tectonics: Princeton University Press, Princeton, New Jersey, p. 251-320.

Kubler, B., 1968, Évaluation quantitative de métamorphisme par la cristallinité de l'illite: Bull. Centre Rech. Pau-SNPA, v. 2, no. 2, p. 385-397.

Maxwell, J. C., 1964, Influence of depth, temperature and geologic age on porosity of quartzose sandstone: American Association of Petroleum Geologsits Bulletin, v. 48, no. 5, p. 697-709.

Mizutani, Shinjiro, 1970, Silica minerals in the early stages of diagenesis: Sedimentology, v. 15, p. 419-436.

Murata, K. J., Friedman, Irving, and Gleason, J. D., 1977, Oxygen isotope relations between diagenetic silica minerals in Monterey Shale, Temblor Range, California: American Journal of Science, v. 277, p. 259-272.

Pisciotto, K. A., 1979, Deduction of past geothermal gradients in Neogene siliceous rocks in Circum-Pacific region: American Association of Petroleum Geologists Annual Meeting, Program, p. 146.

Railroad Commission of the State of California and California Division of Oil and Gas, 1942, Estimate of the natural gas reserves in the State of California as of January 1, 1941: California Department of Natural Resources, Division of Oil and Gas, p. 219.

Tanaka, T., and Sato, K., 1977, Estimation of subsurface temperature in oil and gas producing areas, northeast Japan: Journal of the Japanese Association of Petroleum Technologists, v. 42, no. 4, p. 229-237.

United States Geological Survey, 1973, Draft environmental statement, proposed plan of development, Santa Ynez Unit, Santa Barbara Channel, off California: U.S. Geological Survey, Department of the Interior, v. 1, p. II-145.

Verhoogen, J., Turner, F. J., Weiss, L. E., Wahrhaftig, C., and Fyfe, W. S., 1970, The earth, an introduction to physical geology: Holt, Rinehart and Winston, Inc., 748 p.

LITHOLOGIC DESCRIPTIONS

Hugh McLean
U.S. Geological Survey
Menlo Park. California

The Point Conception OCS-Cal 78-164 No. 1 well penetrated sedimentary rocks of Quaternary, Pliocene, and Miocene age that unconformably overlie rocks of Early Cretaceous or Late Jurassic age. Most if not all of the rocks were deposited in a marine environment. All depths represent drilled depths beginning at the derrick floor. Thus, the sea floor starts at a drilled depth of 1,465 ft (37 ft from the derrick floor to sea level plus a water depth of 1,428 ft). The detailed lithologic log (Table 1) begins at a sub-derrick floor depth of 2,000 ft and continues to 10,500 ft. Total drill depth of the well is 10,571 ft.

TECHNIQUES

Washed well cuttings collected at 30-ft intervals from 2,000 to 10,500 ft, 29 sidewall cores, and one conventional core cut from 9,529 to 9,549 ft were examined visually with a binocular microscope. In addition, 12 grain-mount thin sections prepared from selected intervals of washed cuttings were studied petrographically; 14 thin sections cut from the conventional core were also studied with a petrographic microscope. Detrital modes were determined for three sandstone samples from the cored interval between 9,529 and 9,549 ft; results are tabulated in Table 2.

Geophysical logs including the dual induction-laterolog (DIL), borehole compensated sonic log (BHC), simultaneous compensated neutron, formation-density logs (CNL-FDC) and dip meter were used in conjunction with the drillers mudlog to determine lithologic breaks and major unconformities.

Significant shows of gas occurred between 2,900 and 4,100 ft; and oil and tar shows occurred between 3,400 and 5,800 ft. Mica was added to the drilling mud as lost circulation material at 3,300 ft. Washed cuttings from 3,300 to 3,640 ft consist mainly of the mica additive.

SANDSTONE PETROGRAPHY

Sandstone recovered in the suite of washed cuttings is briefly described in Table 1. The small number and size of sandstone fragments observed in grain-mount thin sections precludes detailed petrographic analysis. For this reason, only the sandstone recovered in core No. 1 (9,529-9,549 ft) is discussed in this chapter.

Detrital modes and QFL ratios for three sandstone samples are listed in Table 2. The sandstone is texturally well to moderately sorted with

subrounded to subangular grains either floating in calcite cement, or has a grain supported framework with silica and chlorite filling pore spaces. Framework grains consist mostly of polycrystalline and monocrystalline quartz, plagioclase, and rock fragments including felsic, microlitic, and vitric volcanics, mica schist, quartz diorite and fragments of greenschist facies metamorphic rock. Accessory minerals include potassium feldspar, epidote, chlorite, opaque minerals, mica, and sparry calcite (Hein, et al., this report).

Provenance

Quartz types, potassium feldspar and quartz-mica schist appear to reflect a granitic source terrane, whereas the presence of abundant chert and altered volcanic rocks such as spilite and keratophyre may reflect erosion of an ophiolite terrane, similar in part to the section exposed at Point Sal located about 45 km north of the drill site. No high pressure-low temperature metamorphic rocks such as glaucophane or lawsonite-bearing schist were observed.

TABLE 1.--Lithologic log of OCS-Cal 78-164 No. 1 well

Depth (in feet)	Unit Lithologic Description
At 2,050*	Mudstone.
At 2,145*	Siltstone.
At 2,210†	Siltstone, carbonaceous; sandstone, silty; pebbles of chert and epidote hornfels.
At 2,238*	Siltstone.
2,240- 2,270	Sandstone, silty, very fine grained, shell fragments.
2,270- 2,390	Sandstone, silty, very fine grained, shell fragments
2,390- 2,420	Sandstone, silty, forams, bone fragments.
2,420- 2,540	Sandstone, silty, forams, bone fragments.
2,540- 2,600	Siltstone, massive; forams.
2,600- 2,690	Sandstone, silty, brownish gray, friable.
At 2,669*	Mud, soft, brown.
2,690- 2,840	Siltstone, grayish brown, rounded white tuff pebbles.
At 2,847	Siltstone, semiconsolidated, brown.
2,840- 2,990	Siltstone, gray, friable; shell fragments.
2,990- 3,015	Siltstone, grayish brown, massive friable.
At 3,025*	Sandstone, silty, semiconsolidated, brown.
3,015- 3,042	Sandstone, fine grained, friable, calcareous.
At 3,142*	Sandstone, silty.
3,142- 3,220	Siltstone, grayish brown, friable, calcareous.
3,220- 3,250†	Tuff and tuffaceous mudstone with rare forams; microlaminated tuffaceous siltstone; pebbly sandstone and siltstone, poorly sorted.
3,250- 3,347	Siltstone, brown, interbedded with light gray tuff.
At 3,347	Silty mudstone, soft and friable.
3,347- 3,415	Siltstone.
At 3,415*	Siltstone, brown, dry and friable.
At 3,450*	Sandstone, light gray, fine grained, friable.
3,450- 3,640	Siltstone, gray, calcareous.
3,640- 3,760	Siltstone, brownish gray, calcareous.
3,760- 3,878	Siltstone, brownish gray, calcareous.
At 3,878*	Mud, soft, brown.
3,878- 3,950	Siltstone, calcareous.
At 3,950*	Silty mud, soft, brown.
3,950- 4,102	Silstone, calcareous.
At 4,102*	Mud, dark grayish brown.
4,102- 4,240	Siltstone.
4,240- 4,270†	Siltstone, brown, contains forams and rare diatoms; sandstone, very fine grained, quartzose, calcite cement; sandstone, fine grained quartz and plagioclase in tuffaceous matrix; sandy siltstone, reddish brown matrix.
At 4,250*	Sandstone, silty, grayish brown, friable.
4,270- 4,350	Siltstone, dark grayish brown.

TABLE 1.cont.--Lithologic log of OCS-Cal 78-164 No. 1 well

Depth (in feet)	Unit lithologic description
At 4,350*	Siltstone, grayish brown with petroleum odor.
4,350- 4,390	Siltstone.
4,390- 4,450	Mudstone, partly siliceous.
At 4,450*	Siltstone mixed with mudstone, siliceous, brown soft.
4,450- 4,550	Mudstone, siliceous, brown, soft.
At 4,550*	Mudstone, siliceous, brown, weak petroleum odor.
4,550- 4,650	Mudstone, siliceous.
At 4,650*	Mudstone, siliceous, grayish brown, friable.
4,650- 4,710	Mudstone, siliceous.
4,710- 4,750	Siltstone, siliceous, grayish brown, friable.
At 4,750*	Siltstone, siliceous, grayish brown, firable.
4,750- 4,850	Siltstone, siliceous, grayish brown, noncalcareous, weakly friable.
At 4,850*	Mudstone, siliceous, grayish brown, noncalcareous, weakly friable.
4,850- 4,950	Mudstone, siliceous, grayish brown, noncalcareous, weakly friable.
At 4,950*	Sandstone, silty, very fine grained, grayish brown, friable.
4,950- 5,357	Mudstone, siliceous, grayish brown, friable.
At 5,357*	Mudstone, siliceous, grayish brown.
5,357- 5,463	Siltstone, siliceous.
5,463- 5,680	Mudstone, siliceous; shale, siliceous; minor porcelanite, thinly laminated; minor dolomite.
5,740- 5,800	Porcelanite, partly thinly laminated; minor dolomite and chert.
5,880- 5,830†	Mudstone, siliceous, red-brown interbedded with calcareous feldspathic fine grained sandstone; dolomitic and siliceous porcelanite.
5,830- 6,310	Porcelanite, partly thinly laminated; minor dolomite and chert.
6,310- 6,764	Porcelanite, partly dolomitic, partly thinly laminated minor dolomite
At 6,764*	Mudstone, siliceous soft and plastic with strong petroleum odor.
6,764- 6,880	Porcelanite, laminated, partly dolomitic, dark gray; chert. Slight petroleum odor.
6,880- 7,060	Porcelanite, partly dolomitic laminated with grayish brown wary laminations. Has petroleum odor.
7,060- 7,090†	Cuttings include: sandy tuffaceous siltstone, recrystallized chert, dolomitic laminated siliceous mudstone, and reddish brown argillaceous laminated siliceous siltstone.

TABLE 1 cont.--Lithologic log of OCS-Cal 78-164 No. 1 well

Depth (in feet)	Unit lithologic description
7,090- 7,351	Porcelanite, silty, dolomitic, partly laminated shale, siliceous, dolomitic; chert; dolomite.
At 7,351*	Porcelanite, dolomitic grayish brown, has weak petroleum odor.
7,351- 7,412	Porcelanite, silty, dolomitic, partly laminated; siltstone, dark gray, slightly sandy with petroleum odor; dolomite; fragments of light gray chert, and sparry calcite (probably vein filling).
7,412- 7,720	Siltstone, light gray calcareous, massive.
7,720- 7,750†	Cuttings include: mudstone, silty and calcareous (limy); sandstone, fine grained, contains quartz chert, mica, plagioclase and chlorite in clayey matrix; sandy mudstone, with reddish brown clayey matrix tuffaceous siltstone with tuff altering to clay and calcite.
7,750- 8,740	Sandy siltstone, and very fine grained calcareous sandstone.
8,740- 8,770†	Cuttings include: sandy siltstone, reddish brown, laminated clayey matrix, contains quartz, plagioclase and forams; sandstone, fine grained, poorly sorted, grains of quartz, plagioclase, chert, opaques, mica and calcite floating in reddish brown clay matrix; silty limestone.
8,770- 9,040*	Sandy siltstone, gray, calcareous.
At 9,040	Siltstone, dark reddish brown with streaks of white colored mineral. Weak petroleum odor.
9,040- 9,450	Sandy siltstone and rare sandstone, dark gray, fine grained, with abundant grains of rock fragments.
9,450- 9,530	Sandstone, dark greenish gray, fine grained, calcite cement. Conglomerate, clasts of green and light brown chert.
9,529- 9,549	Cored interval of sandstone and pebble conglomerate (see core description).
9,549- 9,670	Sandstone, greenish gray, fine to medium grained, composed of rock fragments including well rounded gray and green chert, calcareous cement.
9,670- 9,700†	Cuttings include sandstone as above, silty sandstone, chert grains, and sparry calcite (probably vein filling).
9,700- 9,735	Sandstone, greenish gray, fine to medium grained composed of rock fragments including well rounded gray and green chert, calcareous cement.
At 9,735	Change in lithology.

TABLE 1 cont.--Lithologic log of OCS-Cal 78-164 No. 1 well

Depth (in feet)	Unit lithologic description
9,735-10,300	Siltstone, dark gray and dark greenish gray, massive with calcite cement interbedded with sheared and polished dark gray mudstone.
10,300-10,510	Mudstone, dark gray and dark greenish gray, massive with calcite cement interbedded with sheared and polished dark gray mudstone.
10,510-10 540†	Sandy siltstone, gray, contains grains of quartz, plagioclase, chlorite, mica, calcite, and opague laminae. Zeolite matrix.

* Sidewall core sample
† Grain-mount thin section.

Petrographic Description of Sidewall Core Samples*

Drill Depth (feet	
3,064	Sandstone (arenite), gray, fine grained, well sorted, weakly compacted, subangular grains of quartz, plagioclase, calcite, potassium feldspar, diatoms, epidote, and opaques. Visual estimate of porosity is 20 to 30 percent.
3,102	Pebbly sandstone, gray, fine-grained sandstone matrix; arenite with rounded pebbles 2mm in diameter, moderately sorted, weakly compacted (grains in point contact with adjacent grains), subangular sand-size grains of quartz, plagioclase, calcite, and white mica. Rock fragments of tuffaceous mudstone. A second rock type is fine grained sandstone (wacke) with a red-brown clay matrix and abundant potassium feldspar.
3,199	Sandstone (arenite), very fine grained, well sorted, weakly compacted subangular grains of quartz, plagioclase, potassium feldspar, and diatoms; interbedded with very fine-grained sandstone (wacke) with red-brown clay matrix
3,450	Sandstone (arenite), fine grained, moderately sorted, subanglar grains of quartz and feldspar floating in tuffaceous matrix. Patches of tarry oil fills pore space in parts of sandstone chips.
4,350	Claystone, siliceous, brown, silty, laminated, rare diatoms.
5,054	Sandstone (arenite), fine grained, well sorted, grains of quartz and feldspar, weakly compacted, patches of tarry oil fills pore space; interbedded with siliceous siltstone.
5,253	Siltstone, siliceous, brown, tuffaceous.
5,820	Sandstone (subwacke), gray, fine grained, well sorted, weakly compacted, grains of quartz and feldspar floating in tuffaceous matrix. Matrix locally replaced by patches of calcite.
7,150	Porcelanite, dolomitic, brown.
9,410	Sandstone (subwacke), fine to medium grained, moderately sorted, quartz, feldspar and abundant foraminifers (large chambered forms). Framework tightly cemented by mixture of calcite and clay minerals. No visible porosity. Contains small rounded siltstone pebbles.
9,440	Sandstone (wacke), brownish gray, fine grained, moderately sorted, subround to subangular grains of quartz, feldspar,

chert, calcite, and mica cemented by a mixture of clay minerals, chlorite and possibly zeolite. Small patches of visible porosity within framework Small fractures may also be porous.

9,603 Sandstone (subwacke), fine to medium grained, well sorted, framework grains mainly volcanic rock fragments and chert, rare quartz and plagioclase. Grains tightly packed; fractures filled with secondary quartz. Possible fracture porosity. Cemented by grain contacts and pseudomatrix.

9,721 Sandstone (subwacke), medium grained, well sorted, grains mainly altered volcanic rock fragments, quartz, and plagioclase. Rock cemented by grain contacts and clayey pseudomatrix that is replaced in part by secondary calcite. Visible porosity is minimal.

10,310 Sandstone (arenite), grayish brown, fine grained, well sorted, quartz, plagioclase, altered volcanic rock fragments, mica, chlorite, and opaque minerals. Rare calcite and diatoms? Subangular grains cemented by grain contacts and pseudomatrix. Volcanic groundmass glass altering to chlorite. No visible porosity.

* Thin sections prepared by Mr. K. Bowlis, Denver Research Center, Marathon Oil Company.

CORE DESCRIPTION

ESCI
OCS CAL 78 164 NO. 1 (PT CONCEPTION COST WELL)

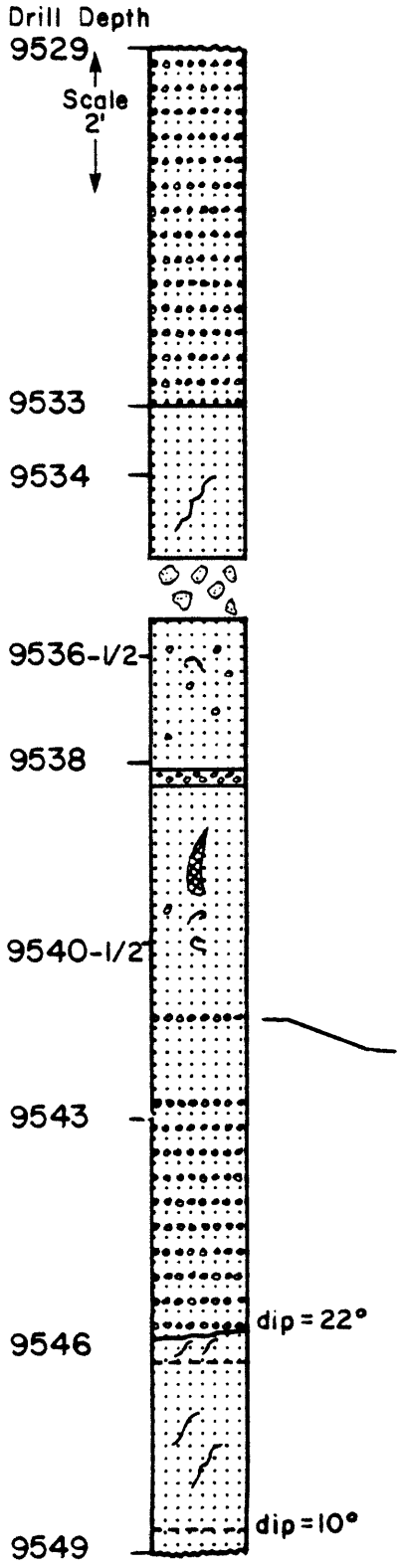

Pebble conglomerate, dark gray, grain supported, poorly sorted, well rounded clasts of gray, green and tan chert, and very fine grained metamorphic rocks 1 - to 3 cm in diameter. Matrix is pebbly fine-grained lithic sandstone with calcite cement.

Sandstone, gray, fine grained, moderately sorted, massive grains of rock fragments and feldspar. Calcite cement; fractures filled with crystalline calcite.

Core broken into several pieces.

Sandstone, gray, massive, fine grained. Contains pelecypod fragments and scattered pebbles of well rounded chert and sandstone 1 - to 2 cm in diameter.

Pebble conglomerate, massive, clasts up to 4 cm in diameter of subangular - to well rounded green and tan chert, and dark gray fine-grained lithic sandstone.

Sandstone, gray, fine grained, massive, fractures filled with crystalline calcite. Contains rare shell fragments.

Pebble conglomerate, matrix supported clasts of tan and gray chert and very fine grained metamorphic rocks, and dark gray fine-grained sandstone. Pebbles up to 3 cm in diameter.

Pebble conglomerate, poorly sorted, matrix supported, massive, well indurated, clasts of fine grained volcanic rock, chert, and fine-grained sandstone. Matrix composed of greenish black, fine-grained, weakly calcareous sandstone

Fractures filled with white crystalline calcite.

Sandstone, greenish black, fine grained, massive, well sorted lithic arenite with interbeds of black mudstone approximately 2 cm thick. Wavy contacts between sandstone and mudstone. Fractures filled with calcite and pyrite.

TABLE 2

DETRITAL MODES OF SANDSTONE CORE

DRILL DEPTH	Quartz (Q)	Feldspar (F)	Lithics (L)	C/Q	P/F	V/L	M/L	Qm/Q	Quartz	K-spar	Plagioclase	Volc. R. Frag.	Meta. R. Frag.	Chert	Mica	Hornblende	Pyroxene	Olivine	Epidote	Opaque	Sphene	Other (CO_3)	Other (Chlorite)	Matrix and/or Cement: Other (Garnet)	Calcite	Zeolite	Phyllosilicate	Matrix
9535.5-9536.5	59	23	18	.55	.90	.82	.10	.45	39	2	16	11	1	G	1	-	-	-	1	2		6	0					13
9538-9538.5	58	24	18	.74	.91	.94	. 6	.26	39	2	16	13	1	16	1	-	-	-	0	2		7	5					13
9540.5-9541.5	46	27	27	.63	.96	.94	. 4	.37	26	1	16	16	1	3	0				1	1				tr	35			
9548.3	30	19	51	.56	1.0	.99	. 1	.44	19	0	14	37	tr	3	1				1	2		1	4				18	

Petrographic description of rock fragments in pebble conglomerate.

Drill Depth

9529-9531

Granulite, greenschist facies, contains quartz chlorite, epidote, opaque mineral, sphene, and plagioclase.

Keratophyre (Na - rich meta volcanic) contains plagioclase, chlorite, calcite, opaques, and serpentine? minerals.

Volcanic porphyry.

Chert.

9531-9532.5

Meta quartz diorite, contains plagioclase, quartz, chlorite, opaques, and epidote.

Quartz keratophyre, contains plagioclase (albite), quartz, chlorite, opaques, and calcite.

Quartz - mica schist.

Chert.

9541.5-9543

Quartz keratophyre, contains plagioclase, chlorite, opaques, and quartz.

Spilite, contains albite, quartz, chlorite, epidote, opaques, and calcite.

Sandstone, fine grained subquartzose feldspathic arenite. (rip up clast ?)

Chert.

9543-9546

Spilite, contains albite, chlorite, and opaque mineral.

Andesite, holocrystalline, contains, plagioclase, chlorite and epidote.

Keratophyre.

Chert.

GEOLOGICAL AND GEOPHYSICAL IMPLICATIONS OF DENSITY AND SONIC LOGS

Larry A. Beyer
U.S. Geological Survey
Menlo Park, California

INTRODUCTION

This chapter analyzes the gamma-gamma density (FDC) and acoustic velocity (sonic) logs from OCS-Cal 78-164 No. 1 and discusses the implications of the density and velocity profiles derived from these logs. The log analysis procedure, density and velocity profiles, and selected published and unpublished data pertinent to the subsequent discussions are presented in the following section. Subsequent sections briefly discuss implications of these data for seismic and gravity exploration, lithologic and stratigraphic analysis, and porosity evaluation of the section penetrated by OCS-Cal 78-164 No. 1. All depths are referenced to the Kelly bushing on the derrick and are taken from the well logs. Thus, the sea floor is at a log depth of about 1,465 ft.

LOG ANALYSIS AND DATA PRESENTATION

Values of gamma-gamma density and interval transit time (reciprocal of velocity) were manually averaged over carefully chosen intervals. These intervals were selected only where, from examination of the caliper log and other considerations, the logging measurements were judged to be reasonably reliable. Although this approach is somewhat biased in favor of more competent rocks that did not cave off into the drill-hole, this approach does minimize the inclusion of erroneous density and interval transit time values. Biases are believed to be negligible below 5,700 ft and small between 3,500 and 5,700 ft. Above 3,500 ft utmost caution was used to choose a few intervals that mostly represent the coarser-grained rocks. Notable and possibly important gaps where caving of the drill-hole made density and(or) interval transit times unreliable occur from 3,265 to 3,510 ft, 5,730 to 5,800 ft, 7,600 to 7,900 ft, 9,480 to 9,520 ft, and 9,895 to 10,130 ft; porous sandstone is thought to occur within several of these intervals.

Errors in the gamma-gamma and sonic logs arise from three sources: Improper bearing of the logging tool pads against the formation due to drill-hole caving or mudcake build-up; formation damage by drilling fluids (especially important in clayey rocks in California); and improper calibration and operation of the logging device. The rudimentary but effective approach used here probably minimized errors due to drill-hole caving and improper calibration and operation of the logging devices. In most cases the long-spaced sonic log probably was not significantly affected by mud-

cake build-up or formation damage. Significant errors in the gamma-gamma density log may have resulted from formation damage to clayey intervals by drilling fluids and, to a lesser degree, from mudcake build-up especially at shallower depths. No independent means was available to directly check the accuracy of the gamma-gamma and sonic logs, because of the absence of substantive coring, a borehole gravity survey, or a well velocity survey. Comparisons with published data suggest that (1) the gamma-gamma log may have systematically underestimated densities of fine-grained rocks over certain intervals of the well by as much as 0.1 to 0.2 g/cm^3 and (2) the sonic log probably recorded reasonably accurate values over intervals where the drill-hole wall was relatively smooth.

Averaged interval transit times and densities are shown in Figures 1 and 2 together with depth scales referenced to the Kelly bushing (KB) and sea floor. The vertical columns of information near the left margin of these figures is discussed in the following section. In Figure 1 a velocity scale in ft/sec is provided across the bottom which corresponds to the scale of interval transit time across the top. Sonic log fluctuations are henceforth referred to as velocity variations. In Figure 2 five different porosity scales are given across the bottom; each corresponds to the bulk density scale across the top for the indicated grain density. Pore fluid was assumed to be 1.00 g/cm^3. With the use of Table 1, these porosity scales allow Figure 2 to be interpreted as a porosity versus depth illustration after selection of lithologic type.

In Figure 1 the dashed curve was included for comparative purposes; it is based on the average of many interview transit times measured at the tops of Pliocene, Miocene, and Oligocene horizons in a California basin and on the "typical compaction gradient of a California Tertiary basin" (Lang, 1978). In Figure 2 the envelope indicated by the letter A was taken from McCulloh (1967). The lower porosity (higher density) boundary of this envelope is "minimum porosity likely to occur in an argillaceous rock associated with a rock of probable maximum porosity " The higher porosity (lower density) boundary is "maximum probable porosity for most sedimentary rocks." Both boundaries are plotted relative to depth below sea floor for a grain density of 2.67 g/cm^3. Envelope A is based on laboratory measurements of more than 4,000 samples of conventional cores from the Los Angeles and Ventura basins and from other scattered localities in the United States, and the P Basin of Italy. Envelope B is the author's extension of envelope A to include diatomaceous mudstone and porcelaneous shale; it is based on hundreds of bulk-density measurements of conventional cores from wells located in the southwest part of the San Joaquin Basin. Envelope B is also shown relative to depth below sea floor Intervals marked with asterisks in both Figures 1 and 2 were reported to have had gas or oil shows.

Geophysical Implications

As shown in Figures 1 and 2, there is a general increase in velocity and density with depth. However, individual portions of the section show reversals of this trend and an unusually rapid step-like increase in

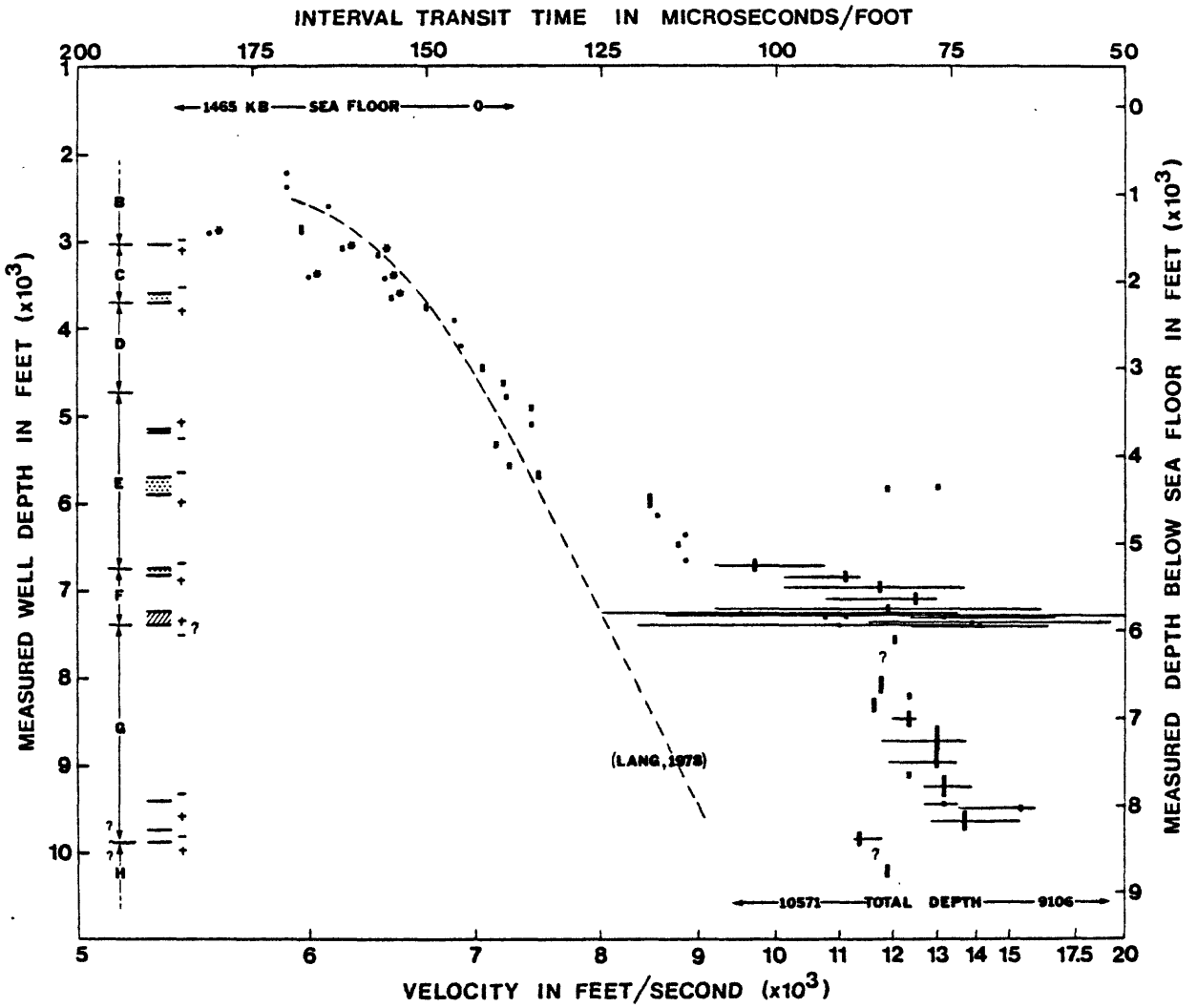

Figure 1. Selected interval transit times taken from the sonic log of OCS-Cal 78-164 No. 1. See text for explanation.

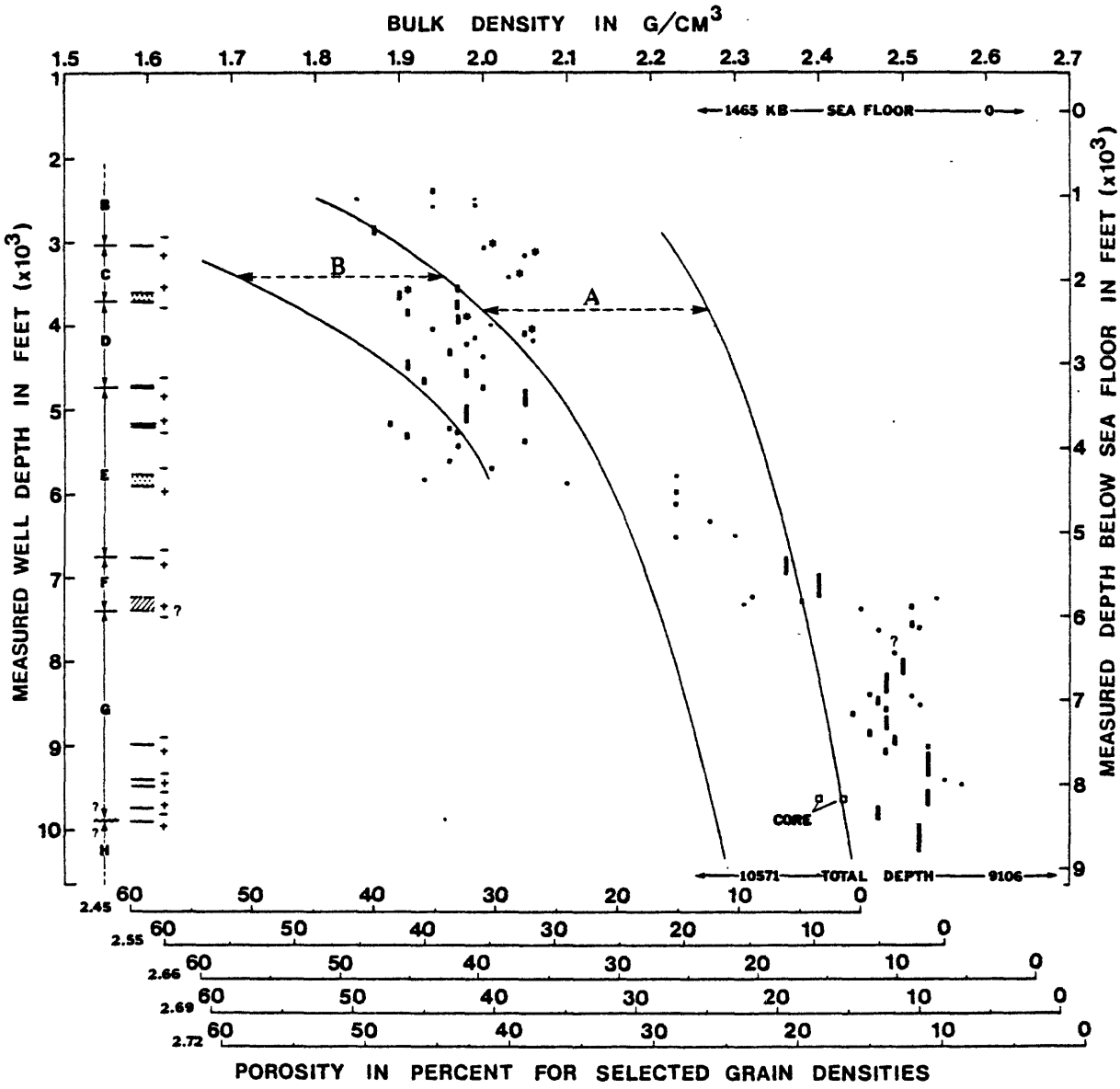

Figure 2. Selected interval densities taken from the gamma-gamma density log of OCS-Cal 78-164 No. 1. See text for explanation.

Table 1.--Typical grain densities for various lithologies of Tertiary marine sedimentary rocks of California (Beyer, Isaacs, McCulloh, unpublished data).

Grain Density (g/cm^3)	Lithologic Types
2.2 -2.3	siliceous rocks with silica as opal-CT and little clay or carbonate
2.3 -2.5	siliceous rocks with silica as opal-CT and some clay or carbonate. siliceous rocks with opal-CT and some quartz
2.5 -2.66	siliceous rocks with substantial proportions of quartz, clay or carbonate relative to opal-CT
2.66	typical "clean" California quartz sandstone; chert
2.66-2.72	lithic and(or) calcareous quartz sandstones; quartzose siliceous shale with carbonate and(or) clay
2.69	typical California marine claystone or clay shale
2.72	limestone

velocity and density occurs between 5,700 and 5,900 ft. Systematic changes in velocity and density are shown along the left side of Figures 1 and 2, together with the seismic-stratigraphic units B through H (McCulloch, Vedder, and Wagner, this report). In some cases the change in velocity or density is abrupt and is indicated by ———. In other cases the change is more gradual or fluctuates back and forth before becoming relatively constant at a higher or lower value (indicated by ⋯⋯). The symbols + over - indicate a downward decrease, while - over + indicates a downward increase, in the value of velocity or density across these boundaries. Many other velocity and density changes occur throughout the section but most of these involve changes of lesser magnitude, very thin intervals, or are unsystematic.

All relatively abrupt changes in velocity and density generate acoustic impedance (velocity times density) contrasts which, in turn, are the sources of reflections when seismic energy is transmitted through the section. Although the reflection seismogram is a display of the total and complex interaction of all perceptible reflections, prominent individual reflections should be correlative with known strong acoustic impedance changes. For example, the abrupt and large increases in velocity and density that occur between 5,700 and 5,900 ft and between 6,700 and 6,900 ft generate large acoustic impedance contrasts. These contrasts are believed to be the sources for the strong seismic reflections observed midway through unit E and at or near the base of unit E (Fig. 1b of McCulloch, Vedder and Wagner this report).

Transfer of other stratigraphic horizons from the well section to the seismic section is possible, though with less assurance in the absence of a more complete analysis. The lower part of seismic-stratigraphic unit F is composed of a sequence of thin beds between which there are large differences in acoustic impedance (diagonal pattern near left side of Fig. 1 and 2). This sequence may be the lowermost part of the section from which readily apparent and coherent reflections were obtained by McCulloch, Vedder, and Wagner (this report). The likelihood that acoustic impedance decreases at the base of unit F or in the upper part of unit G may partly explain why the deeper section is more acoustically opaque. However, sizeable acoustic impedance contrasts are associated with the sequence of sandstone between 9,450 and 9,740 ft and the reported unconformity at about 9,900 ft. Ideally mappable reflections might be obtained from this deeper part of the section as suggested by McCulloch, Vedder, and Wagner (this report).

The large density contrasts (0.4 to 0.5 g/cm^3) between the shallow and deep parts of the section in OCS-Cal 78-164 No. 1 is particularly important for the analysis of offshore gravity maps. Sizeable gravity gradients and anomalies should be found whenever the younger, lower density rocks are buttressed or faulted against the older, higher density rocks, or wherever there is considerable relief on pre-upper Miocene surfaces. For gravity modeling purposes, seismic sections can be used to estimate the depth to the large density increase. Density versus depth functions can be assumed for the shallow section and, after passage through the transition zone, a

higher constant density can be assigned to the deeper rocks. Another increase in density, probably in the range of about 0.2 to 0.3 g/cm^3, should occur upon passage from the lower part of the section into the underlying basment rocks.

LITHOLOGIC AND STRATIGRAPHIC IMPLICATIONS

Careful examination of systematic variations of density and velocity clarify or enhance lithologic and stratigraphic conclusions drawn from examination of the well logs, ditch cuttings, and well history. Starting in the upper part of the section and proceeding downward, variations in density (porosity) and velocity are discussed in terms of lithologic and stratigraphic significance. Only very tentative conclusions were possible above 3,500 ft because of the questionable reliability of the gamma-gamma and sonic logs in that part of the well.

Although reliable density and velocity data in the shallow part of the section are scarce, both velocity and density appear to be higher opposite coarser-grained beds than opposite finer-grained beds down to a depth of about 3,500 to 3,700 ft. Both density and velocity increase downward between 3,000 and 3,050 ft through the transition from predominantly silty claystone above to predominantly silty and conglomeratic sandstone below. This transition corresponds to the boundary between seismic-stratigraphic units B and C (McCulloch Vedder, and Wagner, this report). At a depth of about 3,510 ft, well logs indicate that the coarse-grained rocks of unit C begin to alternate with fine-grained rocks and, after a sequence of interbedded coarse- and fine-grained beds, are mostly underlain by fine-grained rocks at a depth of 3,700 ft. Over this transition from seismic-stratigraphic unit C to D the interbedded coarse-grained rocks also have higher densities than do the fine-grained rocks although no such unambiguous relationship seems to hold for velocities over this interval.

Between 3,700 and about 4,390 ft, density and velocity increase gradually (with minor fluctuations) as might be expected under the influence of normal compaction. From about 4 390 to 4,710 ft density is slightly lower. Ditch cutting suggest that this interval is less silty and, for the first time, biogenic siliceous debris is an important fraction of the rocks. Total organic carbon of ditch cuttings between 4,390 and 4,720 ft is slightly higher than in cuttings above and below this interval, possibly also contributing to a slightly lower density (Geochemical Service Report for OCS-Cal 78-164 No. 1). Hein et al. (this report) first describes opal-CT in ditch cuttings from 4,570 ft but does not report opal-CT in his next shallower sample from 4,150 ft. McLean (this report) describes "rare diatoms" in a claystone from a drilled depth of 4,350 ft. Based on these facts and the onset of lower densities, significant amounts of siliceous material may occur as high, or higher than, 4,390 ft in the well. Densities from this interval lie indisputably within envelope B (Fig. 2) which indicates that these rocks have porosities characteristic of siliceous mudstone or shale. This stratigraphic interval may be equivalent to the lowest part of the Foxen Mudstone. The Foxen Mudstone is described in the Santa Maria Basin by Woodring and Bramlette (1950, p. 37-38) as containing thin layers of diatomaceous shale and abundant phosphatic pellets, particularly where the formation is thin.

From about 4,710 to 5,150 ft densities are higher and ditch cuttings indicate that this interval is slightly more silty than adjacent overlying and underlying clay-rich rocks. The level of natural gamma radiation is lower and quieter downward from about 4,710 ft, as shown by the gamma-ray log. This also can be interpreted as a systematic decrease downward in the relative abundance of clay. The boundary between seismic-stratigraphic units D and E is placed at 4,760 ft (McCulloch, Vedder and Wagner, this report). Velocity increases gradually and fairly uniformly from about 3,700 to 5,170 ft and appears to be generally insensitive to the density and lithologic changes described over this part of the section.

From about 5,150 to 5,350 ft, densities and velocities are somewhat lower. Ditch samples indicate that this interval is dominated by siliceous mudstone and shale with some porcelaneous shale. From 5,350 to 5,710 ft density and velocity increase, decrease and increase again in a vaguely systematic fashion. Ditch samples indicate that this interval contains siliceous shale and mudtone, porcelaneous shale including the first minor amounts of thinly laminated porcelanite, and minor thin beds of dolomite and(or) tightly cemented sandstone. Individual excursions of both density and velocity to higher values between 5,150 and 5,710 ft probably are caused by interbeds of porcelaneous shale or porcelanite, and by thin interbeds of dolomite or tightly cemented sandstone where unusually high density is noted. Between 5,710 and 5,880 ft there is a pronouned increase in velocity and density; very high velocities and high densities alternate with somewhat lower values. Drilling rate slows markedly at about 5,770 ft, indicating that the rocks increase in hardness. Ditch cuttings suggest that sandstone and dolomite beds together with some siliceous units are present in this interval. Below 5,880 ft densities and velocities are relatively high and never return to the lower values observed above 5,710 ft.

The large increase in density and velocity from 5,710 to 5,880 ft probably is caused by a combination of lithologic and diagenetic factors. thinly laminated porcelanite first appears in substantial quantity in ditch cuttings from 5,740 to 5,770 ft. Slightly darker colored, more clay-rich siliceous shale and mudstone decrease in abundance from about 5,300 ft downward until little is observed in cuttings from 5,830 to 5,860 ft. The first few cuttings of banded chert and a few pieces of dolomitic porcelaneous shale appear in ditch samples from 6,010 to 6,130 ft. Individually or in combination these mineralogic and lithologic changes increase density and velocity. The large increase in density and velocity also mean that porosity sharply decreases. Diagenetic transformation of the silica from the opal-CT phase to the quartz phase might cause such a decrease in porosity (Isaacs, 1979).

Another substantial increase in density and velocity occurs between 6,700 and 6,8000 ft in the vicinity of the boundary between seismic-stratigraphic units E and F (McCulloch, Vedder, and Wagner, this report). Chert becomes abundant in ditch cuttings at this depth and the well logs indicate that the chert probably is interbedded with porcelanite and(or) siliceous shale. Between 7,250 and 7,412 ft (base of seismic-stratigraphic unit F), density and velocity fluctuate between high and low values over

short vertical intervals; the electric and gamma-ray logs behave similarly. Beds displaying relatively high electrical resistivity, density, and velocity together with relatively low gamma radiation, may be dolomitic porcelaneous shale or dolomite, both of which appear in ditch cuttings. Beds displaying relatively low electrical resistivity, density, and velocity together with relatively high gamma radiation presumably are more clayey or organic-rich shales. Oil-stained fracture surfaces on ditch cuttings and the presence of some fracture-filling sparry calcite among the cuttings attest to the existence of fractures in this interval. The stratigraphic interval between 7,250 and 7,412 ft is very distinctive. This interval may be lithologically equivalent to the carbonate-rich, fractured shale oil resrevoir in the lower part of the Monterey Shale in the Lompoc oil field described by Dolman (1932).

Density and velocity are not especially diagnostic below 7,412 ft, except to assist in the delineation of distinct rock intervals deeper in the section. Density and velocity are clearly higher in the sequence of sandtone between 9,410 and 9,735 ft. Density and velocity are conspicuously lower in the underlying sequence that extends to about 9 000 ft where the base of the seismic-stratigraphic unit G is placed. At about 9,900 ft a major unconformity exists between Miocene and Lower Cretaceous or Upper Jurassic strata (McCulloch, Vedder, and Wagner, this report). Below 9,900 ft density and velocity increase slightly although caving of the drill-hole between 9,895 and 10,130 ft precludes information from that interval.

POROSITY IMPLICATIONS

A quantitative study of sandstone porosity in OCS-Cal 78-164 No. 1 was not undertaken because of the paucity of conventional cores and lack of independent means for evaluating the accuracy of the gamma-gamma and sonic logs[1]. However, several general inferences about sandstone porosity can be drawn from comparisons of the velocity and density profiles with the average transit time curve (dashed line, Fig. 1) and the predicted range of porosities for rocks from the Los Angeles and Ventura basins (envelope A, Fig. 2). Values of interval transit time from OCS-Cal 78-164 No. 1 generally cluster along the average transit time curve down to a well depth of about 5,700 ft (Fig. 1). These values increase much more rapidly between 5,700 and 7,400 ft, and appear to parallel the average curve but at higher velocities below 7,400 ft (Fig 1). Values of interval density from OCS-Cal 78-164 No. 1 behave in a similar way with respect to envelope A in

---

[1] The porosity and permeability of two conventional and nine sidewall core samples were determined by Core Laboratories, Inc., and are shown in Table 2. The porosity values for the conventional cores are plotted in Figure 2. Measurements of physical properties of sidewall samples must be viewed with extreme caution because of possible physical damage caused by mud or filtrate invasion and percussion (Fertl and others, 1971). For this reason, porosity measurements of sidewall samples were not used in this study.

Table 2 . Lithologic descriptions and porosity and permeability measurements of conventional and sidewall core samples from OCS-CAL 78-164 No. 1 made by Core Laboratories, Inc.

Lithology	Depth (feet)	Porosity (percent)	Permeability (md)
		Conventional Core Samples	
sd; gy, vfgr, vslty, sl calc	9536	15.8	0.07
sd; gy, vf-fgr, vslty, pbls, sl calc	9541	17.9	0.23
		Sidewall Core Samples	
sd; gy, fn grn, sl calc	3064	30.5	494
sd; gy, vf-fgr, sl calc	3102	30.9	685
" " " " " "	3199	34.0	253
" " " " " "	3650	31.3	551
sd; gy, vfgr, sl calc	5054	28.0	345
sd; gy, vfgr, sl slty, sl calc	10222	22.1	9.6
sd; gy, vfgr, vslty, calc	10310	24.3	0.04
sd; gy, vf-vcgr, slty, shy, calc	10318	24.8	1.1
siltstone; gy, vfgr, sdy, calc	10353	22.0	4.2

Figure 2. However, bewteen about 4,400 and 5,700 ft densities lie firmly within envelope B because the rocks are highly siliceous and porous. From these comparisons, it is clear that the acoustic velocity and porosity (or density) trends from Lang (1978) and McCulloh (1967) do not adequately describe the section penetrated by OCS-Cal 78-164 No. 1.

Porosities of sandstone units that occur above 5,700 ft fall within the higher porosity region of envelope A (Fig. 2). The range of porosities for these upper sandstone units may be predicted from the range of sandstone porosities that occur over the same burial depths in the Los Angeles and Ventura basins. In these latter basins normal marine clastic deposits have undergone similar burial histories (no unloading). However, if true, this conclusion may be due to a fortuitous set of circumstances (McCulloh, pers. commun.). The unusually high geothermal gradient (McCulloh and Beyer, this report) may have tended to accelerate porosity-reducing diagenesis (Lowry, 1956).

Sandstone porosities in the deeper part of the section appear to be lower than, or near the end of, the range of porosities predicted by envelope A Organic matter is less abundant and of a different type in the deeper part of the section (Claypool et al., this report; McCulloh, this report) and accelerated porosity-reducing diagenesis due to the high geothermal gradient may not have been inhibited by organic matter.

These hypotheses are admittedly simplistic and ignore the many other factors that are known to affect porosity (McCulloh, 1967). The Pliocene and Holocene sections from which Lang (1978) and McCulloh (1967) drew their conclusions generally are thicker than the Pliocene and Holocene section at the OCS-Cal 78-164 No. 1 well. As a consequence, rocks in the deeper part of the Point Conception well are older than most rocks at comparable depths in portions of the Los Angeles and Ventura basins where no uplift and unloading have taken place. This age difference may, in part, explain the lower porosities in the Point Conception well. Also, geothermal gradients in the California areas studied by Lang and McCulloh are presently lower than, and may never have been as high as, the present geothermal gradient in OCS-Cal 78-164 No. 1 (Lee and Henyey, 1975). Important insights might result from comparisons with sandstone porosities in the Santa Maria Basin where the geothermal gradients are similar to that in OCS-Cal 78-164 No. 1. Such data was not available for this study.

The shale section of the Point Conception well could form potential petroleum reservoirs. This is indicated by the well-documented occurrence of fractured shale reservoirs in the Santa Maria Basin (Regan, 1953), the abundance of shale relative to sandstone in OCS-Cal 78-164 No 1, and by reports in the driller's log of oil and tar on fractured surfaces of ditch cuttings. The stratigraphic interval from 7,250 to 7,412 ft is most likely to contain fractured shale zones, based on an examination of the driller's log, well logs, and ditch cuttings. Although it is not possible to assess the extent or magnitude of fracture porosity development between 7,250 and 7 412 ft, the potential for oil reservoirs in fractured shale in the offshore region of OCS-Cal 78-164 No. 1 is substantial.

REFERENCES CITED

Dolman S. G., 1932, Lompoc oil field, Santa Barbara County: California Oil Fields, Summary of Operations, v. 17, no. 4., p. 13-19.

Fertl, W. H., Cavanaugh, R. J., and Hammack, G. W., 1971 Comparison of conventional core data, well logging analysis, and sidewall samples: Journal of Petroleum Technology, December 1971, p. 1409-1414.

Isaacs, C. M., 1979, Lateral diagenesis in Monterey Shale, Santa Barbara Coast, California (abs.): American Association of Petroleum Geologists Bulletin, v. 63, no. 3, p. 473.

Lang, W. H., Jr , 1978, The determination of prior depth of burial (uplift and erosion) using interval transit time: Annual Logging Symposium of Society of Professional Well Log Analysts, 19th, June 13-16, 1978, El Paso, Texas, Trans., p. B1-B17.

Lee, T., and Henyey, T. L., 1975, Heat flow through the southern California borderland: Journal of Geophysical Research, v. 80, no. 26, p. 3733-3743.

Lowry, W. D., 1956, Factors in loss of porosity by quartzose sandstones of Virginia: American Association of Petroleum Geologists Bulletin, v. 40, no. 3, p. 489-500.

Maxwell, J. C., 1964, Influence of depth, temperature and geologic age on porosity of quartzose sandstone: American Association of Petroleum Geologist Bulletin, v. 48, no. 5, p. 697-709.

McCulloh, T. H., 1967, Mass properties of sedimentary rocks and gravimetric effects of petroleum and natural-gas reservoirs: U.S. Geolgoical Survey Professional Paper 528-A, 50 p.

Regan, L. J., Jr., 1953, Fractured shale reservoirs of California: American Association of Petroleum Geologists Bulletin, v. 37, no. 2, p. 201-216.

Woodring, W. P., and Bramlette, M. N., 1950, Geology and paleontology of the Santa Maria district, California: U.S. Geological Survey Professional Paper 222, 185 p.

WELL LOG CROSS PLOTS

S. E. Prensky
U.S. Geological Survey
Los Angeles, California

INTRODUCTION

A standard suite of electric and geophysical logs (with the exception of proximity log) was run on the Pt. Conception OCS-Cal 78-164 No. 1 well by Schlumberger Ltd. for petrophysical analysis and dip determinations. A lithology log ("mud-log") was made by Exploration Logging Inc. Log quality was good, except in intervals where washouts of the hole resulted in unusuable data The major intervals where hole washout occurred are 2,725 to 2,788 ft, 3,250 to 3,510 ft, 9,950 to 10,010 ft, and 10,058 to 10,071 ft measured depth. Several shows of oil appeared on the lithology log between the intervals 3,400 to 4,100 ft and 5,100 to 5,850 ft measured depth. All depths listed in this report are measured depths from RKB. thus, the sea floor is at a drill depth of 1,465 ft (RKB 37 ft above sea level plus water depth of 1,428 ft).

ROCK CHARACTERISTICS

Preliminary determination of petrophysical characteristics was made using the digitized magnetic tapes of the Dual-Induction Laterolog, Compensated Neutron-Formation Density log and the Borehole Compensated Sonic log. The U.S. Geological Survey's version of Scientific Software Corporation's general log calculation software package LOGCALC was used. The well was drilled to a depth of 10,571 ft and calculations were made from 1,930 to 10,563 ft depths.

Rock characteristics were determined for six major intervals selected on the basis of dominant lithologic components as shown on the lithology log. Table 1 summarizes the data for these six intervals (age data is based on electric log information). In addition to the gross lithologic intervals representative points were selected for lithology determination through cross-plot analysis of the data. The MID (matrix identification) and M-N lithology plots use the following data sonic log interval transit time (Δ_t), density log bulk density (ρ_b) and neutron log porosity on limestone units (ϕ_{Nls}) (Burke, Campbell, and Schmidt, 1971). Table 2 summarizes these data. The point numbers for data in Table 2 correspond to the point numbers in Figures 1 and 2.

Neutron log and sonic log data for the interval 1,930 to 5,400 ft (indicated by the data in Tables 1 and 2) reflect the high degree of undercompaction of the rock. Consequently these values are considered unreliable and if plotted on the MID or M-N crossplots would fall in the shale region.

Table 1. Summary of Interval Rock Characteristics (porosities are in per cent calculated for a sandstone matrix ρ_m 2.65 gm/cc Δt_m 55.5 μsec/ft, n represents the number of values used in determining the mean)

Depth (feet)	Age	Lithology	ρ_b	n	ϕ_D	n	ϕ_N	n	Δt	n	ϕ_S	n
1,930-3,700	Quaternary	ss,sh	1.93	1706	44.4	1772	55.7	1772	173	1727	—[1]	—[1]
3,701-6,760		ss,sh,ls	2.08	3041	34.8	3056	47.5	3056	127	3047	—[1]	—[1]
3,655-4,300	Pliocene	ss,sh,ls	2.00	645	39.2	646	56.3	645	144	643	—[1]	—[1]
4,301-6,760	l. Plio. u. Miocene	ss,sh,ls	2.09	2442	33.8	2456	45.4	2455	123	2447	—[1]	—[1]
5,400-7,420	u. Miocene	ss,sh,ls	2.16	1345	29.8	1361	40.7	1361	114	1361	35.1	361
6,760-7,420	m. Miocene	ss,sh,ls, chert	2.40	661	15.2	661	23.5	661	82	661	18.0	661
7,421-8,010	m. Miocene	sh,ls	2.41	589	14.6	590	27.5	590	88	590	24.0	590
8,011-9,450	m. Miocene	limey siltstone	2.50	1440	9.3	1440	25.8	1440	81	1439	19.1	1440
9,451-10,563		ss,sh	2.45	1103	12.1	1098	31.0	1096	83	1100	22.2	1082
9,451- 9,979	m. Miocene	ss,sh	2.48	529	10.0	528	27.9	524	82	524	21.3	523
9,980-10,563	Jurassic-L. Cret.	ss,sh	2.41	574	14.1	570	33.8	572	85	574	23.0	559

[1] Data from neutron log and sonic log considered unreliable due to undercompaction

Table 2. Summary of Rock Characteristics for Individual Data Points for Cost 78-164 #1 Well (density in gm/cc; sonic log travel time Δt in μsec/ft; neutron porosity in percent).

Point No.	Log Run	Depth	Lithology[1]	ρ_b	ρ_{ma}	Δ_t	Δ_{tma}	ϕN ss	ϕN ls	M	N
1	1	2,030	Mudstone	2.02	—	181	—	54.3	51.5	0.077	0.477
2		2,204	Siltstone	1.92	--	178	--	57.8	55.2	0.089	0.530
3		2,353	Sandstone	1.78	—	192	—	49.7	46.5	-0.032	0.543
4		2,456	Sandstone	1.99	--	161	--	46.9	43.6	0.225	0.579
5		2,609	Sandstone	2.00	—	165	—	54.5	51.6	0.239	0.482
6		2,763	Siltstone	2.00	—	181	--	50.8	47.7	0.079	0.524
7	1	2,904	Siltstone	1.85	—	166	—	64.1	61.8	0.268	0.441
8	2	3,110	Siltstone	1.97	--	168	--	56.3	53.5	0.216	0.480
9		3,240	Tuff	1.92	--	170	—	48.9	45.7	0.205	0.592
10		3,587	Siltstone, calcareous	1.89	--	165	--	51.5	48.4	0.273	0.583
11		3,639	Siltstone	1.95	—	156	—	57.7	55.0	0.352	0.475
12		3,815	Siltstone, calcareous	1.96	--	150	--	57.4	54.7	0.407	0.472
13		3,904	Siltstone, calcareous	2.33	—	90	—	38.9	35.0	0.746	0.490
14		4,060	Siltstone	2.01	—	149	—	59.9	57.4	0.398	0.422
15		4,101		2.20	--	136	--	58.8	56.2	0.444	0.364
16		4,305	Siltstone	1.95	—	145	—	60.5	58.1	0.463	0.440
17		4,550	Siltstone	1.98	--	137	—	50.0	46.8	0.529	0.544
18		4,700	Siltstone	1.99	—	113	—	51.2	48.1	0.771	0.525
19		4,900	Siltstone	2.04	--	139	--	51.1	48.0	0.479	0.502
20		5,032	Siltstone	2.02	2.72	138	—	43.9	40.4	0.479	0.585
21		5,190	Siltstone	1.86	--	143	--	50.1	47.0	0.540	0.619
22	2	5,400	Siltstone	1.94	—	96	—	49.4	46.2	0.990	0.571
23	3	5,463	Siltstone	2.29	2.80	90	46.6	35.5	31.4	0.769	0.532
24		5,512	Siltstone	1.93	—	142	—	45.2	41.8	0.505	0.627
25		5,735	Siltstone	2.21	--	127	--	46.4	43.1	0.509	0.471
26		5,801	Mudstone, calcareous	2.23	2.71	76	44.5	31.5	27.4	0.917	0.589
27		5,822	Mudstone, calcareous	1.94	—	87	42.2	41.3	37.6	1.085	0.662
28		6,150	Siltstone, calcareous	2.24	2.84	123	—	40.5	36.7	0.530	0.511
29		6,431	Siltstone, calcareous	2.23	2.71	107	—	31.3	27.1	0.673	0.595
30		6,600	Siltstone, calcareous	2.41	2.81	99	61	30.7	26.5	0.640	0.523
31		6,751	Siltstone, calcareous	2.23	2.85	108	--	41.2	37.5	0.657	0.507
32	3	6,880	Siltstone	2.43	2.68	86	65.5	16.7	12.4	0.725	0.614
33		6,967	Mudstone	2.42	2.75	80	45.0	25.1	20.8	0.767	0.557
34		7,040	Mudstone	2.43	2.67	81	62.0	15.2	11.0	0.758	0.623
35		7,100	Siltstone	2.41	2.73	83	49.2	23.2	18.9	0.758	0.577
36		7,230	Siltstone	2.42	2.84	92	50.1	32.5	28.3	0.685	0.505
37		7,260	Siltstone	2.44	2.67	115	--	14.9	10.7	0.515	0.622
38		7,330	Siltstone	2.20	2.67	96	56.0	29.9	25.7	0.775	0.621
39		7,370	Siltstone	2.28	2.66	79	50.5	23.2	18.9	0.862	0.634
40		7,414	Siltstone, calcareous	2.36	2.81	98	54.6	32.7	28.5	0.668	0.527

Table 2. Summary of Rock Characteristics for Individual Data Points for Cost 78-164 #1 Well--Continued

Point No.	Log Run	Depth	Lithology[1]	ρ_b	ρ_{ma}	Δt	Δt_{ma}	ϕN ss	ϕN ls	M	N
41		7,510	Siltstone, calcareous	2.50	2.72	70	50.6	16.9	12.7	0.795	0.581
42		7,770	Siltstone, calcareous	2.22	2.69	94	54.0	30.4	26.2	0.778	0.607
43		7,920	Siltstone, calcareous	2.53	2.82	78	47.8	25.4	21.1	0.723	0.513
44		8,200	Siltstone, calcareous	2.50	2.84	79	46.5	28.8	24.6	0.732	0.504
45		8,390	Siltstone, calcareous	2.44	2.76	82	51.3	24.5	20.2	0.742	0.553
46		8,615	Siltstone, calcareous	2.44	2.76	82	52.0	24.5	20.2	0.742	0.553
47		8,800	Siltstone, calcareous	2.47	2.80	84	50.6	26.7	22.4	0.715	0.529
48		9,050	Siltstone	2.48	2.78	75	47.3	24.8	20.5	0.773	0.539
49		9,230	Siltstone	2.52	2.79	74	47.6	22.7	18.4	0.758	0.536
50	3	9,264	Siltstone	2.54	2.82	72	46.3	24.5	20.2	0.761	0.520
51	4	9,405	Siltstone	2.51	2.83	82	49.0	26.9	22.6	0.710	0.511
52		9,480	Sandstone, calcareous	2.59	2.75	65	49.1	14.6	10.4	0.779	0.565
53		9,505	Sandstone, calcareous	2.41	2.68	66	43.7	18.5	14.2	0.870	0.609
54		9,724	Sandstone, calcareous	2.56	2.81	77	49.1	23.2	18.9	0.719	0.519
55		9,923	Siltstone	2.48	2.88	76	43.6	32.9	28.7	0.767	0.482
56		10,100	Siltstone	2.30	2.66	72	47.5	21.5	17.2	0.900	0.636
57		10,190	Siltstone	2.55	2.91	81	45.7	31.4	27.3	0.697	0.468
58		10,279	Siltstone	2.51	2.73	74	52.7	17.4	13.1	0.758	0.574
59		10,348	Mudstone, calcareous	2.60	2.63	61	52.0	8.5	4.7	0.803	0.596
60		10,497	Mudstone, calcareous	2.18	2.67	94	53.5	30.8	26.6	0.805	0.624
61		10,535	Siltstone	2.40	2.79	90	52.0	29.6	25.4	0.708	0.535

[1] From McLean, this report

Figure 1. Matrix Identification Plot (Form Copyright by Schlumberger, Ltd.)

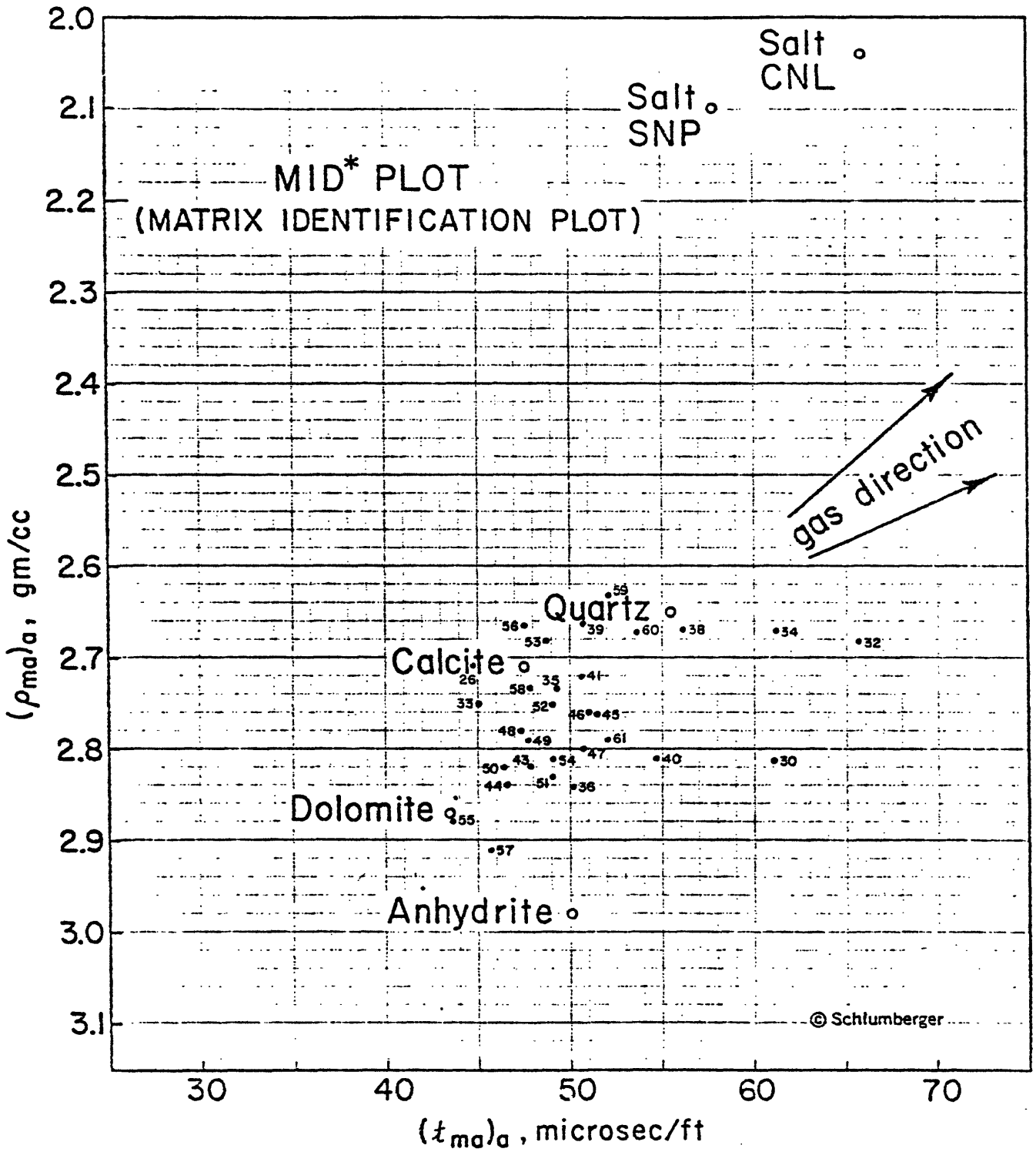

Figure 2. Porosity and Lithology Determination, M-N Plot (Form Copyright by Schlumberger, Inc.)

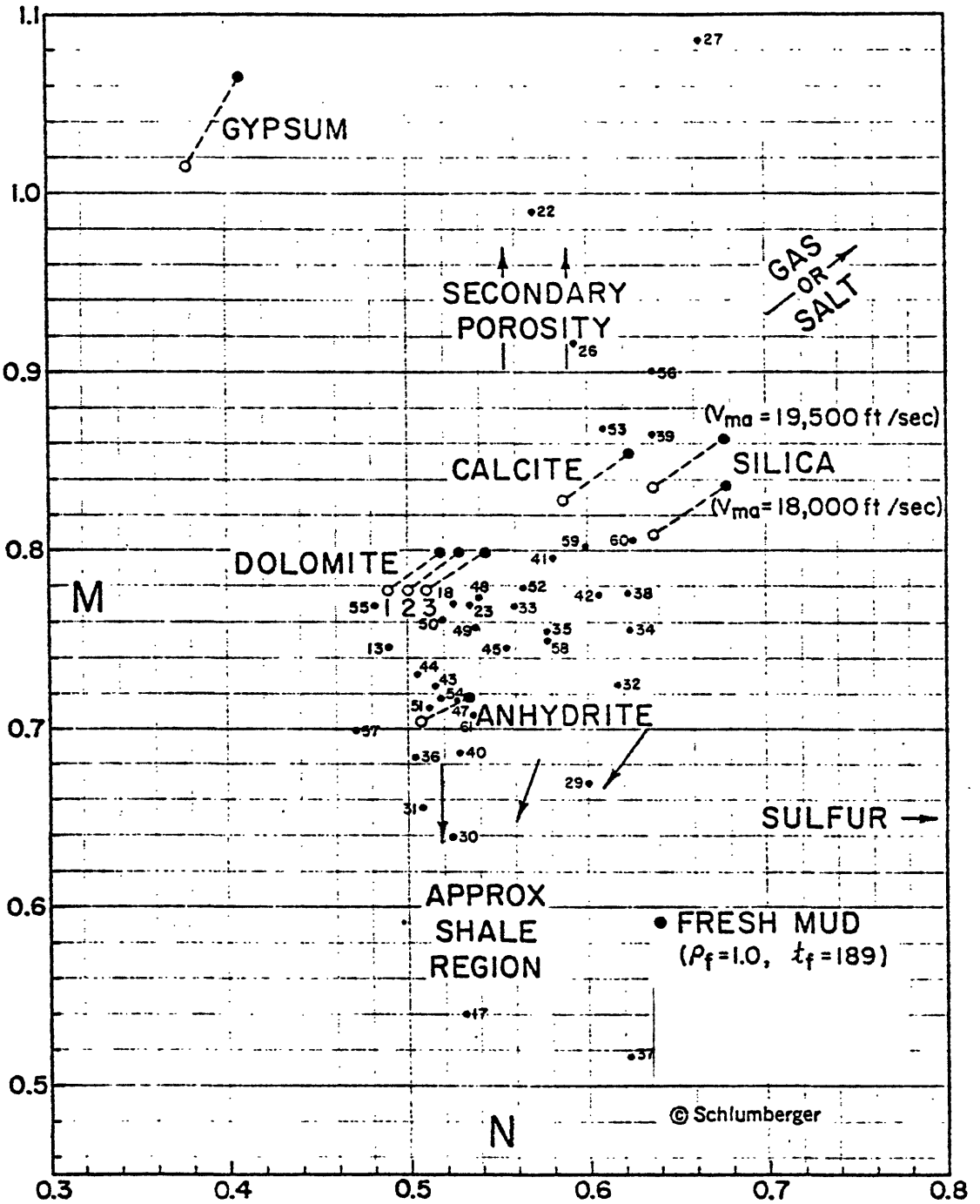

This crossplot may be used to help identify mineral mixtures from Sonic, Density, and Neutron logs. (The Neutron log used in the above chart is the CNL*.) Except in gas-bearing formations, M and N are practically independent of porosity. They are defined as:

$$M = \frac{t_f - t}{\rho_b - \rho_f} \times .01 \qquad N = \frac{(\phi_N)_f - \phi_N}{\rho_b - \rho_f}$$

Points for binary mixtures plot along a line connecting the two mineral points. Ternary mixtures plot within the triangle defined by the three constituent minerals. The effect of gas, shaliness, secondary porosity, etc. is to shift data points in the directions shown by the arrows.

The dolomite lines are divided as to porosity as follows:

1) ϕ = 5.5 to 30 p.u. 2) ϕ = 1.5 to 5.5 p.u. and ϕ > 30 p.u. 3) ϕ = 0 to 1.5 p.u.

Table 3. Dipmeter Survey Summary

Depth (feet)	Age	Lithology[1]	Dip (Degrees)	Direction	Comments
3,000-3,600	Quaternary	ss,sltst	2-8	S-SE	
3,600-4,200	Pliocene	calc. sltst			Random
4,200-4,800	l. Plio.-u. Mio.	ss,sltst	1-6	SE	
4,800-5,090	u. Miocene	ss,sltst	1-4	E-SE	
5,090-5,750		calc. ss,sltst	1-4	NE-E	
5,800-6,900	u.-m. Mio.	ss,sh,chert	3-8	NE-E	
6,900-7,140	m. Miocene	sltst,chert	2-8	SW-SE	
7,140-7,580	m. Miocene	calc. sltst	4-10	NW-NE	
7,580-8,200		calc. sltst,ss	6-12	E	
8,200-9,260		calc. sltst,ss	9-13	N-NE	
9,260-9,370		sltst,ss	8-14	E	
9,370-9,520		sltst,ss	6-10	N-NE	
9,520-9,600		ss	18-22	N	
9,600-10,100	Jurassic-L. Cretaceous	ss,sltst,mdst	--		Random Possible structural change at 9,650
10,100-10,380		ss,sh	18-22	SE	
10,380-10,450		ss,sh	--	NE-E	

[1] From McLean, this report

OIL SHOWS

This well contained the first shows of oil encountered in the series of "COST" wells drilled since 1975. These shows are of particular significance since each well location is selected for position geologically off-structure where such shows of hydrocarbons would be least likely. The best shows occur in sand units at 3,410 to 3,420 ft, 3,550 to 3,620 ft; limestone stringers at 3,875 to 3,880 ft, 3,902 to 3,905 ft, 4,032 to 4,038 ft, 4,100 to 4,102 ft, 5,790 to 5,810 ft; shale 5,050 to 5,450 ft.

DIPMETER ANALYSIS

The Schlumberger Four-Arm Resolution Continuous Dipmeter survey was run between 3,006 to 10,544 ft. Dip readings were recorded on a dipmeter arrow plot. Table 3 summarizes the data for the regional dip for the interval surveyed.

REFERENCES CITED

Burk, J. A., Campbell, R. L., Jr., and Schmidt, A. W., 1971, The litho-porosity cross plot: a method for determining rock characteristics for computation of log data, in Well Logging: Society of Petroleum Engineers Reprint Series No. 1, p. 271-299.

X-RAY MINERALOGY AND DIAGENESIS

J. R. Hein, E. Vanek and Mary Ann Allen
U.S. Geological Survey
Menlo Park, California

INTRODUCTION

The Point Conception deep stratigraphic test well is located on the outer continental shelf about 19 miles west of Point Conception in southern California (see McCulloch et al., this report, Fig. 1a). The drilling site was located in 1,428 ft of water and the well was drilled to a depth of 10,571 ft below the derrick floor (derrick floor was 37 ft above sea level). This paper describes the X-ray mineralogy of 47 samples between drill depths of 2,180 and 10,571 ft. Samples are composite core cuttings from 30-foot intervals. Sample numbers in the tables represent the stratigraphic level (in feet) at the top of each 30-foot interval studied. Depth below the seafloor is obtained by subtracting 1,465 ft (37 + 1,428) from the sample depth. We also discuss aspects of diagenesis that are based on interpretations of the X-ray data.

Methods

Four sets of X-ray data are presented: general, clay, silica, and carbonate mineralogies. A Norelco diffractometer with Cuka radiation set at 40 kv and 20 ma, a curved-crystal carbon monochrometer, and theta compensating slit was used in the X-ray work.

To obtain general mineralogy, splits of samples were powdered and run from 4° to 60° 2θ at 1°/min. Electronic settings were the same for all samples. Peak heights for the major minerals are recorded in Table 1. Numbers are peak heights relative to a scale of 100 for each mineral within each sample. Values for each mineral can be compared down section. Qualitative impressions of relative mineral abundances can be gained from Table 1. Weighting factors must be used for quantitative work (Schultz, 1964).

Clay mineralogy was determined on rock cuttings that were disaggregated by an ultrasonic probe. Techniques of sample preparation and clay mineral identification have been discussed by Hein et al. (1976). A brief outline of the procedure follows: carbonate and organic matter are removed by Morgan's solution (sodium acetate plus glacial acetic acid diluted with distilled water) and 30% hydrogen peroxide respectively. The < 2 m size fraction is isolated by centrifugation. This clay-size fraction is Mg-saturated and glycolated, an X-ray diffractogram being taken after each treatment. Clay mineral percentages are calculated from measurements of peak areas. Biscaye's (1965) weighting factors are used in calculating the percentages of kaolinite, chlorite, illite and smectite/illite, which are summed to equal 100 percent. In general, percentages are reproducible

Table 1.--Relative Intensity of Peak Heights from X-ray Diffractograms
For OCS-Cal 78-164 No. 1 Well

[1]Numbers represent mole % $MgCO_3$ in the protodolomite and calcite.

[2]Mostly from McLean, Lithologic Descriptions, this volume.

[3]Numbers represent relative intensities on a scale of 100.

[4]Contamination by mica added to drilling mud.

x=present, s/s=sandstone, qtz=quartz, m/s=mudstone

Sample No.	Quartz	Plagioclase	K-feldspar	Protodolomite	Calcite	Clay Minerals	Pyroxene	Pyrite	Others	Quartz / Feldspar	Plagioclase / K-feldspar	Mole % [1] $MgCO_3$	Lithology [2]
2180	90[3]	90	54		20	10	10			.63	1.67		siltstone with shell fragments
2240	93	90	25		17	12	13			.81	3.60		s/s. silty with shell fragments
2300	93	56	19	94		6	12			1.24	2.95	47.5=P	s/s, silty, calcareous, shell fragments
2360	93	40	18	94		2	10			1.60	2.22	49.0=P	s/s, silty, calcareous, forams
2420	55	19	19	83	32	4			apatite?8	1.45	1.00	44.0=D? 0.0=C	s/s, silty, calcareous, forams
2480	84	28	19	94	13	2				1.79	1.47	42.0=D? 0.0=C	s/s, silty, calcareous, forams
2540	92	53	22	79	19		x		apatite?	1.23	2.41	45.0=P 0.0=C	siltstone, calcareous, forams
3180	77	16	16	28	10	4			apatite?	2.41	1.00		pebbly m/s, calcareous
3250	100+	28	32		10			10	apatite?	1.67	.88		s/s, well sorted, sub-rounded
3700	68	22	16	65	8		x?			1.79	1.38		siltstone, calcareous
3790	95	48	39	98	11				mica*[4]	1.09	1.23		mica, siltstone, calcareous
3880	17?	17?		90	8				mica*	1.00			mica & dolostone
3970	21?	39	17	98	20				mica*	.54	2.29	42.0=P 1.0=C	mica, siltstone, calcareous

3970A									amphibole				reddish-brown grain
4060	53	26	16	70	46	8		9		1.29	1.56		siltstone, calcareous
4150	38?	51	16	100						.57	3.19	46.0=P	siltstone, calcareous
4570	80	20	10	40		4		5	opal CT-14	2.67	2.00		siltstone, calcareous
4750	78	21	14	11		5	11?	8	apatite?10 opal CT-22	2.23	1.50		siltstone
5110	78	50	18	100		5	8		opal CT-10?	1.15	2.78		siltstone, calcareous, minor s/s
5200	57	28	33	54		3	8	8	apatite?10 mica* opal CT-40?	.93	.85		siltstone, calcareous, minor s/s
5290	72	34	28	100		7			opal CT-22	1.16	1.21	45.0=P	siltstone, calcareous, minor s/s
5380	80	31	21	77		15	9	9	apatite-11 opal CT-31	1.54	1.48		siltstone, calcareous, minor s/s
5380A	43	26	17			7			apatite-10	1.00	1.53		siltstone
6100	100++	14	10	24	6	9		4	apatite-5	4.17	1.40		siltstone, calcareous
6190	100+	13	9	41	5	6		4	apatite-5	4.55	1.44		siltstone, calcareous
6280	79	20	14	91		6		14	apatite-14	2.32	1.43		siltstone, calcareous
6370	100	17	11		11	10		8	apatite-10	3.57	1.55		siltstone, calcareous
6640	100	14	10	51	10	8		7	apatite-8	4.17	1.40		siltstone, calcareous, minor s/s
6730	100+	12	7?	71		5		6		5.26	1.71		siltstone, calcareous, minor s/s
7000	100	12		9	17				opal CT-9?	8.33			m/s, calcareous, chert, minor s/s, tar
7090	100+	6?		74				16	mica*?	16.67		44.0=P	siltstone, calcareous, sandy, minor chert, tar
7270	100			100+									siltstone, calcareous, sandy, minor chert, tar
7360	100+	9?	9?	100+		3		8	apatite?8	5.56	1.00	47.5=P	siltstone, calcareous, s/s chert
7450	98	12	9	95		2		11	apatite?6	4.67	1.33		siltstone, calcareous, sandy, chert
7810	74	15	7?	54		12		19	apatite?16	3.36	2.14		silstone, calcareous, sandy, minor chert, qtz s/s
8440	98	70		36	49	11		14		1.40			siltstone, calcareous,sandy, some are rounded

8530	98	18	9?	77	51	8		9	apatite?2	3.63	2.00	44.0=P 1.0=C	siltstone, calcareous, tar
8620	92	23	11	63	60	2		8	apatite?7	2.71	2.09		siltstone, calcareous, minor qtz s/s
8710	98	22		92	25	5		6		4.45			siltstone, calcareous
8800	90	25		95	31	2		9		3.60			siltstone, calcareous, minor qtz s/s
9070	77	11	6?	98	6			6		4.53	1.83		siltstone, calcareous, minor qtz s/s with calcareous cement
9160	100	26		48	21	7		9	apatite?3	3.85			siltstone, calcareous, qtz s/s with calcareous cement
9250	100	29	9?	53	18	11		8		2.63	3.22		siltstone, calcareous, qtz s/s with calcareous cement
9340	100	20	9	82	46	1		7		3.45	2.22	42.0=P 2.0=C	siltstone, calcareous, qtz s/s
9430	95	26		40	55	8		7	pyroxene? apatite-3	3.52			siltstone, calcareous, qtz s/s with calcareous cement minor chert, a few pyrite cubes
10,330	100	16			41	12		6		6.25			siltstone, s/s, m/s, chert - some are rounded, some grains are sheared and polished.
10,330A	73	33			68	5			pyroxene?	2.21			rounded chert granules within calcareously cemented qtz s/s
10,330B	76	19			29	18				4.00			m/s, dark grey, polished & a green grain
10,420	100	22		11	18	12		4?	pyroxene-7	4.55		44.0=P 1.0=C	m/s, dark grey, chert, minor s/s and pyrite cubes
10,420A	98	39			12	19	6	7		2.51			s/s, greenish grey, well sorted
10,510	95	18	10?		40	25	6	3		3.39	1.80		m/s, grey, polished & minor s/s, chert
10,510A	100	45		32		14	7	10	rhodochro-site?8	2.22			s/s, green and brown grains
10,510B	100	22				25	6		rhodochrosite ?5 pyroxene?6	4.55			m/s, grey
10,540	84	18			47	27	5		rhodo?8 pyroxene?5 apatite?2	4.67		42.0=P 2.0=C	siltstone, sandy, green s/s & minor chert
10,540A	100	29				24	5		rhodochrosite ?5 pyroxene?5	3.45			siltstone, grey

to within three percentage points of the values given. Percentages of chlorite and kaolinite are obtained by a slow scan of the 24° to 26° 2θ region (Biscaye, 1964). Other minerals, however, often mask the clay mineral peaks in this region, or the distinction between the two minerals may not be clear, so kaolinite plus chlorite values are also listed in Table 2. Illite crystallinity (Y, Table 2) is measured as the ratio of the 10 A peak width at mid-height to the peak height. "X" in Table 2 represents the percent expandable layers (smectite) in the smectite/illite mixed layer phase. Discrete smectite (100% expandable) was not detected

Silica mineralogy is presented for four porcelanites from the 4,750 to 5,380-foot section (Tables 1 and 5). Cristobalite d-spacings were determined by the technique of Murata and Larson (1975). Cristobalite crystallite sizes were measured perpendicular to d(101) by the technique of Scherrer (described in Klug and Alexander, 1954). Silica polymorph terminalogy is adopted from Jones and Segnit (1971). Percentages of quartz and opal-CT (Table 5) were determined by peak heights and were summed to equal 100 percent.

Assuming no interference from noncarbonate reflections, the mole percent $MgCo_3$ (includes $FeCO_3$ and $MnCo_3$) was determined by measuring the 2θ shift in the calcite (or dolomite) peaks and comparing the values with calibration curves of Goldsmith, Graf, and Heard (1961) and Goldsmith and Graf (1958). This technique has an accuracy of about 1 mole percent. A silicon standard was used to measure d-spacings precisely for both the silica and carbonate mineralogies.

Results

General mineralogy

Quartz, feldspar, and protodolomite (discussed below) are the dominant minerals overall (Table 1). Locally, calcite, apatite, and opal-CT are abundant. Clay minerals are a significant fraction only in the Mesozoic section (below 10,000 ft). Pyroxene occurs in many samples, and pyrite is a widespread but minor component. Rhodochrosite appears in the Mesozoic section below 10,420 ft. Mica, abundant in several samples, is a contaminant that was added to the drilling mud when the well reached 3,300 ft (Table 1).

In general, the rocks become more mineralogically mature with depth in the section. Quartz is the dominant mineral at depth; plagioclase and K-feldspar decrease signficantly, K-feldspar becoming uncommon below 7,700 ft and essentially disappearing below 9,000 ft. Protodolomite decreases in the lowermost units, while, as mentioned, clay minerals increase and rhodochrosite appears.

Although considerable variability occurs for each mineral, there are several stratigraphic horizons where statistically significant changes occur for all major minerals. The best defined change occurs somewhere between 5,410 and 6,100 ft, an unsampled interval. This level may be near

Table 2--Clay Minerology for OCS-Cal 78-164 No. 1 Well

[1]X=percent expandable layers in the smectite/illite mixed layer phase

[2]Y=illite crystallinity

dash=indeterminate

[3]9070-10,540 feet have 0-30% expandable clay component in the mixed layer phase

[4]illite masked by muscovite

Sample No.	Kaolinite & Chlorite (%)	Kaolinite (%)	Chlorite (%)	Illite (%)	Smectite/ Illite (%)	Others	X[1]	Y[2]
2180	17	6	11	43	39		55	.76
2240	31	-	-	36	33	halloysite?	65	.31
2300	28	13	15	39	33	palygorskite	57	.33
2360	23	12	11	31	46	laumontite?	63	.42
2420	23	13	10	41	36		64	.48
2480	22	-	-	45	33		50	.61
2540	21	14	8	45	34	palygorskite laumontite?	56	.43
3180	10	-	-	37	53	halloysite	84	.41
3700	10	6	4	43	47	halloysite, palygorskite, mixed layer clays	88	.31
3790	11	-	-	64[4]	25	muscovite	65	.15
3880	27	-	-	73[4]	0	muscovite	-	.09
3970	10	7	3	74[4]	16	muscovite	65	.12
4060	11	6	5	37	52	palygorskite, mixed layer clay	60	.32
4150	11	-	-	36	53	palygorskite	63	.20
4570	4	-	-	56	40	halloysite, palygorskite, mixed layer	75	.35

4750	6	4	2	61	33	palygorskite	75	.45
5110	15	12	3	35	51	halloysite, mixed layer clays	49	.38
5200	15	11	4	44	41	halloysite, palygorskite	50	.32
5290	18	6	12	55	27	halloysite, laumontite?, mixed layer clays	58	.26
5380	12	10	2	52	36	palygorskite, halloysite, mixed layer clays	59	.33
6100	30	24	6	44	26		52	.37
6190	21	16	5	50	29	palygorskite, mixed layer clays	55	.47
6280	12	8	4	44	44		57	.52
6370	12	-	-	48	39		51	.47
6640	10	10	0	59	31	mixed layer clays	70	.16
6730	17	17	0	63	20	palygorskite	62	.31
7000	44	44	0	46	10	halloysite	-	.40
7090	22	17	4	38	40		77	.63
7270	26	18	8	69	5?		-	.50
7360	13?	13	0	87	0		-	.56
7450	18	14	4	48	34		70	.50
7810	31	0	31	49	21		70	.24
8440	37	11	26	50	13		60	.34
8530	50	-	-	47	3?		60	.37
8620	51?	15?	36?	49?	Tr		-	.26
8710	44	13	31	56	Tr	laumontite?	0-30	.29
8800	50	-	-	43	8		65?+ 0-30	.13

9070	41	9	32	59	-[3]		0-30	.52
9160	64	54	10	36?	-		0-30	.80
9250	71	-	-	29	-		0-30	.63
9340	55	-	-	45	-		0-30	.35
9430	45	12	33	55	-	vermiculite?	0-30	.32
10,330	61	0	61	39	-		0-30	.48
10,420	54	0	54	46?	-		0-30	.46
10,510	63	24?	39?	37	-		0-30	.32
10,540	53	0	53	47	-		0-30	.29

the Pliocene-Miocene boundary, but does not contain age diagnostic fossils (Bukry, this report; McDougall, et al., this report). Below this unsampled interval quartz increases significantly relative to feldspar (see quartz/feldspar ratios, Table 1), however, the plagioclase/K-feldspar ratios are remarkably uniform both above and below the 5,410 to 6,100-ft stratigraphic level. Although the relative abundance of the two feldspars changes across this interval, they change by the same magnitude, which is not true for quartz and feldspar. There is also a large increase in kaolinite + chlorite below this interval (see next section).

Changes in many minerals occur at various horizons within the stratigraphic interval from 3,730 to 4,570 ft (Table 1). This encompasses the boundary between Pliocene rocks and rocks that do not contain age diagnostic fossils (Bukry, this report; McDougall et al., this report). This stratigraphic interval also represents a transition zone from middle to lower bathyal depositional environments occurring above to lower bathyal or deeper environments below (McDougall et al., this report). All major minerals, including clay minerals, change through this interval (Tables 1 and 2), and the lower boundary (4,570 ft) marks the top of the porcelanite (opal-CT) section.

A third level, defined by changes only in authigenic minerals, occurs in the middle Miocene section in the interval 8,620 to 8,710 ft. Here, protodolomite increases whereas calcite, and to a lesser extent pyrite, decrease.

Tar and oil

Pretreatment of rocks with H_2O_2 for clay mineralogy indicated several stratigraphic zones of abundant organic matter (tar and oil). Five samples especially reacted vigorously, almost violently, with the H_2O_2 treatment: 3,700, 4,570, 4,750, and 6,730. The uppermost three rocks occur within the zone (3,400-5,800 ft) stated by McLean (this report) to contain oil and tar. The lowest two samples, however, occur below this zone, and thus suggest a larger stratigraphic occurrence of oil and tar. These lower occurrences also lie just above a chert-rich section which may correspond to the Monterey Formation. Within the chert-rich Monterey-like section per se, tar was seen with the binocular microscope in samples 7,000, 7,090, and 7,270; a petroleum odor was noted by McLean (this report) from samples from this section. Deeper in the section, tar was noted in samples 8,530 and 9,340.

Clay mineralogy

The clay mineralogy averaged over the entire section is 30 percent, 47 percent, and 30 percent respectively for kaolinite + chlorite, illite, and smectite/illite (Table 3). Statistically signficant changes in clay minerals, however, occur down section (Tables 2 and 3). Kaolinite + chlorite fluctuates between 10 and 25 percent down to about 6 200 ft, then, on the average, increases to the bottom of the hole. Significant step increases are shown in Table 3. Kaolinite is most abundant between 6,100

Table 3--Basic Statistics of the Stratigraphic Distribution of Clay Minerals for the OCS-Cal 78-164 No. 1 Well

Kaolinite & Chlorite				Illite				Smectite/Illite			
Sample Nos.	Mean %	Standard Deviation	No. of Samples	Sample Nos.	Mean %	Standard Deviation	No. of Samples	Sample Nos.	Mean %	Standard Deviation	No. of Samples
2180 to 2540	24	4.61	7	2180 to 4150	39	4.43	11	2180 to 2540	36	4.82	7
3180 to 5380	11	4.44	9	4570 to 6640	50	7.77	11	3180 to 5200	46	7.46	8
6100 to 6190	26	6.36	2	6730 to 7360	61	19.35	5	5290 to 6640	33	6.72	7
6280 to 6730	13	2.99	4	7450 to 10,540	46	7.83	16	6730 to 8800	14	13.34	11
7000 to 8440	28	10.86	7								
8530 to 10,540	54	8.72	13								
All Samples	30		43	All Samples	47		43	All Samples	30		34

and 8,800 ft, the same section where quartz greatly increases relative to feldspar. Chlorite increases markedly below about 8,000 ft (Table 2).

Illite content remains relatively constant throughout the section. An apparent small increase in illite between 6,700 and 7,400 ft is not statistically significant because of its great variability (Tables 2 and 3). Illite, however, does seem to increase slightly below about 4,200 ft (Table 3).

On the average, smectite/illite increases down to about 5 300 ft then decreases to the bottom of the hole; however, there is a tremendous variability in the smectite/illite content (Tables 2 and 3). Below 8 600 ft smectite/illite content is uniform, being characterized by a low percent of expandable smectite layers. Percentages of smectite/illite cannot be listed in Table 2 for this lowermost section because a complete range of mineralogic compositions exist from discrete illite to smectite/illite with about 30 percent expandable layers, which makes the diffractions difficult to interpret.

Unlike the great variability in the smectite/illite content over narrow stratigraphic intervals, the amount of expandable layers ("X", Table 2) in the mixed layer phase is uniform within relatively wide stratigraphic intervals (Table 4). The average "X" and "Y" value for the entire section is 63 percent and 0.35 respectively.

Statistically significant changes in several clay minerals occur at three stratigraphic levels. First, below the unsampled interval of 2,570 to 3,180 ft, kaolinite + chlorite decreases, smectite/illite increases, and the percent expandable layers in the mixed layer phase increases. This stratigraphic interval encompasses the Quaternary-Pliocene boundary (Bukry, this report; McDougall _at al._, this report), and the area where the first gas shows occurred (McLean this report). The second interval where significant changes in clay minerals occur is from about 3,700 to 4,600 ft, which is the same interval, discussed above, where significant changes occur in the nonclay fraction. The third major change occurs between 8,600 and 9,080 ft, where the smectite/illite content dramatically changes, as do the "X" and "Y" values. This interval occurs about 200 ft below the stratigraphic level where major changes in the nonclay fraction occur.

Although laumontite was not detected in the general mineralogy, at the higher power range used for clay mineralogy, a 9.3° 2θ(9.4 Å) peak showed up on several diffractograms (Table 2). As 9.4 Å is the primary spacing for laumontite we tentatively list it in Table 2. There is apparently no stratigraphic or lithologic control on laumontite occurrence, which is found sporadically from about 2,300 to 8,600 ft.

Silica mineralogy

Opal-CT bearing rocks (porcelanite?) occur through the interval 4,750 to 5,410 ft (Table 5). A sample occurring lower in the section (7,000 ft) contains a very small amount of opal-CT and was most likely contaminated by

Table 4--Basic Statistics of the Stratigraphic Distribution of the Amount of Expandable Layers (X) in the Smectite/Illite Phase and of Illite Crystallinity (Y) for the OCS-Cal 78-164 No. 1 Well

[1] illite masked by muscovite

X				Y			
Sample Nos.	Mean %	Standard Deviation	No. of Samples	Sample Nos.	Mean	Standard Deviation	No. of Samples
2180 to 2540	59	5.56	7	2180	.76	0.00	1
3180 to 3700	86	2.83	2	2240 to 3700	.41	.10	8
3790 to 4150	63	2.36	4	3790 to[1] 3970	.12	.03	3
4570 to 4750	75	0.00	2	4060 to 7000	.35	.10	15
5110 to 6370	54	3.87	8	7090 to 7450	.55	.06	4
6640 to 8800	67	6.02	8	7810 to 8800	.27	.08	6
				9070 to 9250	.65	.14	3
				9340 to 10,540	.37	.08	6
All Samples	63		31	All Samples	.39		46

Table 5--X-ray Characteristics of Opal-CT
OCS-Cal 78-164 No. 1 Well

[1]Exact spacing masked by the 4.256 Å spacing of quartz.
[2]Measured perpendicular to d(101) using Scherrer's equations described in Klug and Alexander (1954).

Sample No.	Quartz (%)	Opal-CT (%)	Cristobalite d(101) (Å)	Cristobalite d(200) (Å)	Cristobalite Crystallite[2] Size (Å)	Tridymite (Å)
4750	68	32	4.0602	2.4933	76.40	-[1]
5200	59	41	4.0693	2.4893	86.15	-
5290	65	35	4.0620	2.4913	86.15	-
5380	76	24	4.0565	2.4980	77.86	-

rocks from upsection. The opal-CT section probably occurs near the Pliocene-Miocene boundary (Bukry, this report; McDougall et al., this report).

Opal-CT d(101) spacings commonly range from about 4.12 to 4.05 Å (Murata and Nakata, 1974; Murata and Larson, 1975; Hein et al., 1978); thus, our values, all near 4.06 Å, are near the smaller d-spacing end of this range (Table 5). This suggests that the Point Conception samples are relatively well ordered and may be near the temperature necessary for transformation to quartz (Fig. 1). The size of the crystallites, 76 to 86 Å [perpendicular to d(101)], that make up the opal-CT are also near the upper end of the size range (40 to 81 Å) described by Hein et al. (1978), further indicating a late stage of opal-CT diagenesis (Table 5).

If the chert-rich interval between about 6,800 and 7,500 ft is the Monterey Formation then only the quartz-rich lower part of the formation is represented; the opal-A (diatomite) and opal-CT (porcelanite) upper sections are not present. The opal-CT section at 4,750 to 5 410 ft probably represents part of a Pliocene porcelanite-bearing formation.

Carbonate mineralogy

Protodolomite is a common constitutent down to about 9,400 ft (Table 1). It always contains excess $CaCO_3$ (1.0 to 8.0 mole %) relative to ideal dolomite and has broad, low amplitude ordering peaks (Table 1). Calcite, commonly occurring with protodolomite, is consistently a low-magnesium variety (0.0 to 2.0 mole % $MgCO_3$).

The origin of the low-magnesium calcites is probably biogenic carbonate, foraminifers, nannofossils, mollusks, etc. Fragmented mollusk shells were seen with a binocular microscope in samples ranging down to about 2,570 ft. Biogenic calcite most commonly has a low $MgCO_3$ content. The stratigraphic interval from about 4,000 to 8,000 ft was noted by the paleontologists (Bukry, this volume; McDougall et al., this volume) not to contain many calcareous microfossils; this is the interval where few samples contain calcite (Table 1).

The protodolomite is probably a cement for the sandstones and siltstones found throughout the section. The origin of the protodolomite is not as easily explained as the calcite. Several possibilities exist for the sources of Ca, Mg, and C: (1) dissolution of biogenic calcite provides Ca, C; (2) alteration of volcanic ash provides Ca, Mg; (3) alteration of ferromagnesium mineals provides Mg; (4) dissolution of plagioclase provides Ca; (5) bacteriogenically or thermocatalytically produced CO_2 provides C (6) sea water provides Mg. Without carbon and oxygen isotopic analysis of the protodolomite, the origin of its constitutent elements cannot be determined. Alteration of ash probably did not supply much Ca and Mg because the main product of ash alteration--clay minerals, especially smectite--are not common in the Point Conception section. Thus, the magnesium must have been derived from alteration of ferromagnesium minerals and from Mg-rich interstitial waters. If protodolomite was an early diagenetic phase then a sea water source for the Mg is most likely.

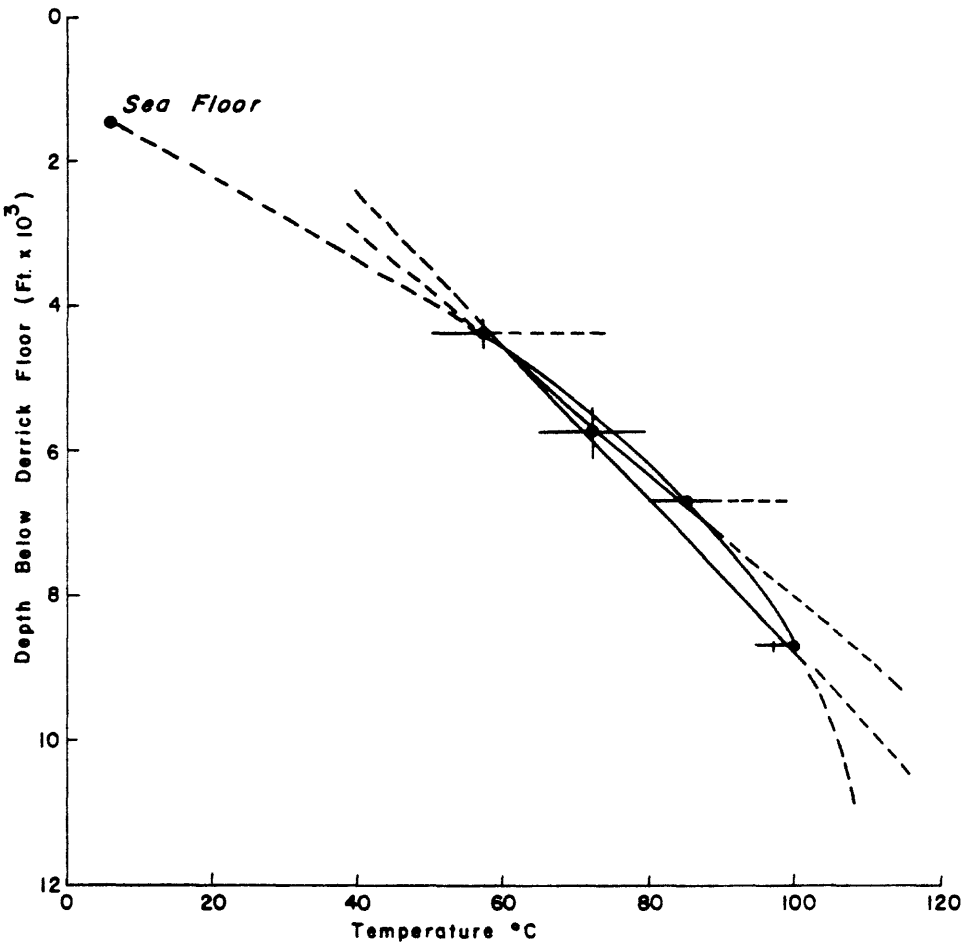

Figure 1. Depth-temperature curves determined from temperature controlled diagenetic mineral transformations. The upper three points are from silica mineral transformations and the stratigraphically lowest point from clay mineral changes. The points on the error bars that the curves are drawn through are favored interpretations of the data on the basis of all the mineralogic data presented here and on our experience with other similar section.

DISCUSSION

There is a great deal of variation in the mineralogy of rocks from the Point Conception well. Variations appear to occur randomly on a small scale as well as with discernable trends with depth. Diagenesis, source area changes, and variations in lithologic types account for these changes. Much of the local, small-scale variations are probably due to different mixtures of lithologic types in the core cuttings. Analysis of single lithologic types downsection would no doubt give a clearer picture of the mineralogy and of the mechanisms that cause the changes.

Major changes occurring for many minerals over a certain interval may reflect variations in source areas, for example, those changes that occur near the Quaternary-Pliocene boundary and the Pliocene-Miocene boundary discussed earlier. Significant deepening or shoaling of the depositional environment could produce similar sweeping mineralogical changes.

We wish to emphasize diagenetic changes here, however, and to use the diagenetic changes in the minerals as geothermometers in order to construct a depth-temperature curve for the section. Most mineralogic transformations deep in the section are obviously due to diagenesis because the changes span an unconformity at about 10,000 ft that separates middle Micoene from Early Cretaceous rocks. In fact, no significant mineralogic variations occur across this greater than 100 m.y. hiatus, providing striking evidence that diagenesis is the controlling influence on mineralogy below at least about 8,500 to 9,000 ft. The best defined changes that can be attributed to diagenesis are the loss of K-feldspar, probably by dissolution, and the increase in the illite component of the smectite/illite phase. Similar changes have been noted from deep wells in the Gulf Coast and other areas (for example, Perry and Hower, 1970, 1972). At high temperatures, illite forms at the expense of smectite, the potassium needed for illite genesis being derived from K-feldspar dissolution (Perry and Hower, 1970, 1972). A decrease in expandable layers to about 30 to 40 percent occurs near a temperature range of about 95° to 100° C and is accompanied by an increase in ordering of the mixed layer phase. This mineralogic transformation occurs at a depth of about 8,600 ft in the Point Conception section (Fig. 1).

Mineralogic transformations of silica polymorphs are mainly temperature controlled. Opal-A (biogenic silica) is transformed to poorly ordered opal-CT (porcelanite) over a temperature range from about 35° to 55° C, depending partly on the amount of clay fraction in the rocks, and on the amount of time lapsed before initiation of the transformation (for a detailed discussion see Hein et al., 1978). Considering the ordered character of Point Conception opal-CT and assuming that the first occurrence is at about 4,300 ft, temperature limits can be estimated for this stratigraphic level (Fig. 1). Similarily, temperature constraints can be placed on the last occurrence of opal-CT (Table 1 and Fig. 1).

The transformation from opal-CT to microcrystalline quartz (chert) is

initiated at a temperature of about 80° C (Murata et al., 1977). Thus, temperature constraints for the first occurrence of the Monterey chert sequences can also be estimated (Fig. 1).

Several possible depth-temperature curves can be constructed using the four mineralogically determined temperature estimates (Fig. 1): (1) a straight line connecting the three points determined from silica mineralogy (2) a straight line connecting the point determined from clay minerals and two of the silica points; and (3) a curve connecting our four points with the 6° C temperature of the sea floor where the well as drilled. These curves agree reasonably well with curves constructed by Beyer and McCulloh (this report) by correcting the unadjusted temperatures taken from headings of well logs. However, the curve connecting our data with the sea floor temperature, when projected deeper than 9,000 ft gives a much shallower geothermal gradient than do Beyer and McCulloh's corrected curves. Our curve should also give a slightly steeper gradient down to about 4,500 ft.

REFERENCES CITED

Biscaye P E., 1964, Distinction between kaolinite and chlorite in recent sediments by X-ray diffraction: American Mineralogist, v. 49, p. 1281-2189.

_____ 1965, Mineralogy and sedimentation of recent deep sea clay in the Atlantic Ocean and adjacent seas and oceans: Geological Society of America Bulletin 761. p. 803-832.

Goldsmith, J. R., and Graf, D. L., 1958, Relocation between lattice constants and composition of the Ca-Mg carbonates: American Mineralogists v. 43, p. 84-101.

Goldmsith, J. R., Graf, D. L., and Heard, H. C., 1961, Lattice constants of calcium-magnesium carbonates: American Minerlogists, v. 46, p. 453-457.

Hein, J. R., Scholl, D W. and Gutmacher, C E., 1976, Neogene diatomaceous sediment from the far northwest Pacific and southern Bering Sea, in Bailey, S. W., ed., AIPEA Proceedings, 1975 International Clay Conference, Mexico City: Applied Publishing Ltd., Illinois, p. 71-80.

Hein, J. R., Scholl, D. W., Barron, J. A , Jones, M. G., and Miller, Jacquelyn, 1978, Diagenesis of late Cenozoic diatomaceous deposits and formation of the bottom simulating reflector in the southern Bering Sea: Sedimentology, v. 25, p. 155-181.

Jones, J. B., and Segnit, E. R., 1971, The nature of Opal 1. Nomenclature and constituent phases: Journal of

Klug, H. P., and Alexander L. E., 1954, X-ray diffraction procedures: John Wiley and Sons, Inc., New York.

Murata, K. J., Friedman, I., and Gleason, J. D., 1977, Oxygen isotope relations between diagenetic silica minerals in Monterey Shale, Temblor Range, California: American Journal of Science, v. 277, p. 64-65.

Murata, K. J., and Larson R. R., 1975, Diagenesis of Miocene siliceous shales Temblor Range, California: U.S. Geological Survey Journal of Research v. 3, p. 553-566.

Murata, K. J., and Nakata, J. K., 1974, Cristobalite stage in the diagenesis of diatomaceous shale: Science, v. 184, p. 567-568.

Perry E. A., and Hower J., 1970, Burial diagenesis in Gulf Coast pelitic sediments: Clays and Clay Mineralogy, v. 18, p. 165-177.

_____ 1972, Late-stage dehydration in deeply buried pelatic sediments American Association of Petroleum Geologists Bulletin, v. 56, no. 10, p. 2013-2021.

Schultz, L. G., 1964, Quantitative interpretation of mineralogical composition from X-ray and chemical data for the Pierre Shale: U.S. Geological Survey Professional Paper 391-C 31 p.

SEDIMENT CHEMISTRY

D. Z. Piper and B Fowler
U.S. Geological Survey
Menlo Park California

INTRODUCTION

Thirty-six samples from Point Conception well have been analyzed by X-ray fluorescence for the ten major oxides (Table 1). All sample numbers represent drilled depths starting at the derrick floor. Thus, the sea floor is at a drilled depth of 1,465 ft (derrick floor to sea level is 37 ft plus water depth of 1,428 ft). Samples were washed, dried at 110°C, mixed with a flux in a sample to flux ratio of 0.85 to 0 15, and pelletized. Analytical accuracy is better than 8% for all determinations and is usually better than 5%. Several of the samples however, were contaminated by drill-bit fragments and mica used in the drilling mud. Although organic carbon values for individual samples were not available for this report, eight organic carbon analyses of composite samples, each from a depth interval of approximately 400 ft and at a spacing of 1,000 ft, were made by Claypool et al. (this report) and have been included (Table 3) for comparison with the major oxide analyses. The major oxide concentrations were averaged over these same intervals to permit comparison with the organic carbon values. Although the two sets of samples were taken from the same depth intervals, they do not come from the same drill cuttings

The major oxides are present in marine sediment largely as lithogenic material. Lesser amounts are present as exchangeable ions. Iron and manganese may be present also as amorphous metal oxides (iron may also occur as pyrite). CaO and SiO_2 might be present as biogenic $CaCO_3$ and silica and/or sparry calcite and chert respectively (McLean, this report). Carbon, nitrogen, and phosphorus accumulate in the sediment as organic detritus.

During diagenesis these elements may behave quite differently. Most of the nitrogen is returned to the water column during early diagenesis as NH_3. Some of the phosphorus may be trapped in the sediment as fluoroapatite, or possibly incorporated in $CaCO_3$. The organic carbon retained in the sediment is present as one of several substances (Claypool et al., this report). The largest fraction of metals, that incorporated within the lithogenic phase, is relatively non-reactive during diagenesis. Thus, the relation between the distributions of these elements may elucidate the nature of sediment diagenesis. Although we observe several interesting elemental relations for the samples from this well, we require more analyses to ascertain the significance of these trends.

Table 1

Major Oxide Composition of Samples from Point Conception COST Well No. 1. Concentrations are in Percent.

	(Quaternary)							(Pliocene)				
Depths (ft)	2180-2210*	2300-2330	2360-2390	2420-2450	2480-2510	2540-2570	Av.	3790-3820	3880-3910*	3970-4000	4150-4180	Av.
SiO_2	40.05	34.61	36.52	36.68	38.12	38.59	36.90	41.54	39.25	31.75	30.77	34.69
Al_2O_3	22.87	8.00	6.71	6.99	5.88	6.05	6.73	7.02	14.19	5.63	5.31	5.99
Fe_2O_3	7.26	3.99	4.34	4.53	5.80	4.24	4.58	3.58	5.38	4.59	4.52	4.23
MgO	1.91	8.15	8.43	8.14	8.08	8.14	8.19	7.16	5.53	9.46	10.29	8.97
CaO	11.55	20.66	19.81	19.36	18.31	20.25	19.68	18.24	12.44	24.33	24.34	22.30
Na_2O	1.23	0.53	0.66	0.70	0.82	0.76	0.69	0.68	0.74	0.41	0.41	0.50
K_2O	1.07	1.40	1.47	1.44	1.52	1.50	1.47	1.72	4.30	1.37	1.44	1.51
TiO_2	0.27	0.29	0.28	0.25	0.24	0.24	0.26	0.32	0.53	0.29	0.25	0.29
P_2O_5	0.30	0.45	0.45	0.46	0.45	0.48	0.46	0.45	0.33	0.58	0.54	0.52
MnO	0.095	0.052	0.045	0.050	0.047	0.042	0.047	0.030	0.055	0.054	0.059	0.048
S	4.18	0.74	0.67	0.89	1.59	0.75		0.92	0.69	1.12	0.92	
L.O.I.	3.25	23.4	23.9	23.3	22.6	24.7		24.5	18.9	30.4	31.4	
Total	94.1	102.3	103.2	102.8	103.5	105.8		106.1	102.3	110.0	110.2	

* Sample was omitted from the average because of contamination

TABLE 1

(Miocene)

Depths (ft.)	5110-5140	5200-5230	5290-5320	5380-5410	Av.
SiO_2	67.94	72.64	74.10	71.54	71.56
Al_2O_3	8.60	7.55	8.68	8.93	8.44
Fe_2O_3	4.82	4.33	4.64	4.86	4.66
MgO	2.47	2.91	2.19	2.06	2.41
CaO	3.73	5.23	3.55	3.47	4.00
Na_2O	1.24	0.78	1.04	1.00	1.02
K_2O	1.65	1.38	1.56	1.65	1.56
TiO_2	0.51	0.44	0.51	0.54	0.50
P_2O_5	0.31	0.26	0.28	0.35	0.30
MnO	0.039	0.030	0.031	0.035	.034
S	1.35	0.79	0.98	1.08	
L.O.I.	11.9	13.0	10.7	10.8	
Total	104.5	109.4	108.3	107.0	

(Miocene)

6100-6130	6190-6220	6280-6310	6370-6400	Av.
82.49	76.82	69.46	80.54	77.33
7.29	7.01	6.55	7.93	7.20
3.71	4.17	4.38	4.23	4.12
1.48	2.01	2.81	1.57	1.97
2.47	3.93	5.34	2.13	3.47
0.85	0.89	0.83	1.09	0.92
1.16	1.16	1.14	1.29	1.19
0.42	0.41	0.41	0.48	0.43
0.24	0.26	0.28	0.24	0.26
0.028	0.032	0.035	0.030	.031
0.81	1.00	0.95	1.10	
8.1	9.7	11.6	7.5	
109.0	107.4	103.8	108.4	

TABLE 1

(Miocene)

Depths (ft)	7090-7120	7180-7210	7270-7300	7360-7390	7450-7480	Av.
SiO_2	77.59	74.48	52.61	65.45	51.52	64.33
Al_2O_3	2.84	3.29	3.21	1.60	4.70	3.13
Fe_2O_3	1.51	1.96	1.80	1.21	2.81	1.86
MgO	3.03	3.26	6.20	5.06	6.45	4.80
CaO	7.33	8.84	14.97	12.08	15.66	11.78
Na_2O	0.25	0.30	0.27	0.13	0.47	0.28
K_2O	0.46	0.60	0.59	0.32	0.87	0.57
TiO_2	0.16	0.20	0.19	0.10	0.29	0.19
P_2O_5	0.27	0.80	0.69	0.42	0.73	0.58
MnO	0.010	0.017	0.013	0.009	0.026	.015
S	0.83	1.33	1.29	1.09	1.64	1.24
L.O.I.	13.1	15.1	23.0	20.1	22.7	
Total	107.4	110.1	104.8	107.6	107.8	

(Miocene)

8440-8470	8530-8560	8620-8650	8710-8740	Av.
62.01	66.55	68.40	59.47	64.11
6.21	6.62	6.86	6.20	6.47
4.24	3.92	3.88	4.63	4.17
3.77	2.62	2.52	4.30	3.30
9.19	9.90	8.39	11.40	9.72
0.97	0.92	1.00	0.91	0.95
1.06	1.15	1.25	1.20	1.16
0.41	0.42	0.44	0.43	0.43
0.31	0.35	0.36	0.38	0.35
0.063	0.051	0.047	0.067	0.05
1.09	0.99	1.10	1.15	1.08
13.7	12.7	12.0	16.2	
103.0	106.2	106.3	106.3	

TABLE 1

Depth (ft)	(Miocene) 9070-9100	9160-9190	9250-9280	9340-9370	9430-9460	Av.	(Cretaceous) 10330-10360	10420-10450	10510-10540	10540-10571	Av.
SiO_2	62.52	54.21	56.95	50.95	52.86	55.50	63.13	54.09	55.21	55.11	56.88
Al_2O_3	5.27	6.44	7.33	6.90	7.90	6.77	10.14	13.25	14.86	13.83	13.02
Fe_2O_3	3.06	4.22	4.38	4.54	4.92	4.22	6.04	7.86	8.64	8.69	7.81
MgO	4.45	5.48	4.46	5.75	4.69	4.97	2.28	3.57	3.67	3.79	3.33
CaO	10.07	13.07	11.00	15.16	11.38	12.14	5.78	4.59	1.54	3.53	3.86
Na_2O	0.82	0.91	1.07	0.92	1.25	0.99	1.49	1.75	1.73	1.90	1.72
K_2O	1.01	1.18	1.33	1.19	1.36	1.21	1.23	1.88	2.38	1.91	1.85
TiO_2	0.35	0.47	0.52	0.51	0.55	0.48	0.58	0.84	0.95	0.91	0.82
P_2O_5	0.35	0.39	0.38	0.42	0.38	0.38	0.26	0.23	0.13	0.19	0.20
MnO	0.044	0.061	0.061	0.075	0.077	0.064	0.113	0.089	0.057	0.094	0.088
S	1.01	1.07	1.11	1.03	1.19	1.08	0.41	0.42	0.42	0.26	0.38
L.O.I.	15.8	17.6	15.1	17.9	14.6		7.1	7.5	6.5	7.3	
Total	104.7	105.1	103.7	105.3	101.2		98.5	96.0	97.1	97.5	

Table 3

Average Concentrations, in Percent, of Major Components in Sediment Samples Collected from Approximately 400 ft. Depth Intervals and at a Spacing of 1000 ft.

Depth (ft)	2180-2570	3790-4180	5110-5410	6100-6400	7090-7480	8440-8740	9070-9460	10330-10571
Organic Carbon	0.55	1.31	2.23	1.51	2.57	1.72	1.48	0.88
$CaCO_3$	32.8	37.7	1.8	3.6	20.0	15.1	19.3	2.2
$MgCO_3$	14.9	16.8	2.2	1.7	9.0	4.8	8.2	2.6
SiO_2	10.9	11.6	40.0	49.5	52.3	39.1	29.4	6.6
Al-silicates	39.4	29.1	47.8	39.7	9.3	34.7	37.2	85.4

Table 2

Ratios of Major Oxides to Al_2O_3, Averaged for Approximately 1000 ft. Intervals

	Quat.	Plio.	Miocene					Cret.	
Depth (ft)	2180-2570	3780-4160	5110-5410	6150-6400	7090-7480	8440-8740	9070-9460	10330-10571	Shale
$SiO_2:Al_2O_3$	5.48	5.79	8.48	10.74	20.53	9.91	8.20	4.37	3.86
$Fe_2O_3:Al_2O_3$	0.68	0.71	0.55	0.57	0.59	0.64	0.62	0.60	0.45
$MgO:Al_2O_3$	0.76	1.22	0.29	0.27	1.53	0.51	0.73	0.26	0.16
$CaO:Al_2O_3$	2.92	3.72	0.47	0.48	3.76	1.50	1.79	0.30	0.20
$Na_2O:Al_2O_3$	0.10	0.08	0.12	0.13	0.09	0.15	0.15	0.13	0.085
$K_2O:Al_2O_3$	0.17	0.25	0.18	0.17	0.18	0.18	0.18	0.14	0.21
$TiO_2:Al_2O_3$	0.039	0.048	0.059	0.060	.061	0.066	0.071	0.063	0.051
$P_2O_5:Al_2O_3$	0.068	0.087	0.036	0.036	0.18	0.054	0.056	0.015	0.011
$MnO:Al_2O_3$	0.007	0.008	0.004	0.004	0.005	0.009	0.009	0.007	0.007

RESULTS AND DISCUSSION

Chemical analyses of the samples are given in Table 1. The high concentrations of SiO_2 and CaO support the lithologic descriptions that report chert and calcite. The third major component is alumino-silicates.

The relative abundances of these components can be estimated by assuming an "idealized" composition for the lithogenic alumino-silicate component. Variations in the mineralogy of this component certainly place a limit on the accuracy of such calculations. Thus, we have calculated the concentrations of these components averaged over 1,000-ft intervals. The composition of shale (Turekian and Wedepohl, 1961) is taken as the composition of the lithogenic component. The shale composition is essentially identical to that of North Pacific pelagic clay, which was free of biogenic silica and was leached of $CaCO_3$ and amorphous metal oxides (Piper et al., 1979). The ratios of the major oxides to Al_2O_3 for shale are listed in Table 2. Also listed in Table 2 are the average ratios for the samples from each 1,000-ft interval. All sample intervals have excess SiO_2 and CaO.

The amount of excess SiO_2 in sample interval 10,330 to 10,571 ft is determined by the following relation:

$$SiO_{2_{excess}} = SiO_{2_{sample}} - Al_2O_{3_{sample}} \cdot \frac{SiO_2}{Al_2O_3}_{shale}$$

$$= 56.88\% - (13.02\%)\ 3.96$$
$$= 6.62\%$$

and is given in Table 3. Excess CaO for this same sample interval is:

$$Ca_{excess} = 3.86\% - (13.02\%)\ 0.20$$
$$= 1.26\%$$

and CaO as CaO_3 = 2.25%.
These same calculations have also been made for $MgCo_3$ (Table 3).

From the amount of $CaCo_3$ and $MgCo_3$ calculated and the amount of organic carbon measured, the expected concentration of CO_2 can be estimated. This value for each 1,000-ft interval agrees extremely well with the average CO_2 concentration measured directly on these samples (Table 4). This close agressment suggests that the accuracy of the analyses may be much better than the 5 to 8% reported and the selection of shale as an idealized composition for the lithogenic component in these sediments may be quite valid.

The agreement between Mno:Al_2O_3 for samples and shale suggests that all of the MnO is present solely in lithogenic material.

Iron, however, shows an excess in the samples. Its occurrence as pyrite was examined by comparing excess Fe with sulfur. The average values

Table 4

Concentration of CO_2 measured gasometrically and computed from the concentrations of organic carbon, $CaCO_3$, and $MgCO_3$. The method whereby the concentrations of $CaCO_3$ and $MgCO_3$ were calculated is given in the text. Each value represents an average for the specified depth interval

Depth (ft)	Concentration (%)	
	Measured	Computed
2180-2570	24.0	24.2
2490-4180	30.6	30.2
5110-5410	12.9	10.2
6100-6400	10.2	8.0
7090-7480	23.9	22.9
8440-8740	16.7	15.4
9070-9460	19.1	18.6
10330-10571	5.2	5.4

for each 1,000-ft interval are plotted in Figure 1 Several points are close to the curve for FeS_2. The scatter of the data require, however, that both Fe and S occur in other phases. In the case of sulfur, it may be associated with organic material. The two points which live below the curve represent the 5,000-ft and 7,000-ft intervals. Organic carbon, given in Table 3, was higher for these intervals than for the other 6 intervals. The samples that lie above the curve, i.e., those with high Fe, may contain an iron oxide mineral or an iron rich clay, such as chlorite.

The fraction of P_2O_5 associated with the terrigenous material can be subtracted from the bulk analyses. Similarily, the lithogenic CaO can be substracted from the total CaO values to give "excess" CaO, along with "excess" P_2O_5. A plot of these values (Fig. 2) shows that the distribution of P_2O_5 is strongly dependent upon the distribution of $CaCo_3$ The main exceptions are the samples from the interval 7,000 to 8,000 ft, which fall well above the curve of best fit.

Correlations between some of the components have been computed using the compositions listed in Table 1. These suggest a strong relation between titanium and aluminum (r = .89) and between iron and aluminum (r= .83). Correlation between P_2O_5 and CaO (r = .67) also was observed and a negative correlation was found between SiO_2 and $CaCo_3$ (r = 85).

The weight ratio of C:P in organic matter is 41:1 (Svendrup et al., 1942). All eight of the averaged values (Fig. 3) fall below this value that is, they have a high P_2O_5 concentration relative to that of plankton. No trend in the data is apparent. However, the four samples which approach most closely that or ogranic matter, come from Miocene age sediment. The method used to obtain the carbon values (analysis of composite samples) and P_2O_5 values (averaging 4 to 5 individual analyses) may largely mask any trends that would otherwise be observed. Certainly, more date are needed before any interpretation can be made from this relation. Organic carbon analyses are needed for individual samples for which major oxide analyses also are available.

REFERENCES CITED

Piper, D. Z., Leong, K., and Cannon, W. F., 1979, Manganese nodule and surface sediment compositions: DOMES Sites A, b, and C, in Bischoff, J. L., and Piper D. Z , eds., Marine geology and oceanography of the Pacific manganese nodule province: Plenum Publishing Corporation, New York, in press.

Svendrup, H. U., Johnson, M. W., and Fleming, R. H., 1942, The oceans: Prentice-Hall, Inc., Englewood Cliffs, New Jersey, 1060 p.

Turekian, K. K., and Wedepohl, K. H., 1961, Distribution of the elements in some major units of the earth's crust: Geological Society of America Bulletin, v. 72, p. 175-192.

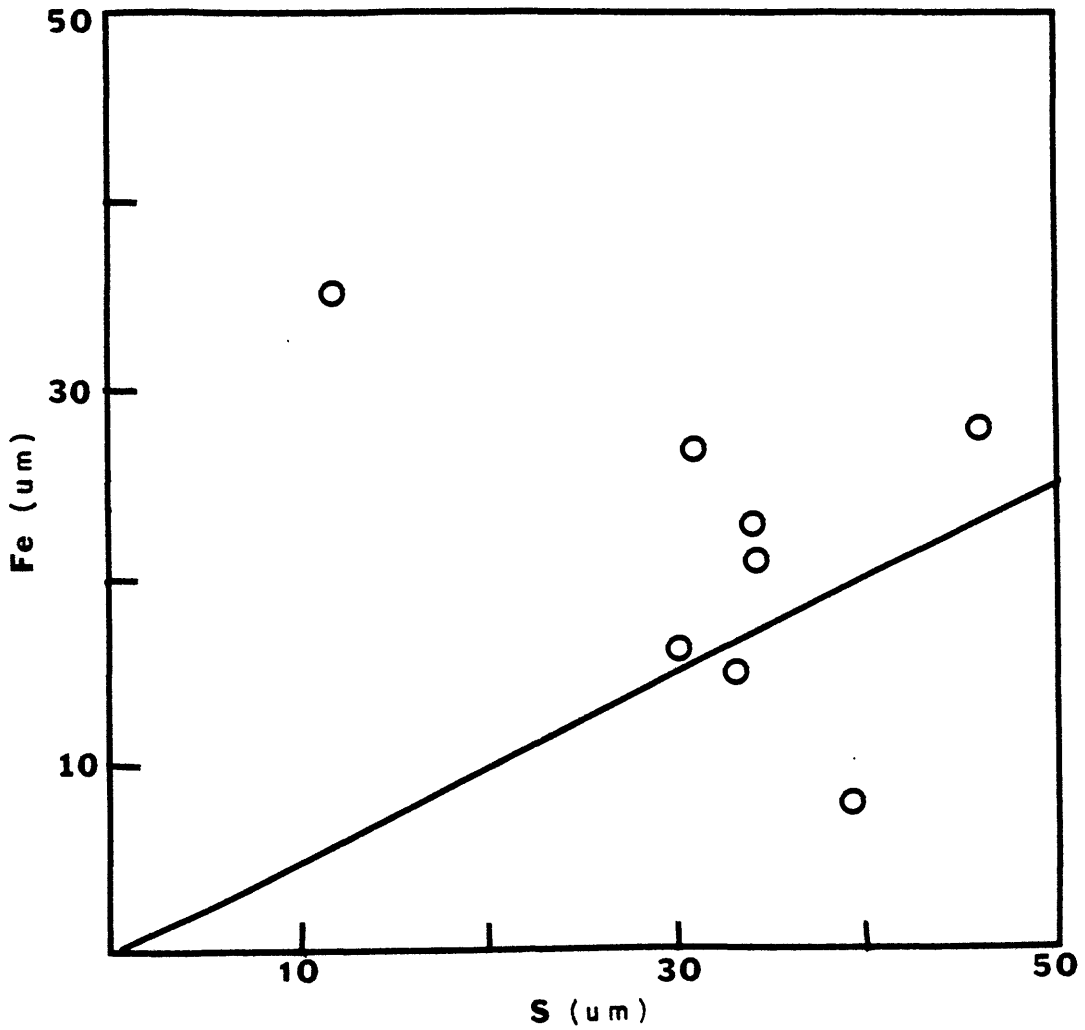

Figure 1. Relation between "excess" Fe and sulfur. The curve gives this relation for FeS_2.

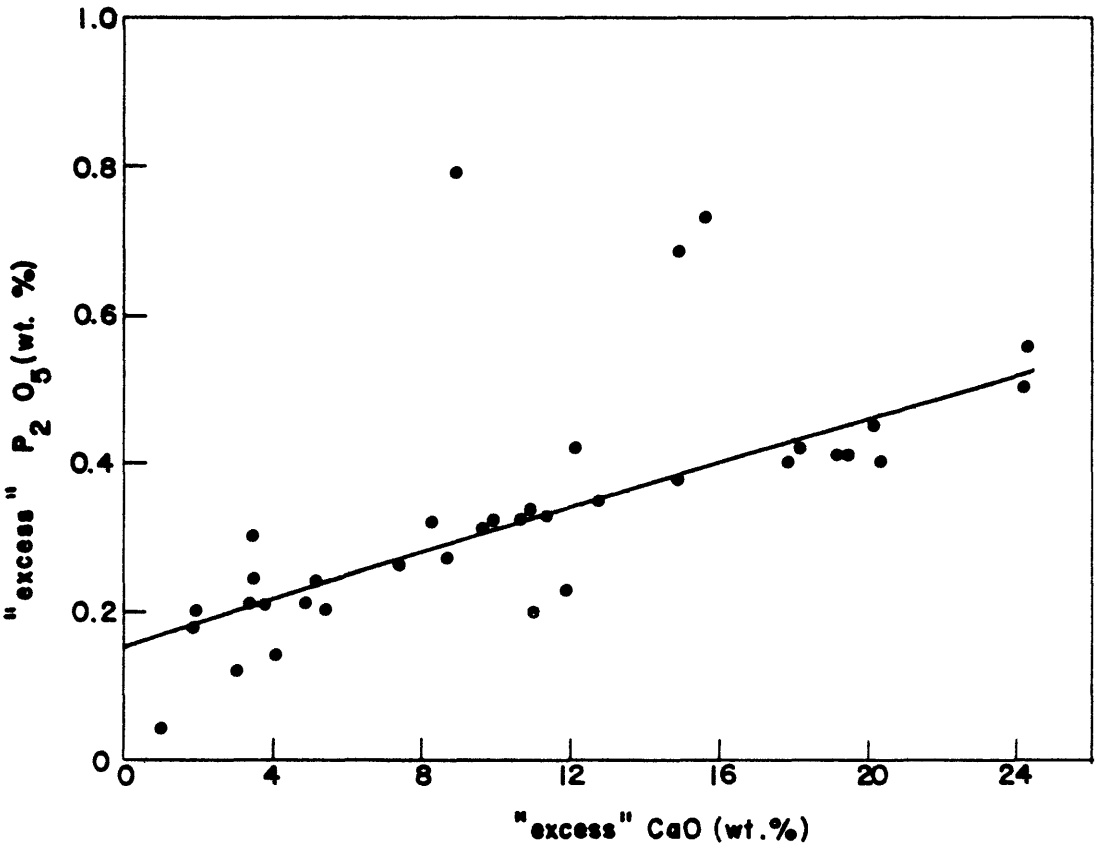

Figure 2. Relation between P_2O_5 concentrations which are in excess of those for "ideal" lithogenic matter.

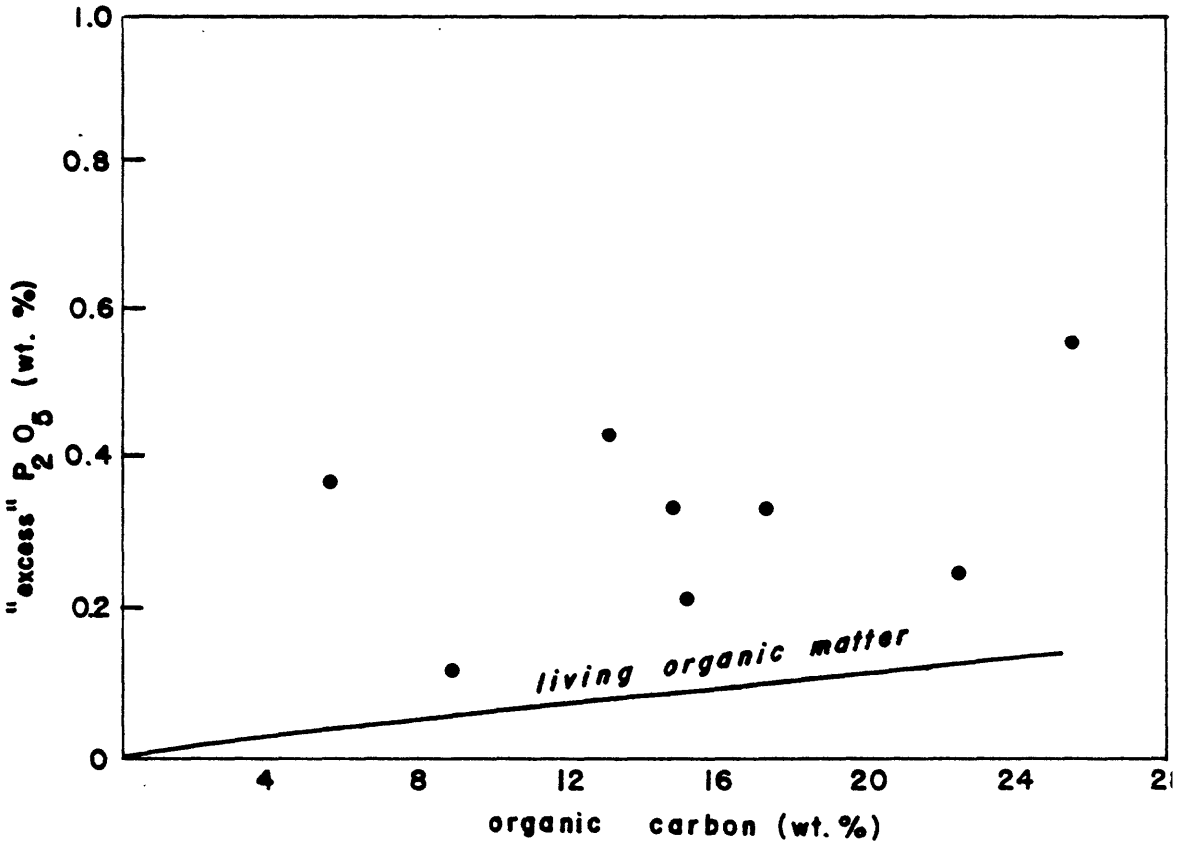

Figure 3. Relation between organic carbon and "excess" P_2O_5.

ORGANIC GEOCHEMISTRY

G. E. Claypool, J. P. Baysinger, C. M. Lubeck, and A. H. Love
U.S. Geological Survey
Denver Colorado

SUMMARY

Eight samples of drill cuttings composited over 300 to 400-ft depth intervals at approximately 1,000-ft spacing were analyzed to provide basic information on the content, type, and thermal maturity of organic matter in the sedimentary section penetrated by the Pt. Conception deep stratigraphic test well. All depths and sample numbers in the tables, figures, and text represent drilled depths beginning at the derrick floor. Thus, the sea floor is at a drilled depth of 1,465 ft (derrick floor 37 ft above sea level plus water depth of 1,428 ft).

Neogene rocks have above average organic matter content when compared to fine-grained rocks in general, but are less than average for sediments of the same age in other petroleum-producing areas of California. The organic matter is dominantly of a type which has excellent oil-generating capacity. The organic matter in Neogene rocks is immature to marginally mature with respect to the degree of thermochemical transformation usually required for abundant petroleum generation However, a very large proportion of the organic matter is extractable by organic solvents. If the high content of extractable hydrocarbons is characteristic of the organic matter type, and is not due to contamination or presence of nonindigenous hydrocarbons, then it suggests the possibility of expulsion and accumulation of oil at low apparent stages of thermal maturity.

RESULTS AND DISCUSSION

Organic carbon content (Table 1) was measured by a wet oxidation technique modified after Bush (1971). The analyses were performed by Rinehart Laboratories, Arvada, Colorado. Excluding the shallowest and deepest samples, the organic carbon content ranges from 1.31 to 2.57 percent. The depth intervals with the highest organic carbon content are at 5,110 to 5,410 ft (2.23 percent) and at 7090 to 7480 ft (2.57 percent). It is likely that rocks with higher organic carbon content are present in these intervals, but are diluted by organically lean rocks.

Richness, type and maturity of organic matter in the composite samples from the Pt. Conception COST well were evaluated by MP-3 thermal analysis (Claypool and Reed, 1976; Table 1) and Rock-Eval pyrolysis (Espitalie, et al., 1977; Table 2) In these procedures, a small sample of rock is heated in a flowing stream of helium at a rapid rate of temperature increase. The hydrocarbons (or other organic-carbon containing compounds) evolved from the rock are measured as a function of the temperature of

MP-3

Table 1. -- Organic carbon and thermal analysis of composited drill cuttings, Pt. Conception Well No. 1

Depth Interval (feet)	Rock Unit	Organic Carbon (wt. %)	(Total) Pyrolytic Hydrocarbon Yield (wt. %)	Volatile Hydrocarbon Content (ppm)	Pyrol. Hc. / Org. C (%)	Vol. HC / Pyrol. HC	Temperature of Maximum Pyrolysis Yield (°C)
2180-2570'	Pico	0.55	0.16	300	28.9	0.19	462
3790-4180'	Pico	1.31	0.47	420	36.1	0.09	467
5110-5410'	Repetto	2.23	0.81	470	36.4	0.06	464
6100-6400'	Repetto	1.51	0.66	340	43.5	0.05	456
7090-7480'	Monterey	2.57	1.27	1900	49.4	0.15	468
8440-8740'	Miocene	1.72	0.74	950	43.2	0.13	466
9070-9460'	Miocene	1.48	0.60	1100	40.7	0.18	472
10330-10571'	Cret. or Jur.	0.88	0.09	120	10.1	0.13	483

Table 2. -- Rock-Eval pyrolysis of composited drill cuttings,

Pt. Conception Well No. 1

Depth Interval (feet)	S1 (mg/g)	S2 (mg/g)	S3 (mg/g)	$T_{(s2)}$ (°C)	Genetic Potential, $S_1 + S_2$ (ppm)	Hydrogen Index S_2/Corg (mg HC/gC)	Oxygen Index S_c/Corg (mgCO2/gC)	Transformation ratio $S_1/S_1 + S_2$
2180-2570'	0.35	1.06	0.56	427	1410	193	102	0.25
3790-4180'	0.36	4.39	1.10	420	4750	335	84	0.08
5110-5410'	0.04	7.14	0.69	414	7180	320	31	0.01
6100-6400'	0.22	4.65	0.41	408	4870	308	27	0.05
7090-7480'	1.20	14.47	0.74	416	15,670	563	29	0.08
8440-8740'	1.77	7.29	0.34	422	9060	424	20	0.20
9070-9460'	1.15	5.80	0.42	421	6950	392	28	0.17
10330-10571'	0.12	0.54	0.27	440	660	61	31	0.18

heating. The basic analytical results of MP-3 thermal analysis reportd in Table 1 (in addition to organic carbon) are: the total pyrolytic hydrocarbon-yield, which is the total weight of hydrocarbons (or hydrocarbon-like compounds) given off during the heating of the sample; the volatile hydrocarbon content, which is the portion of the total hydrocarbon yield produced at lower heating temperatures; and the temperature at which the yield of pyrolysis products is at a maximum. The basic determinations for Rock-Eval pyrolysis (Table 2) are: S_1, the weight of hydrocarbons given off by the rock at 250°C heating temperature; S_2, the weight of hydrocarbons given off by higher temperature (up to 55°C) pyrolysis of the solid organic matter; S_3, the weight of carbon dioxide given off during 250 to 390°C pyrolysis of the solid organic matter; and $T_{(S2)}$, the temperature of maximum pyrolysis yield.

On the basis of the total pyrolytic hydrocarbon yield, or the genetic potential ($S_1 + S_2$, Tissot and Welte, 1978, p. 447) all except the shallowest and deepest samples analyzed can be classified as potential oil source rocks. (Potential source rock here means a rock with an adequate content of oil-generating organic matter at an immature stage of thermochemical transformation.) High proportions of relatively hydrogen-rich ("sapropelic") organic matter are indicated by pyrolytic hydrocarbon-to-organic carbon ratios of 36 to 49 percent and hydrogen indices of 308 to 563 mg HC/g C for samples between 3,790 and 9,460 ft. Evidence for maturity based on interpretation of thermal analysis is mixed. Values of the volatile hydrocarbon-to-pyrolytic hydrocarbon ratio or $S_1/S_1 + S_2$ (the "transformation ratio" of Tissot and Welte, 1978, p. 453, and the "production index" of Barker, 1974) of 0.1 or more indicate organic matter which has advanced to the oil-generating stage of thermal maturity. On this basis, the samples below 7,090 ft are mature, if the volatile hydrocarbon content is indigenous. Another, independent estimate of maturity is provided by the temperature of maximum pyrolysis yield, where the transition from immature to mature is indicated by a pyrolysis temperature of about 475°C for MP-3 pyrolysis and about 425°C for Rock-Eval pyrolysis. By this criterion, most of the samples are immature-to-marginally mature, with only the deepest sample giving a clear indication of thermal maturity.

The samples were also analyzed by conventional source rock evaluation techniques (Claypool *et al.*, 1978) and these results are summarized in Table 3. Contents of extractable organic matter--chloroform extractable bitumen and hydrocarbons determined by elution chromatography--are exceptionally high, both in an absolute sense and relative to organic carbon. Hydrocarbon concentrations range from 180 ppm (10,330-10,571 ft) to 4800 ppm (7,090-7,480 ft). All samples have hydrocarbon-to-organic carbon ratios of greater than one percent which suggests some degree of transformation of organic matter to hydrocarbons. This ratio exceeds ten percent for three of the samples (2,180-2,570 ft, 7,090-7,480, and 9,070-9,460 ft) suggesting that nonindigenous hydrocarbons may be present. However, it was noted previously (Taylor 1976, p. 25) that organic matter of the Monterey Shale in this region has unusual geochemical characteristics, including a high fraction of extractable hydrocarbons at an apparently immature stage of thermal alteration.

Elemental analyses of kerogen concentrates from chloroform-extracted rock samples are also shown in Table 3. The atomic H/C ratios confirm the sapropelic nature of the organic matter in rocks between 5,000 and 10,000 ft. There is a slight trend of decreasing H/C with increasing depth of burial over the interval 6,100 to 9,460 ft. This may be due to a trend of increasing (but still very early) stages of thermal maturity. The atomic H/C ratio of 0.86 at 10,330 to 10 571 ft may be partially due to increased thermal maturity, but it also suggests a major change in the type of organic matter.

The saturated hydrocarbon fractions were analyzed by gas chromatography and the chromatograms are shown in Figure 1. The shallowest sample (2,180 to 2,570 ft) appears to be contaminated with diesel fuel or some other refined hydrocarbon substance. However, the rest of the samples (especially those between 5,110 and 9,460 ft) contain hydrocarbon mixtures typical of thermally immature organic matter in offshore California Tertiary sediments (Taylor, 1976; Paul et al., 1976). Several significant points can be made regarding the detailed hydrocarbon distributiions shown in the chromatograms:

1. The saturated hydrocarbons from the sample at 5,110 to 5,410 ft (Fig. 1C) are composed predominantly of isoprenoids (pristane and phytane), steranes, and pentacyclic teriterpanes. Normal paraffins are absent or at low concentration. This mixture of hydrocarbons is characteristically associated with sedimentary organic matter derived from aquatic algae, and which is at low, early stages of thermal maturity.

2. The n-paraffin content of the saturated hydrocarbon mixtures (relative to the isoprenoids, steranes, and triterpanes) increases regularly with increasing depth of burial below 6,100 ft. This is probably due to early thermogenic hydrocarbon generation rather than changes in the type of organic matter.

3. The n-paraffins in samples between 6,100 and 9,760 ft show an even carbon number preference over the range of $\underline{n}$-C_{16} to $\underline{n}$-C_{24}, which is most pronounced in the sample from 7,090 to 7,480 ft (the interval which contains the Monterey Shale). This feature is most commonly associated with organic matter deposited in carbonate-evaporite sediments, but it is also characteristic of oils produced from fractured Monterey Shale in the Santa Maria Basin (Milner et al., 1977, p. 138).

4. Saturated hydrocarbon mixtures below 8,440 ft show a reversal of the pristane:phytane ratio, from less than to greater than one This probably indicates a change in the type of organic matter and the environment of deposition, but may also be an effect of increasing thermal maturity.

5. There is a distinct odd carbon number preference in the n-paraffins from the sample at 10,330 to 10,571 ft. This indicates a significant land plant source of the organic matter in this sample, and a level of thermal maturity slightly less than that required for abundant generation of petroleum hydrocarbons from land plant-derived organic matter.

Table 3.--Extractable organic matter and elemental analysis of kerogen concentrates, Pt. Conception Well No. 1.

Depth Interval (feet)	$CHCl_3$ extractable Bitumen (ppm)	Total Hydrocarbons (ppm)	Hydrocarbon / Org. carbon %	Saturated / Aromatic	Hydrocarbon / Bitumen	Kerogen Concentrate H/C	Kerogen Concentrate C/N
2180- 2570	1320	780	14.2	0.96	0.59	1.01	33.1
3790- 4180	860	440	3.4	0.76	0.51	1.23	20.9
5110- 5410	660	244	1.1	0.71	0.37	1.32	19.3
6100- 6400	1180	415	2.8	0.94	0.35	1.36	23.2
7090- 7480	8850	4800	18.7	0.17	0.54	1.32	34.5
8440- 8740	2750	1390	8.1	0.95	0.51	1.30	28.3
9070- 9460	3650	1720	11.6	1.16	0.47	1.26	26.9
10330-10571	400	180	2.1	0.84	0.45	0.86	39.1

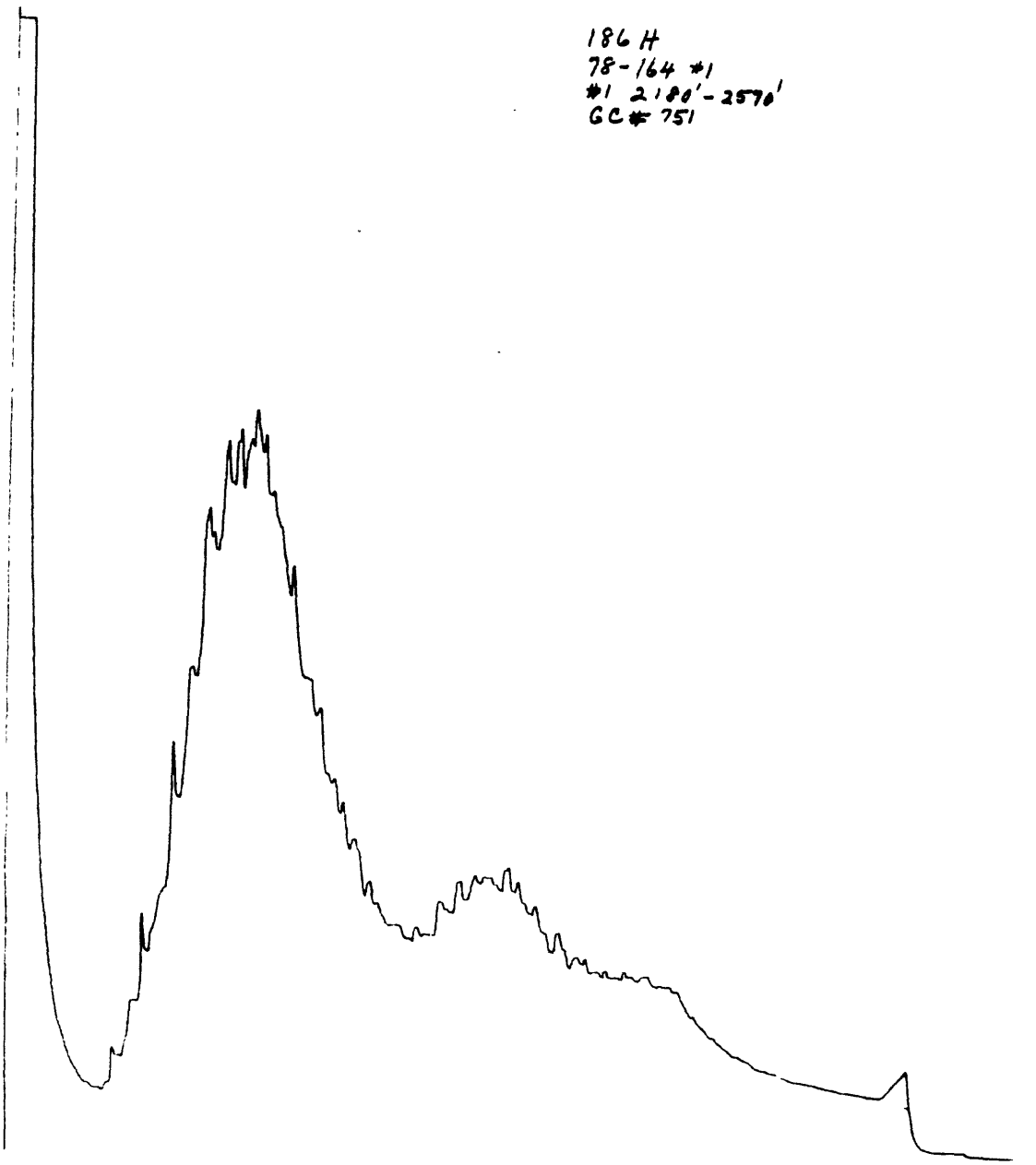

Figure 1.--Gas chromatographic analyses of saturated hydrocarbons in samples from Pt. Conception COST well, A through H with depths as indicated in Table 1. Tentative compound identifications based on relative retention times and shown for index purposes only.

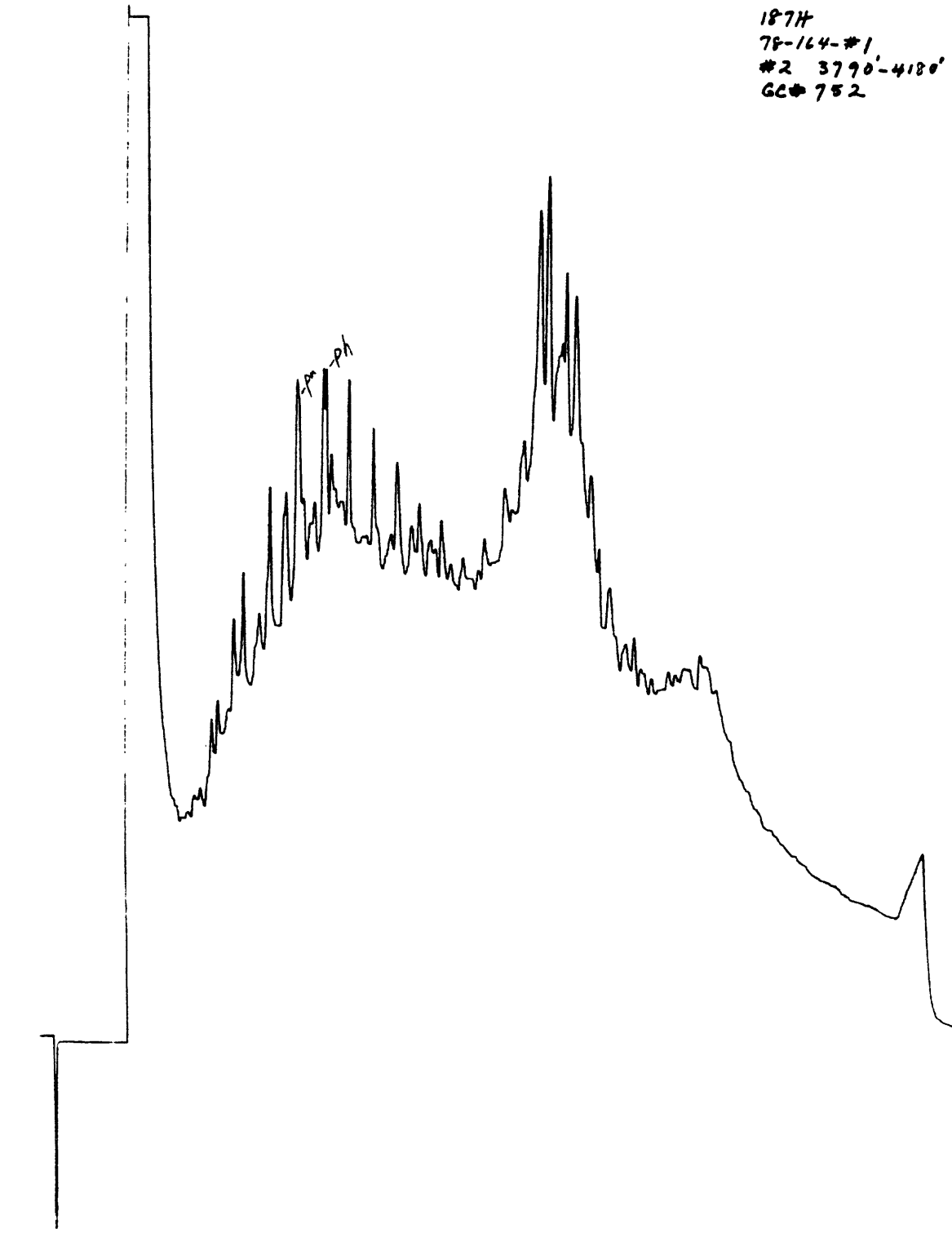

Figure 1b.

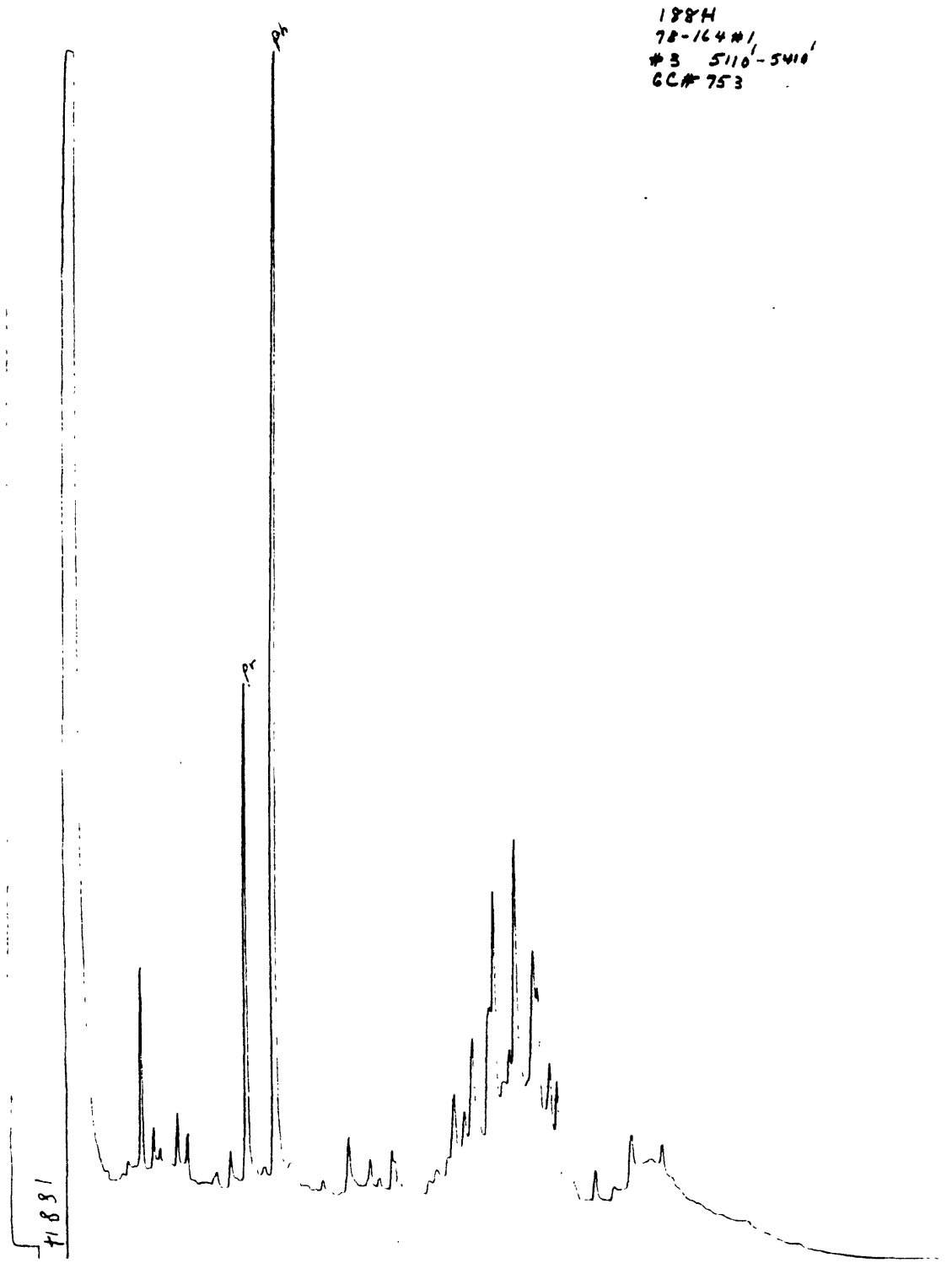

Figure 1c.

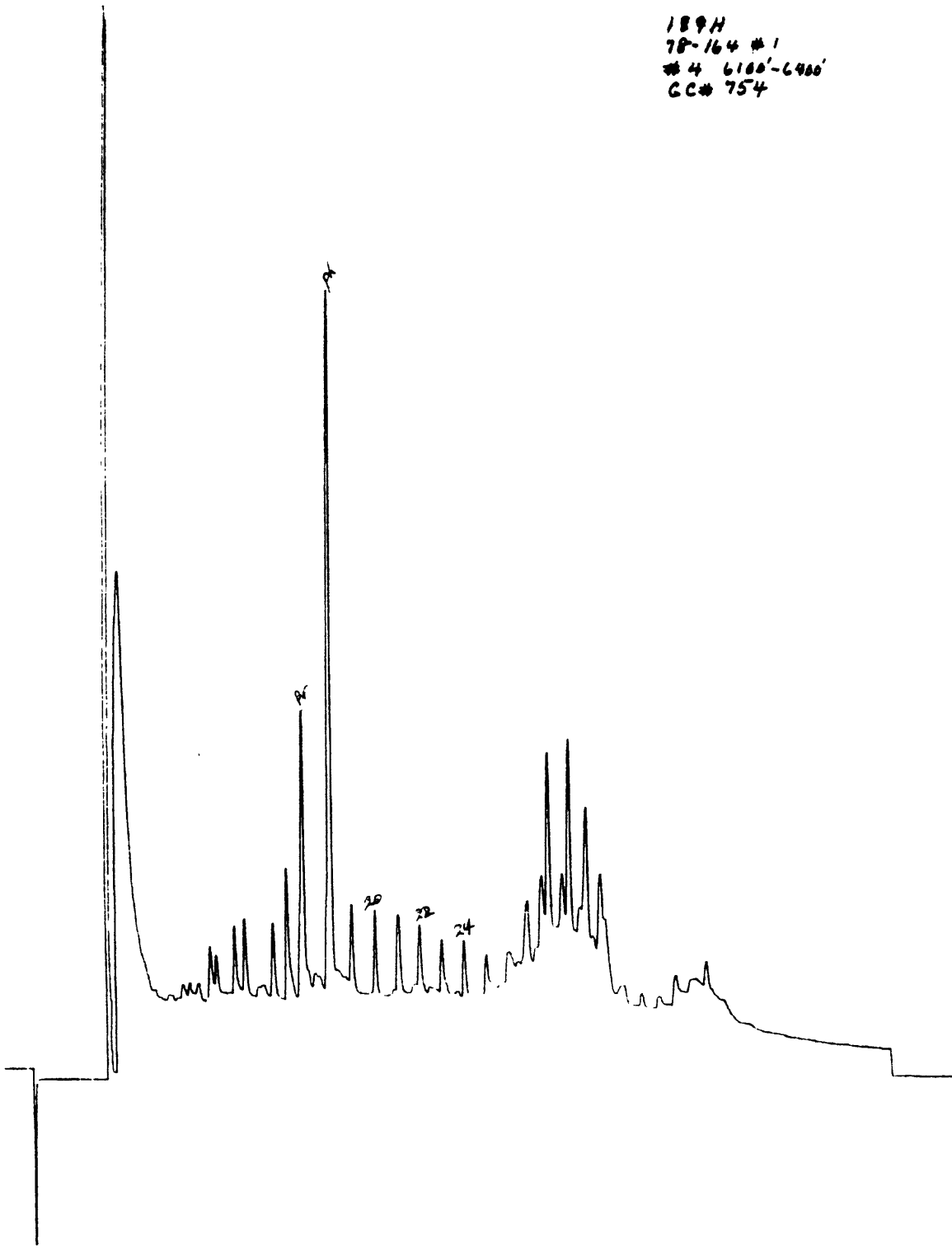

Figure 1d.

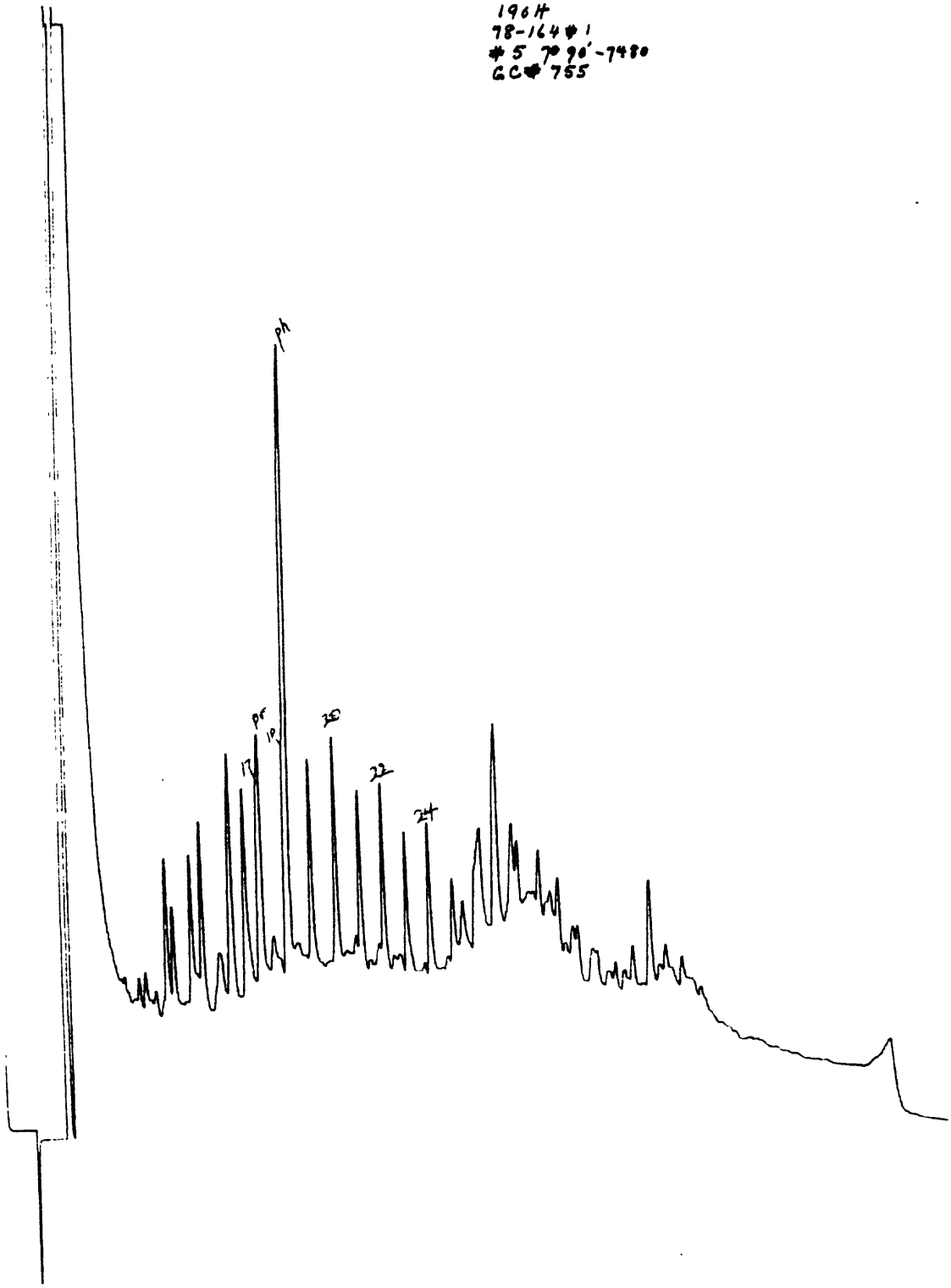

Figure 1e.

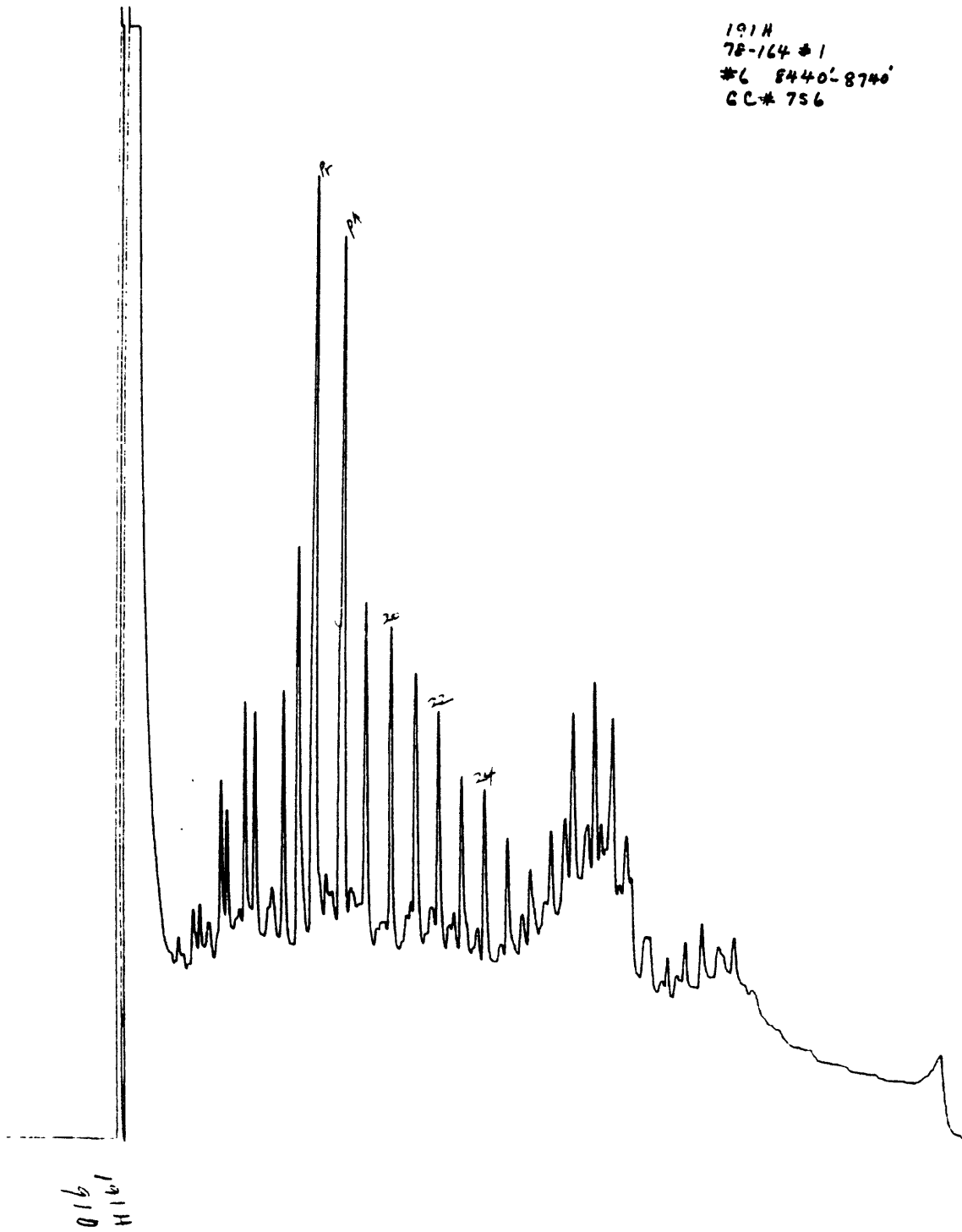

Figure 1f.

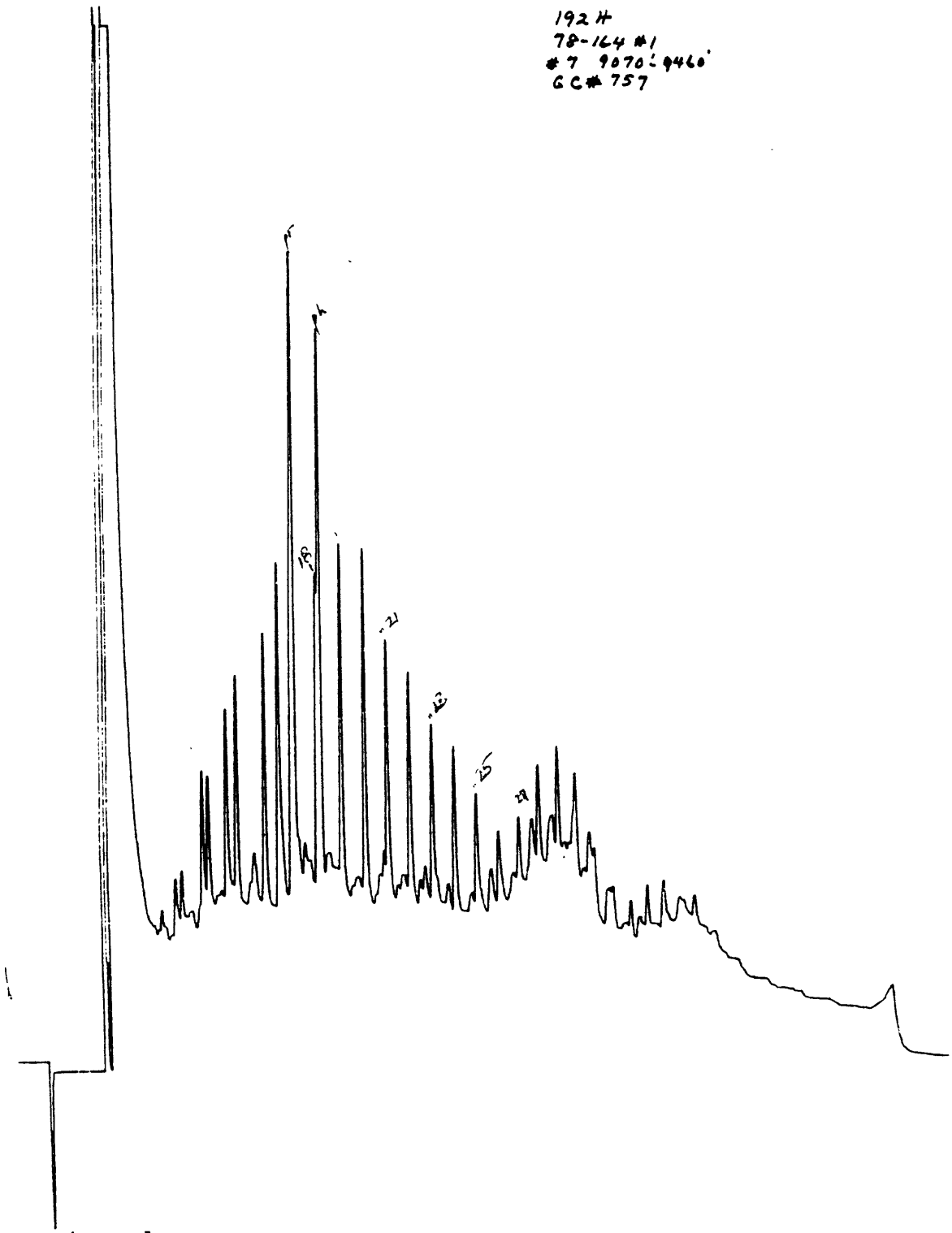

Figure 1g.

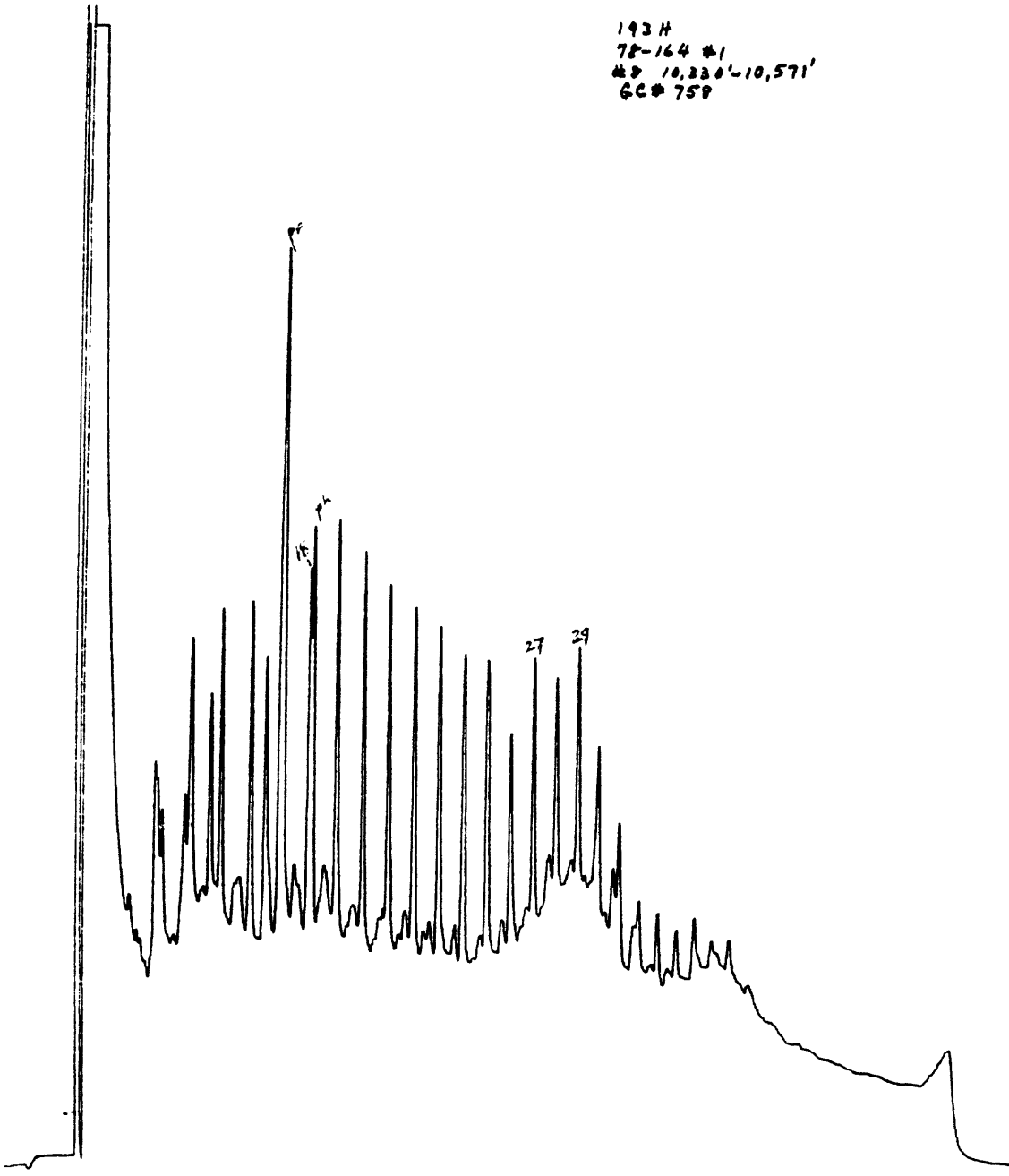

Figure 1h.

CONCLUSIONS AND IMPLICATIONS FOR PETROLEUM OCCURRENCE

Organic matter in the prospective source rock section from 5,000 to 10,000 ft in the Pt. Conception well is thermally immature to submature, based on qualitative characteristics (molecular composition of saturated hydrocarbons, pyrolysis characteristics and elemental analysis of solid organic matter). However, the concentration of extractable hydrocarbons is exceptionally high, and these extractable hydrocarbons have many characteristics in common with crude oils from the Santa Maria Basin a nearby onshore oil-producing area. If these hydrocarbons are indigenous to the fine-grained rocks sampled and analyzed, it indicates that significant amounts of petroleum hydrocarbons are present at a lower apparent integrated time-temperature history than commonly is believed to be required for petroleum generation.

An oil show was reported during the drilling of this well (Menard, 1978). No information was available at the time this report was prepared concerning the details of the reported show (magnitude, composition, etc.). The presence of migrated hydrocarbons may account for the unusually high concentration of extractable hydrocarbons in samples from this well, especially in the sample at 7,090 to 7,480 ft. If these high concentrations are due to oil-staining, it would diminish the probability that the section penetrated in this well contains effective or possible oil source rocks, although they meet all the requirements for potential oil source rocks and should have generated oil if the same rocks are more deeply buried in the immediate vicinity. The alternative possibility is that these rocks contain high concentrations of indigenous extractable organic matter and expellable "immature" petroleum at an early stage of thermal transformation. If this is the case, then the requirement of locating source rocks that are "mature" in the conventional sense may not be relevant in this case. Certainly the presence of an oil show is itself evidence for effective source rocks somewhere in the area. Chemical analysis of the oil show and comparison with the hydrocarbons extracted from the drill cuttings could provide a better basis for assessing the significance of the rock analyses.

The detailed compositions of saturated hydrocarbons by themselves (Fig. 1) do not support the interpretation of contamination by migrating petroleum. The variation of relative proportions of different hydrocarbons and hydrocarbon types (odd-even n-alkanes, isoprenoid, normal alkanes, sterones/triterpanes) appears to be controlled by depth of burial rather than the possible degree of staining as indicated by extractable hydrocarbon/organic carbon ratios. This suggests that the organic matter in these rocks may yield significant amounts of hydrocarbons at an early stage of thermochemical transformation.

REFERENCES CITED

Barker, C., 1974, Pyrolysis techniques for source rock evaluation American Association of Petroleum Geologists Bulletin, v. 58, p. 2349-2361.

Claypool, G. E., and Reed, P. R , 1976, Thermal analysis technique for source-rock evaluation: quantitative estimate of organic richness and effects of lithologic variation: American Association of Petroleum Geologists Bulletin, v. 60, p. 608-612.

Espitalie, J., Laporte J. L., Madec M., Marquis, F., Leplat, P., Paulet, J., and Boutefeu, A., 1977, Methode rapide de caracterisation des rockes meres, de leur potential petrolier et de leur degre d'evolution: Rev. Inst. Fr. Pet., v. 32, p. 23-42.

Menard, H. W., 1978, Stratigraphic test well yields oil and gas "shows" offshore California: U.S. Geological Survey News Release, 1 November 1978, 2 p.

Milner, C. W. D., Rogers, M. A , and Evans, C. R , 1977, Petroleum Transformations in reservoirs: Journal of Geochemical Exploration, v. 7, p. 101-153.

Paul, R. G., et al., 1976, Geological and operational summary, Southern California Deep Stratigraphic Test OCS-CAL 75-70 No. 1, Cortes Bank area offshore southern California: U.S. Geological Survey Open-file Report. 76-232.

Taylor, J. C., 1976, Geologic appraisal of the petroleum potential of offshore southern California: The Borderland compared to onshore coastal basins: U.S. Geological Survey Circular 730, 43 p

Tissot, B. P., and Welte, D. H., 1978, Petroleum formation and occurrence--a new approach to oil and gas exploration: New York, Springer-Verlag, 538 p.

VITRINITE REFLECTANCE

N. H Bostick
U.S. Geological Survey
Denver, Colorado

Eight samples of cuttings, each composite over several hundred feet of depth, were crushed and extracted with chloroform (see Claypool et al., this report). They were then demineralized with HCl and HF and made into polished sections of kerogen concentrate. All depths and sample numbers represent drilled depths beginning at the derrick floor. Thus, the sea floor starts at a drilled depth of 1,465 ft (derrick floor 37 ft above sea level plus water depth of 1,428 ft).

Reflectance of first-cycle vitrinite was measured with a microphotometer. Histograms of the data are compiled in Figure 1 for the eight samples. The operators' "best picks" for average vitrinite reflectance, with an estimate of the uncertainty ranges are tabulated below.

Drilled Depth (ft)	Vitrinite Reflectance, % R_{oil}		Uncertainty Range	N
	First choice	Possible		
2,375	.28	.22	.22-.32	50
3,985	.27	.25	.23-.31	90
5,260	.27	.31	.24-.32	64
6,250	.29	.35	.26-.34	39
7,285	.32	.28	28-.35	47
8.615	.32	.26	.28-.36	73
9,265	.34	.31	.30-.37	53
10,450	.68	--	.61-.75	89

The ogranic grains were generally sparse on the mounts and small, though polish quality was good. Analyses of reflectances at this low level of maturation commonly have considerably more scatter than these, so the reliability of the general maturation level and the suggestion of a depth gradient for these samples can be considered quite good. In order to help determine the first cycle vitrinite grains, resinite was also measured.

Note that the deepest sample appears to be from distinctly older rocks than the others (for example, see Bukry, this report); also it has much more humic or terrestrial kerogen than in shallower samples. Also the shallowest two samples stand apart.

2375 contains fragments of microspores, especially disaccate pollen, more abundantly than the other samples. 3985 contains an unusual abundance

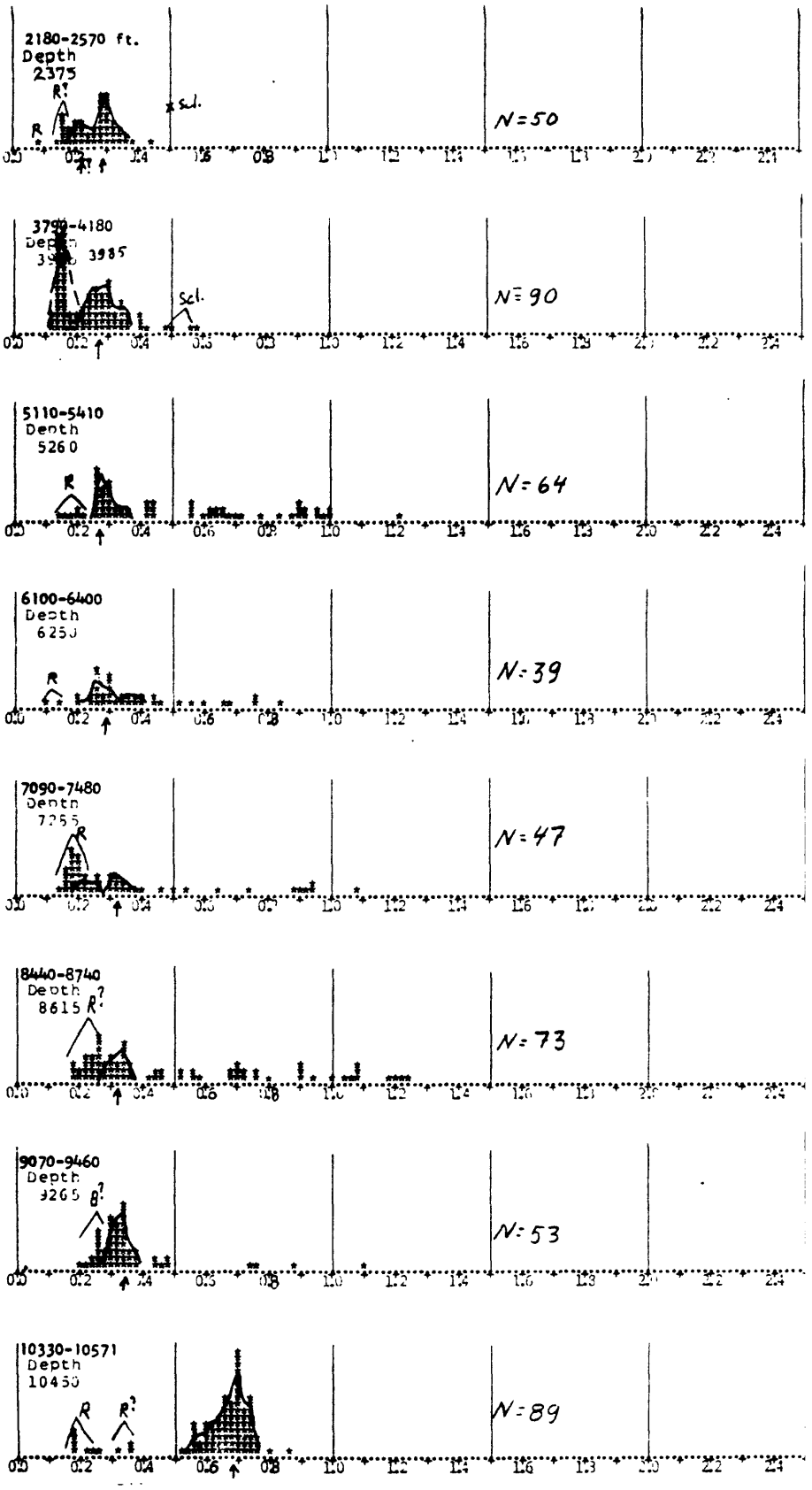

Figure 1. Reflectance histograms for eight samples of cuttings from the COST "Pt. Conception" 1 borehole. The range and mean depth for each sample is not at the left. The operators' selection of first cycle vitrinite within t kerogen assemblage is outlined by a heavy solid line on each histogram, and the "best pick" value (approximately the modal value in most cases) marked below by an arrow. Readings on definite (R) and possible (R?, B? resinite and solid bitumen are below most of those for vitrinite. Only two sclerotia were measurable--in sample 3985.

of coarse resinite and resinite-vitrinite bimacerite, several fragments of uncompressed wood tissue and a fragment of high volatile bituminous coal that looks like Carboniferous coal. These suggest possible contamination, at least the coal. Bits of microspores are abundant.

Further notes from the analyses indicate that sporinite fluorescence is generally greenish yellow in samples 2375 and 3985, but is yellowish orange or "bright" orange in deeper samples. This suggests that the $\%R_o$ of vitrinite in the top two samples could be picked slightly lower in the histograms than done by the operator.

In both 2375 and 3985 the mounting polyester has not "extracted fluorescence" from the organic matter as much as in deeper samples. This could represent different procedure during the geochemists' extraction, different organic makeup, or less hydrocarbon presence than in deeper samples.

The most likely explanation for the slightly anomalous properties of the two shallowest samples is twofold: they have more terrestrial humic organic matter than deeper samples (except the bottom sample). They are somewhat less mature than deeper samples. Both these conclusions agree with the pyrolysis analysis (Claypool et al., this report).

The 0.68% vitrinite reflectance level for sample 10,450 was compared with the reflectance profile of the Standard "Gerber"-1 borehole on Pt. Conception, 28 km distant. This comparison indicates burial of the 10,450 sample (Jurasic or Upper Cretaceous) by no more than about 6,000 ft before erosion and later sedimentation by the Miocene section.

The Pt. Conception reflectance data (Fig. 1) are very similar to those from the Ventura Central Syncline (Bostick, et al., 1979)--with perhaps slightly shorter effective burial time or even lower temperatures for a given depth. Because the very short effective burial time seems to be about the same, the borehole reflectance values in Figure 1 indicate temperatures at least as low as in the Ventura Syncline.

Several reflectance analyses from above 8,000 ft in the Santa Maria Basin have the same general level as in Figure 1, but below 8,000 ft the Santa Maria values rise abruptly.

With regard to petroleum generation our analysis indicates favorable type of organic matter in samples from 5,200 to 9,300 ft, and oragnic carbon analyses in this range are all above 1%. So this part of the section contains potential oil source rocks. Since each sample was a composite from several hundred feet, the section may contain some rocks with very high potential that were not recognized because of dilution in the composite samples.

Although a good part of the section in this well contains potential oil source rocks, our analysis of vitrinite reflectance indicates that the maturity is less than that needed for initiation of petroleum generation in

commercial amounts. Experience in most petroleum basins indicates that vitrinite reflectance levels of 0.5 to 0.6 $\%R_o$ are associated with the shallowest occurrence of indigenous petroleum. Yet the driller's report of an oil show and some of the geochemical data indicate that the rocks contain some oil

This discrepancy occurs in several oil basins in southern California. In some cases it can be explained by indications that the oil has migrated into the section from elsewhere. But where migration seems to be unlikely I suspect part of the section--the "Monterey type" rocks in particular--contains organic matter that matures to oil at vitrinite reflectance levels as low as 0.4 to 0.3 $\%R_o$. So in conventional terms the rocks are too immature to yield commercial oil, but there is some suspicion that even at the low maturity level this section could have generated oil in modest commercial quantity.

REFERENCES CITED

Bostick, N. H., Cashman, S. M., McCulloh, T. H., and Waddell, C. T., 1979, Gradients of vitrinite reflectance and present temperature in the Los Angeles and Ventura Basins, California, in Oltz, D. F , ed., A Symposium in Geochemistry: Low temperature metamorphism of kerogen and clay minerals: Society of Economic Paleontologists and Mineralogists, Pacific Section, Los Angeles, California, p. 65-96.

BIOSTRATIGRAPHY AND PALEOECOLOGY OF FORAMINIFERS, RADIOLARIANS, AND DIATOMS

Kristin McDougall[1], John. A. Barron[1], Stanley Kling[2], and Richard Z. Poore[1]

[1]U.S. Geological Survey
Menlo Park, California

[2]Scripps Institute of Oceanography
La Jolla, California

INTRODUCTION

This report describes the biostratigraphy and paleoecology of the Point Conception deep stratigraphic test well drilled in 1 428 ft of water, 19 mi west of Point Conception, California. Drill cuttings, sampled in 30-ft intervals were examined for radiolarians (Kling), diatoms (Barron), and foraminifers (McDougall and Poore).

All depths and sample numbers in Fig. 1 and the tables represent drilled depths. beginning at the derrick floor. Thus, the sea floor is at a drilled depth of 1,465 ft (derrick floor 37 ft above sea level plus water depth of 1,428 ft).

BIOSTRATIGRAPHIC SUMMARY

Siliceous microfossils are common and well preserved in the upper 4,000 ft of the well but are sparse and poorly preserved or absent below 4,000 ft. Diatoms and radiolarians indicate the Pliocene-Quaternary boundary is between the 2,840-2,870-ft and 2,960-2,990-ft samples, and that the interval from there through 3,820 to 3,850 ft is late Pliocene. Samples below this level down to 4,090 to 4,120 ft are assigned to the undifferentiated Pliocene. Stratigraphically diagnostic siliceous microfossils are sparse or absent in the remaining samples; however, a diatom assemblage recovered at 4,210 to 4,240 ft is no older than latest Miocene (Fig. 1).

Benthic foraminiferal assemblages are indicative of the Venturian-Repettian Stage from 3,020 to 2,060 ft through 3,640 to 3,670 ft, the Repettian Stage from, 3820 to 3,850 ft through 10,450 to 10 480 ft. The agglutinated foraminiferal assemblages from 4,150 to 4,180 ft and 7,900 to 7,930 ft are not age diagnostic. Evidence for pre-middle Miocene sediments was not detected (Fig. 1).

Planktic foraminifers in samples from 2,030 ft through 3,850 ft are not particularly age diagnostic but are compatible with determinations derived from the other microfossil groups. Planktic foraminifers found

Fig. 1 BIOSTRATIGRAPHIC ZONATION OF THE PT. CONCEPTION COST WELL NO. 1

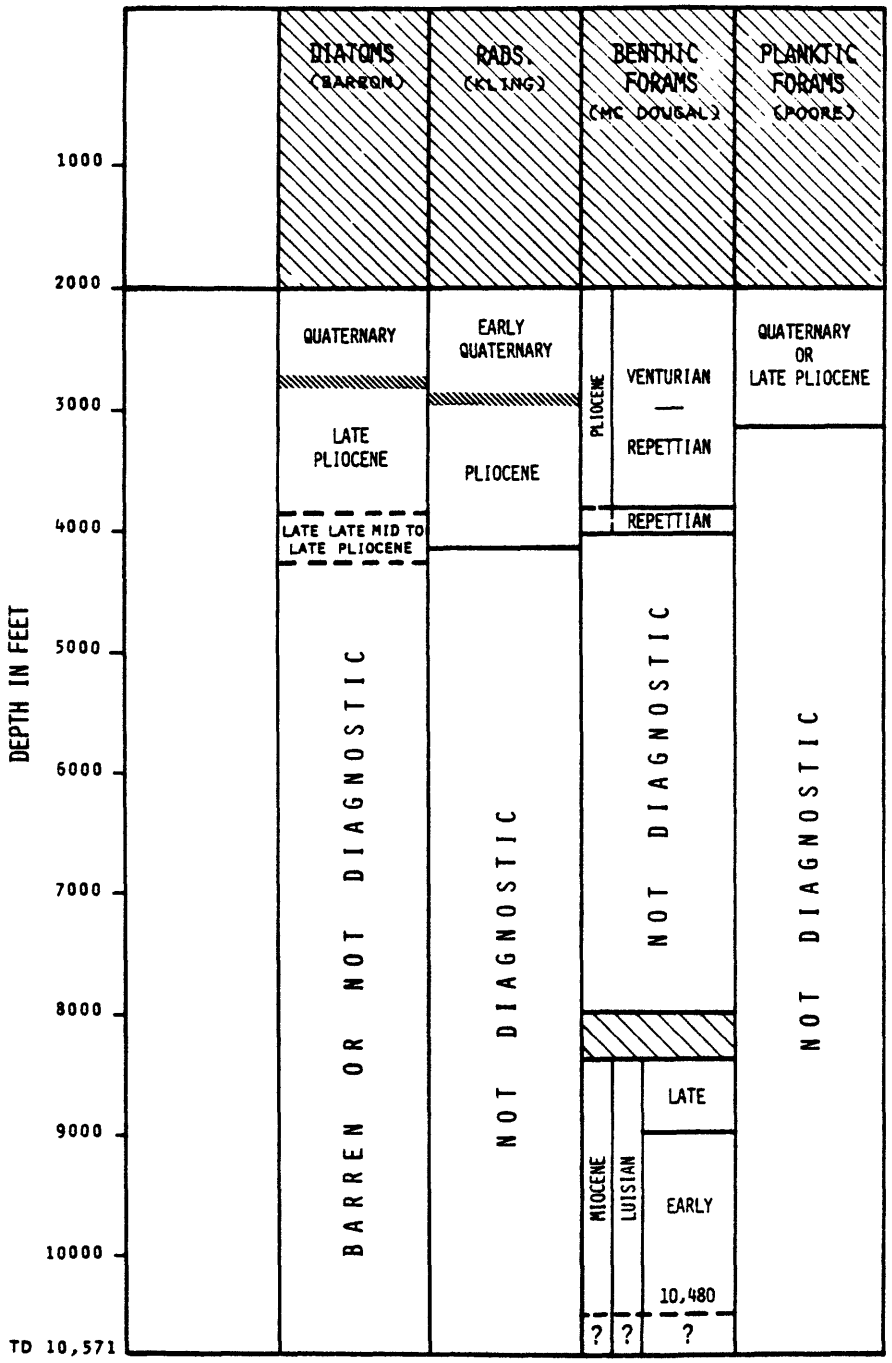

below 3,970 ft are too poorly preserved for accurate identification or are long-ranging taxa that could be downhole contaminants (Fig. 1).

DIATOMS

Ditch cuttings were examined at 90-ft intervals above a depth of 4,300 ft. Below that level, diatoms are absent or are represented by very poorly preserved fragments.

As at nearby Deep Sea Drilling Site 467 in the San Miguel Gap, middle Miocene and upper Miocene diatoms are reworked into most of the younger section. Consequently, last occurrences are difficult to determine. In this study, reliance has been placed on first occurrences, because a normal downhole sequence of Quaternary and Pliocene datums indicates no appreciable downhole contamination.

The last occurrence of Thalassiosira antiqua at 2 660 to 2,690 ft and the first occurrence of Pseudoeunotia doliolus at 2,840 to 2,870 ft are datum levels that both approximate the Pliocene-Quaternary boundary in middle latitudes of the North Pacific. The latter is here considered most reliable to approximate the Pliocene-Quaternary boundary because reworking of Miocene material--and therefore, possibly T. antiqua in the intermediate sample from 2,750 to 2,780 ft is supportive of this conclusion.

At 3,670 to 3,700 ft Denticula kamtschatica and Thalassiosira convexa var. aspinosa have their last occurrences. These late Pliocene datum levels have been assigned absolute ages of 2.4 and 2.15 m.y.B.P. respectively on the basis of correlation to paleomagnetic stratigraphy elsewhere in the Pacific (Koizumi, 1975). Thalassiosira convexa var. aspinosa, however, is a warm-water taxon; and Koizumi (1975) notes that its last occurrence of D. kamtschatica in high latitudes.

The first occurrence of Denticula seminae var. fossils at 3 820 to 3,850 ft is tentatively assigned an absolute age of 2.5 m.y.B.P., corresponding with its first common occurrence in cold-temperature areas of the North Pacific. Relationships at nearby Deep Sea Drilling Site 467 in the San Miguel Gap are supportive of this assignment.

Samples below 3,900 ft are largely undiagnostic, but the sample from 4,210 to 4,240 ft can be no older than late late Miocene because of the presence of Thalassiosira sp. (precursor - T. oestrupii) and Nitzschia rolandii.

RADIOLARIANS

Radiolarians occur in the interval between 2,180 to 2,210 ft and 4,090 to 4,120 ft. They are rare in all samples and very few species are represented. Individuals are reasonably well preserved but the assemblages are poorly preserved from the point of view of completeness.

Few species of biostratigraphic significance are present. No zones

are recognizable with confidence but the general age relationships can be recognized. Samples in the range 2,180-2,210 ft through 2,960-2,990 ft contain Lamprocyrtis neoheteroporos, and toward the bottom of the sequence Eucyrtidium matuyamai is also present, indicating the early Quaternary.

The Pliocene-Quaternary boundary at Deep Sea Drilling Site 173 off Cape Mendocino corresponds to the bottom of the range of Eucyrtidium matuyamai (Kling, 1973). In well cuttings, however, tops of ranges can be recognized with greater confidence and the boundary can be approximated by the (slightly younger) top Lamprocyrtis heteroporos, between the 2,840-2,870-ft and 2,960-2,990-ft samples.

Below 2,960-2,990 ft, Lamprocyrtis heteroporos is consistently present, indicating the Pliocene. No species useful in subdividing the Pliocene were recognized. One specimen of the late Miocene-early Pliocene species Stichocorys peregrina in sample 2,570-2,600 is apparently reworked or contaminated.

Species occurrences are included in Table 1. Abundances are recorded as "very rare" (+: 1-2 specimens per strewn slide of the >44-um fraction), "rare" (R 3-10 specimens per slide), "few" (F: 10-20 per slide), and "common" (C: >20 per slide). Preservation is recorded as M for "moderately good" in a potential sequence of "poor," "moderately good," and "good" preservation based on visual estimates of condition of individual specimens.

BENTHIC FORAMINIFERS

Benthic foraminifers are present in most samples analyzed for this study (Table 2). Quality of preservation and diversity of the benthic foraminifers decreases with depth, varying from well-preserved, fragile, highly diverse assemblages at the top of the hole to low diversity assemblages composed of siliceous molds and poorly preserved calcareous specimens. Pliocene and middle Miocene (early Luisian) benthic foraminiferal species are present (Fig. 1).

Pliocene benthic foraminiferal assemblages are identified in samples 2,030-2,060 to 3,970-4,000. The upper portion (samples 2,030-2,060 to 3,640-3,670) is assigned to the Venturian-Repettian Stages (early-middle Pliocene) whereas the lower portion (samples 3,820-3,850 to 3,970-4,000) is assigned to the early Pliocene, Repettian Stage. The presence of Uvigerina hootsi suggests assignment of the upper interval to the Repettian Stage, but abundances of Bolivina argentea, Bolvinia seminuda, and Buliminella subfusiformis are more characteristic of the Biofacies IV, 900-2,000 ft of Natland (1957), the lower Pico Formation of the Los Angeles Basin (Martin, 1952), and thus diagnostic of the younger Venturian Stage. Assemblages of the lower interval indicate an increase in bathymetry, a decrese in Venturian species and the first appearances downhole of Bulimina subacuminata, Buliminia subcalva, Melonis pompilioides, Siphotextularia flintii, and other species typical of the Repetto Formation (Martin, 1952), Biofacies IV, 2,000-7,500 ± ft (Natland, 1957), and the Repettian Stage (Natland, 1933; Natland and Rothwell, 1954).

Table 1.--Radiolarian species occurrences in the Pt. Conception OCS-Cal 78-164 No. 1 well.

78-164-#1 Interval (ft)	ABUNDANCE PRESERVATION	Artostrobium miralestense	Siphocampe corbula	Siphocampe arachnea	Cornutella profunda	Sphaeropyle langii	Eucyrtidium calvertense	Bathropyramis woodringi	Theocalyptra davisiana	Stylodictya validispina	Pterocanium korotnevi	Pterocorys clausus	Lamprocyrtis nigriniae	Eucyrtidium matuyamai	Lamprocyrtis neoheteroporos	Lamprocyrtis heteroporos	Stichocorys peregrina
2060-2090	B																
2180-2210	R M	R	+	R	-	-	-	-	-	-	-	-	+	-	+	-	-
2270-2300	R M	F	R	-	-	-	-	-	F	-	-	-	-	-	R	-	-
2360-2390	R M	+	R	-	-	-	-	-	+	R	-	-	-	-	+	-	-
2450-2480	R M	R	-	+	-	-	-	-	-	-	-	-	+	-	-	-	-
2570-2600	R M	+	+	R	-	-	-	-	R	-	-	+	-	-	-	-	+
2660-2690	R M	R	-	F	-	-	-	+	R	R	-	-	+	+	+	-	-
2750-2780	R M	R	+	R	+	-	-	-	-	R	-	-	-	-	-	-	-
2840-2870	R M	R	+	C	R	+	-	+	F	R	-	-	-	+	+	-	-
2960-2990	F M	F	-	F	F	-	-	-	F	R	+	-	-	R	R	R	-
3040-3070	R M	R	+	F	+	-	-	-	-	+	-	-	-	-	-	+	-
3130-3160	R M	R	-	C	-	-	-	-	+	R	-	-	-	-	-	+	-
3220-3250	R M	R	-	F	-	-	-	-	+	R	-	-	-	-	-	+	-
3310-3340	R M	-	-	R	-	-	-	-	+	+	-	-	-	-	-	-	-
3400-3430	R M	R	+	F	+	-	-	-	+	+	-	-	-	-	-	+	-
3490-3520	R M	R	-	R	-	-	+	-	-	R	-	-	-	-	-	R	-
3580-3610	R M	R	-	R	-	-	-	-	+	+	-	-	-	-	-	-	-
3670-3700	R M	R	+	C	+	-	+	-	-	R	-	-	-	-	-	R	-
3760-3790	R M	F	-	F	R	-	R	-	-	R	-	-	-	-	-	R	-
3910-3940	R M	R	-	F	R	-	R	-	-	R	-	-	-	-	-	R	-
4000-4030	R M	R	-	F	R	-	-	-	-	R	+	-	-	-	-	+	-
4090-4120	R M	+	-	F	+	-	+	+	-	R	-	-	-	-	-	+	-
4210-4240 through 10,510-10,530	B A R R E N																

Table 2
Pt. Conception cost well

FEET	2030-2060	2240-2270	2330-2360	2540-2570	2720-2750	2930-2960	3100-3130	3289-3310	3460-3490	3640-3670	3820-3850	3970-4000	4150-4180	4570-4600	4960-4990	5350-5380	5770-5800	6160-6190	6610-6640	6820-6850	7030-7060	7210-7240	7450-7480	7900-7930	8350-8380	8560-8590	8740-8770	8920-8950	9100-9130	9310-9340	9520-9550	9730-9760	9810-9940	10090-11126	10270-10300	10450-10480
Bolivina argentea	A	-	A	-	C	-	C	-	C	-	F	-	-	-	-	-	-	-	-	-	-	-	-	-	-	-	-	-	-	-	-	-	-	-	-
Bolivina seminuda	C	-	A	-	-	-	R	-	-	-	-	-	-	-	-	-	-	-	-	-	-	-	-	-	-	-	-	-	-	-	-	-	-	-	-
Bolivina sinuata	F	-	-	-	-	-	-	-	-	-	-	-	-	-	-	-	-	-	-	-	-	-	-	-	-	-	-	-	-	-	-	-	-	-	-
Bulimina auriculata	F	-	F	-	-	-	R	-	-	-	-	-	-	-	-	-	-	-	-	-	-	-	-	-	-	-	-	-	-	-	-	-	-	-	-
Bulimina pagoda	R	-	-	-	-	-	-	-	-	-	-	-	-	-	-	-	-	-	-	-	-	-	-	-	-	-	-	-	-	-	-	-	-	-	-
Bulliminella subfusiformis	F	-	C	-	-	-	-	-	-	-	-	-	-	-	-	-	-	-	-	-	-	-	-	-	-	-	-	-	-	-	-	-	-	-	-
Cassidulina cushmani	F	-	F	-	R	-	-	-	-	-	-	-	-	-	-	-	-	-	-	-	-	-	-	-	-	-	-	-	-	-	-	-	-	-	-
Cassidulina tumida	A	-	C	-	-	-	-	-	-	-	-	-	-	-	-	-	-	-	-	-	-	-	-	-	-	-	-	-	-	-	-	-	-	-	-
Cassidulinoides bradyi	F	-	-	-	-	-	-	-	-	-	-	-	-	-	-	-	-	-	-	-	-	-	-	-	-	-	-	-	-	-	-	-	-	-	-
Cibicides mckannai	F	F	F	-	-	-	R	-	F	-	C	F	-	-	-	-	-	-	-	-	-	-	-	-	-	-	-	-	-	-	-	-	-	-	-
Epistominella bradyana	C	-	F	-	-	-	-	-	R	-	-	-	-	-	-	-	-	-	-	-	-	-	-	-	-	-	-	-	-	-	-	-	-	-	-
Epistominella pacifica	C	F	A	-	C	-	C	-	C	R	A	F	-	-	-	-	-	-	-	-	-	-	-	-	-	-	-	-	-	-	-	-	-	-	-
Globobulimina affinis	C	C	C	F	-	-	R	-	-	-	-	-	-	-	-	-	-	-	-	-	-	-	-	-	-	-	-	-	-	-	-	-	-	-	-
Gyroidina multilocula	F	-	-	-	-	-	R	-	F	-	F	-	-	-	-	-	-	-	-	-	-	-	-	-	-	-	-	-	-	-	-	-	-	-	-
Gyroidina sp.	R	-	-	-	-	-	-	-	-	R	-	-	-	-	-	-	-	-	-	-	-	-	-	-	-	-	-	-	-	-	-	-	-	-	-
Loxostomum pseudobeyrichi	F	-	R	-	-	-	-	-	-	-	-	-	-	-	-	-	-	-	-	-	-	-	-	-	-	-	-	-	-	-	-	-	-	-	-
Nonionella labradorica	R	-	-	-	-	-	-	-	-	-	-	-	-	-	-	-	-	-	-	-	-	-	-	-	-	-	-	-	-	-	-	-	-	-	-
Oridorsalis umbonatus	C	-	-	-	-	-	F	-	-	-	F	-	-	-	-	-	-	-	-	-	-	-	-	-	-	-	-	-	-	-	-	-	-	-	-
Planulina ornata	F	F	F	F	R	-	F	-	F	-	-	-	-	-	-	-	-	-	-	-	-	-	-	-	-	-	-	-	-	-	-	-	-	-	-
Pullenia salkinae	F	-	-	-	-	-	-	-	-	-	-	-	-	-	-	-	-	-	-	-	-	-	-	-	-	-	-	-	-	-	-	-	-	-	-
Pyrgo cf. P. murrhina	R	R	-	-	-	-	-	-	-	-	-	-	-	-	-	-	-	-	-	-	-	-	-	-	-	-	-	-	-	-	-	-	-	-	-
Uvigerina hispidacostata	F	-	-	-	-	-	F	-	C	-	F	-	-	-	-	-	-	-	-	-	-	-	-	-	-	-	-	-	-	-	-	-	-	-	-
Uvigerina hootsi	F	-	F	-	-	-	-	-	-	-	-	-	-	-	-	-	-	-	-	-	-	-	-	-	-	-	-	-	-	-	-	-	-	-	-
Uvigerina peregrina	C	A	A	C	C	-	A	-	A	-	F	C	-	-	-	-	-	-	-	-	-	-	-	-	-	-	-	-	-	-	-	-	-	-	-
Valvulineria araucana	F	-	R	-	-	-	-	-	-	-	-	-	-	-	-	-	-	-	-	-	-	-	-	-	-	-	-	-	-	-	-	-	-	-	-
Bolivina sp.	-	F	-	F	-	-	R	-	-	-	-	-	-	-	-	-	-	-	-	-	-	-	-	-	-	-	-	-	-	-	-	-	-	-	-
Cassidulina californica	-	R	A	-	R	-	R	-	F	-	F	-	-	-	-	-	-	-	-	-	-	-	-	-	-	-	-	-	-	-	-	-	-	-	-
Lenticulina sp.	-	F	F	F	-	-	R	F	R	R	F	F	-	-	-	-	-	-	-	-	-	-	-	-	-	-	-	-	R	-	-	-	-	-	-
Hoeglundina elegans	-	F	F	F	-	-	-	-	-	-	-	-	-	-	-	-	-	-	-	-	-	-	-	-	-	-	-	-	-	-	-	-	-	-	-
Quinqueloculina lamarckiana	-	R	R	-	F	-	R	-	C	-	-	-	-	-	-	-	-	-	-	-	-	-	-	-	-	-	-	-	-	-	-	-	-	-	-
Siphotextularia flintii	-	R	R	-	-	-	-	-	-	-	-	-	-	-	-	-	-	-	-	-	-	-	-	-	-	-	-	-	-	-	-	-	-	-	-
Bolivina spissa	-	-	A	-	-	-	-	-	-	-	-	-	-	-	-	-	-	-	-	-	-	-	-	-	-	-	-	-	-	-	-	-	-	-	-
Dentalina albatrossi	-	-	R	-	-	-	-	-	-	-	-	-	-	-	-	-	-	-	-	-	-	-	-	-	-	-	-	-	-	-	-	-	-	-	-
Fissurina orbignyana elliptica	-	-	R	-	-	-	-	-	-	-	R	-	-	-	-	-	-	-	-	-	-	-	-	-	-	-	-	-	-	-	-	-	-	-	-
Fissurina tricostulata	-	-	R	-	-	-	-	-	-	-	-	-	-	-	-	-	-	-	-	-	-	-	-	-	-	-	-	-	-	-	-	-	-	-	-
Gyroidina soldanii	-	-	F	-	-	-	-	-	-	-	-	-	-	-	-	-	-	-	-	-	-	-	-	-	-	-	-	-	-	-	-	-	-	-	-
Melonis barleeanus	-	-	R	-	-	-	-	-	-	-	-	-	-	-	-	-	-	-	-	-	-	-	-	-	-	-	-	-	-	-	-	-	-	-	-
Nodosaria anomala	-	-	F	-	-	-	F	-	R	-	-	-	-	-	-	-	-	-	-	-	-	-	-	-	-	-	-	-	-	-	-	-	-	-	-
Nodosaria longiscata	-	-	F	-	-	-	-	-	-	-	-	-	-	-	-	-	-	-	-	-	-	-	-	-	-	-	-	-	-	-	-	-	-	-	-

Table 2 (CONT.)
Pt. Conception cost well

	FEET	2030-2060	2246-2270	2330-2360	2546-2570	2720-2750	2930-2960	3100-3130	3289-3320	3460-3490	3640-3670	3820-3850	3957-4020	4150-4180	4570-4600	4960-4990	5350-5380	5770-5800	6160-6190	6610-6640	6820-6850	7030-7060	7210-7240	7450-7480	7900-7930	8350-8380	8560-8590	8740-8770	8927-8957	9110-9140	9310-9340	9520-9550	9730-9760	9910-9940	10090-10120	10270-10300	10450-10480
Oridorsalis tenera		-	-	R	-	-	-	-	-	-	-	-	-	-	-	-	-	-	-	-	-	-	-	-	-	-	-	-	-	-	-	-	-	-	-	-	-
Planulina wuellerstorfi		-	-	F	-	-	-	-	-	-	-	-	-	-	-	-	-	-	-	-	-	-	-	-	-	-	-	-	-	-	-	-	-	-	-	-	-
Plectofrondicularia advena		-	-	F	-	R	-	F	-	F	-	-	-	-	-	-	-	-	-	-	-	-	-	-	-	-	-	-	-	-	-	-	-	-	-	-	-
Cassidulina translucens		-	-	-	F	-	-	C	-	-	-	A	-	-	-	-	-	-	-	-	-	-	-	-	-	-	-	-	-	-	-	-	-	-	-	-	-
Dentalina soluta		-	-	-	R	-	-	-	-	F	-	F	-	-	-	-	-	-	-	-	-	-	-	-	-	-	-	-	-	-	-	-	-	-	-	-	-
Trichohyalus ornatissima		-	-	-	-	R	-	-	-	F	-	-	-	-	-	-	-	-	-	-	-	-	-	-	-	-	-	-	-	-	-	-	-	-	-	-	-
Bulimina subacuminata		-	-	-	-	-	-	F	-	A	-	A	-	-	-	-	-	-	-	-	-	-	-	-	-	-	-	-	-	-	-	-	-	-	-	-	-
Bulimina pseudoaffinis		-	-	-	-	-	-	R	-	-	-	-	-	-	-	-	-	-	-	-	-	-	-	-	-	-	-	-	-	-	-	-	-	-	-	-	-
Cassidulina limbata		-	-	-	-	-	-	F	-	F	-	-	-	-	-	-	-	-	-	-	-	-	-	-	-	-	-	-	-	-	-	-	-	-	-	-	-
Elphidiella hannai		-	-	-	-	-	-	F	F	A	-	-	-	-	-	-	-	-	-	-	-	-	-	-	R	-	-	-	-	-	-	-	-	-	-	-	-
Uvigerina hispida		-	-	-	-	-	-	F	-	F	-	A	-	-	-	-	-	-	-	-	-	-	-	-	-	-	-	-	-	-	-	-	-	-	-	-	-
Uvigerina peregrina dirupta		-	-	-	-	-	-	F	-	F	-	-	-	-	-	-	-	-	-	-	-	-	-	-	-	-	-	-	-	-	-	-	-	-	-	-	-
Buliminella curta basispinata		-	-	-	-	-	-	-	-	R	-	-	-	-	-	-	-	-	-	-	-	-	-	-	-	-	-	-	-	-	-	-	-	-	-	-	-
Eponides healdi		-	-	-	-	-	-	-	-	R	-	-	-	-	-	-	-	-	-	-	-	-	-	-	-	-	-	-	-	-	-	-	-	-	-	-	-
Lagena costata		-	-	-	-	-	-	-	-	F	-	R	-	-	-	-	-	-	-	-	-	-	-	-	-	-	-	-	-	-	-	-	-	-	-	-	-
Polymorphina charlottensis		-	-	-	-	-	-	-	-	F	-	-	-	-	-	-	-	-	-	-	-	-	-	-	-	-	-	-	-	-	-	-	-	-	-	-	-
Bulimina rostrata		-	-	-	-	-	-	-	-	-	-	F	-	-	-	-	-	-	-	-	-	-	-	-	-	-	-	-	-	-	-	-	-	-	-	-	-
Bulimina subclava		-	-	-	-	-	-	-	-	-	-	F	-	-	-	-	-	-	-	-	-	-	-	-	-	-	-	-	-	-	-	-	-	-	-	-	-
Marginulina sp.		-	-	-	-	-	-	-	-	-	-	R	-	-	-	-	-	-	-	-	-	-	-	-	-	-	-	-	-	-	-	-	-	-	-	-	-
Melonis pompilioides		-	-	-	-	-	-	-	-	-	-	F	R	-	-	-	-	-	-	-	-	-	-	-	-	-	-	-	-	-	-	-	-	-	-	-	-
Sigmoilina tenuis		-	-	-	-	-	-	-	-	-	-	R	-	-	-	-	-	-	-	-	-	-	-	-	-	-	-	-	-	-	-	-	-	-	-	-	-
Sphaeroidina bulloides		-	-	-	-	-	-	-	-	-	-	R	-	-	-	-	-	-	-	-	-	-	-	-	-	-	-	-	-	-	-	-	-	-	-	-	-
Uvigerina proboscidea		-	-	-	-	-	-	-	-	-	-	R	-	-	-	-	-	-	-	-	-	-	-	-	-	-	-	-	-	-	-	-	-	-	-	-	-
Agglutinated fragments		-	-	-	-	-	-	-	-	-	-	-	-	F	-	C	-	A	C	C	-	C	-	C	C	-	-	F	-	F	F	F	F	F	F	-	A
Bathysiphon sp.		-	-	-	-	-	-	-	-	-	-	-	-	-	-	F	-	-	F	F	-	-	-	-	-	-	-	-	-	-	-	-	-	-	-	-	-
?Karreriella milleri		-	-	-	-	-	-	-	-	-	-	-	-	-	-	F	-	-	F	F	-	-	-	-	F	-	-	-	-	-	-	-	-	-	-	-	-
Martinottiella sp.		-	-	-	-	-	-	-	-	-	-	-	-	-	-	F	-	-	-	-	-	-	-	-	-	-	-	-	-	-	-	-	-	-	-	-	-
Bolivina cf. B. advena striatella		-	-	-	-	-	-	-	-	-	-	-	-	-	-	-	-	-	-	-	-	-	-	-	-	F	-	-	-	F	C	C	-	C	-	-	F
Valvulineria sp.		-	-	-	-	-	-	-	-	-	-	-	-	-	-	-	-	-	-	-	-	-	-	-	-	F	-	-	-	-	-	-	-	-	-	-	-
Pullenia miocenica globula		-	-	-	-	-	-	-	-	-	-	-	-	-	-	-	-	-	-	-	-	-	-	-	-	-	-	R	-	-	-	-	-	-	-	-	-
Valvulineria californica var.		-	-	-	-	-	-	-	-	-	-	-	-	-	-	-	-	-	-	-	-	-	-	-	-	-	-	-	-	C	A	A	C	A	F	F	A
Baggina robusta		-	-	-	-	-	-	-	-	-	-	-	-	-	-	-	-	-	-	-	-	-	-	-	-	-	-	-	-	-	F	-	-	-	-	-	R
Bulimina sp.		-	-	-	-	-	-	-	-	-	-	-	-	-	-	-	-	-	-	-	-	-	-	-	-	-	-	-	-	-	F	-	-	-	-	-	-
Siphogenerina branneri		-	-	-	-	-	-	-	-	-	-	-	-	-	-	-	-	-	-	-	-	-	-	-	-	-	-	-	-	-	A	-	-	-	-	-	-
Uvigerina sp.		-	-	-	-	-	-	-	-	-	-	-	-	-	-	-	-	-	-	-	-	-	-	-	-	-	-	-	-	-	F	C	-	-	-	-	-
Bulimina mexicana		-	-	-	-	-	-	-	-	-	-	-	-	-	-	-	-	-	-	-	-	-	-	-	-	-	-	-	-	-	-	C	F	F	R	R	F
Marginulina beali		-	-	-	-	-	-	-	-	-	-	-	-	-	-	-	-	-	-	-	-	-	-	-	-	-	-	-	-	-	F	-	-	-	-	-	R
																															F	-	-	-	-	-	-

Table 2 (CONT.)

Pt. Conception cost well

FEET	2030-2060	2240-2270	2330-2360	2540-2570	2720-2750	2930-2960	3100-3130	3289-3310	3460-3490	3640-3670	3820-3850	3970-4000	4150-4180	4570-4600	4960-4990	5350-5380	5770-5800	6160-6190	6610-6640	6820-6850	7030-7060	7210-7240	7450-7480	7900-7930	8350-8380	8560-8590	8740-8770	8920-8950	9100-9130	9310-9340	9520-9550	9730-9760	9910-9940	10090-10120	10270-10300	10450-10480
Orthomorphina rohri	-	-	-	-	-	-	-	-	-	-	-	-	-	-	-	-	-	-	-	-	-	-	-	-	-	-	-	-	-	-	F	-	-	-	-	-
Siphogenerina reedi	-	-	-	-	-	-	-	-	-	-	-	-	-	-	-	-	-	-	-	-	-	-	-	-	-	-	-	-	-	-	R	-	-	-	-	-
Uvigerina joaquinensis	-	-	-	-	-	-	-	-	-	-	-	-	-	-	-	-	-	-	-	-	-	-	-	-	-	-	-	-	-	-	F	-	-	-	-	C
Bolivina tumida	-	-	-	-	-	-	-	-	-	-	-	-	-	-	-	-	-	-	-	-	-	-	-	-	-	-	-	-	-	-	-	R	F	-	-	-
Siphogenerina sp.	-	-	-	-	-	-	-	-	-	-	-	-	-	-	-	-	-	-	-	-	-	-	-	-	-	-	-	-	-	-	-	F	-	-	-	-
Cibicides sp.	-	-	-	-	-	-	-	-	-	-	-	-	-	-	-	-	-	-	-	-	-	-	-	-	-	-	-	-	-	-	-	-	R	R	-	-
Nonionella miocenica	-	-	-	-	-	-	-	-	-	-	-	-	-	-	-	-	-	-	-	-	-	-	-	-	-	-	-	-	-	-	-	-	R	R	-	-
Eggerella sp.	-	-	-	-	-	-	-	-	-	-	-	-	-	-	-	-	-	-	-	-	-	-	-	-	-	-	-	-	-	-	-	-	-	R	-	-
Dentalina sp.	-	-	-	-	-	-	-	-	-	-	-	-	-	-	-	-	-	-	-	-	-	-	-	-	-	-	-	-	-	-	-	-	-	-	R	-
Lenticulina smileyi	-	-	-	-	-	-	-	-	-	-	-	-	-	-	-	-	-	-	-	-	-	-	-	-	-	-	-	-	-	-	-	-	-	-	-	F
ASSOCIATED MICROFOSSILS																																				
Diatoms	F	F	-	-	F	-	-	F	A	F	-	-	-	-	-	F	-	-	-	-	-	-	-	-	-	-	-	-	-	-	-	-	-	-	-	-
Radiolarians	F	F	F	R	F	A	C	-	F	A	C	-	-	-	-	-	-	-	-	-	-	-	-	-	-	-	-	-	R	-	-	-	-	-	-	-
Sponge spicules	F	C	-	F	-	A	-	-	F	F	C	-	-	-	-	-	-	-	-	-	-	-	-	-	-	-	-	-	-	-	-	-	-	-	-	-
Megafossil fragments	C	F	A	-	F	R	-	F	A	F	-	-	-	-	-	-	-	-	-	-	-	-	-	R	-	-	-	-	-	-	R	-	F	-	F	-
Planktic foraminifera	C	C	C	-	F	-	F	F	F	-	F	-	-	-	-	-	-	F	-	-	-	-	R	R	C	C	F	C	F	F	F	F	F	R	-	-
Echinoid spines	-	-	-	F	F	R	-	-	-	F	-	-	-	-	-	-	-	-	-	-	-	-	-	R	-	-	-	-	-	-	R	-	-	-	-	-
Fish debris	-	-	-	-	F	-	-	-	-	H	-	H	-	-	-	-	-	-	F	-	-	-	-	-	-	-	-	-	-	-	-	-	-	-	-	-

KEY:
A = Abundant (>50 specimens)
C = Common (20-50 specimens)
F = Few (2-19 specimens)
R = Rare (1 specimen)

The early-middle Pliocene age assignment does not agree with the diatom or radiolarian evidence presented in this paper for the same interval. The ecologic facies aspect of the Pliocene stages was recognized years ago (Ingle, 1967), and usage requires a knowledge of local ecology and geography. Many Pliocene species are still living and stage assignments are based on species abundances and depth associations. This Point Conception well lies far to the north and east of the type sections and the stages may therefore have different chronostratigraphic relations.

Below the Pliocene interval, arenaceous foraminifers dominate the asemblages (samples 4,150-4,180 to 7,900-7,930). These specimens are fine-grained, acid-resistant, crushed forms and are not age diagnostic. One form resembling Karreriella milleri first appears in sample 4,960-4,990. The first appearance (downsection) of this species is indicative of the middle Repettian Stage in the Los Angeles Basin (Natland and Rothwell, 1954). A similar age relation is probable for this well. The Pliocene-Miocene boundary and the Mohnian and Delmontian Stages cannot be recognized.

Miocene calcareous benthic foraminifers occur in samples 8,350-8,380 to 10,450-10,480. The appearances of Bolvinia advena striatella and Pullenia miocenica globula in samples 8,350-8,380 to 8,920-8,950 are diagnostic of the late Luisian Stage. Valvulineria californica sensu lato, Marginulina beali, Siphogenerina reedi, and Siphogenerina branneri, which appear in samples 9,100-9,130 to 10,450-10,480, suggest assignment to the early Luisian Stage. Zonal assignments are not possible.

Benthic foraminifer (Miocene, this paper) and calcareous nannofossil (lower Cretaceous or Jurassic, Bukry, this report) age determinations in this lower interval, 9,970 to 10,571 ft, disagree. This discrepancy can be attributed to either downhole contamination or reworking. Additional samples below 9,000 ft (Table 3), contain benthic foraminifers in siltstone and sandstone chips typical of lithologies stratigraphically higher but not in the dark gray siltstones below 9,735 ft (McLean, this report). This evidence strongly supports contamination. The second hypothesis, reworking of the calcareous nannofossils into younger sediment, cannot be discounted as no other fossil group corroborates the lower Cretaceous or Jurassic age and nannofossils are frequently and easily reworked.

PLANKTIC FORAMINIFERS

Planktic foraminifers are sparse to common and moderately well preserved in samples from 2,030 ft through 3,850 ft. Samples from 2,330 ft through 3,130 ft contain Neogloboquadrina pachyderma (s.s.), Globigerinita glutinata, Turborotalita quinqueloba, Globigerina bulloides, and Globoratolia bulloides, and Globorotalia inflata (sample 2,030-2,060 ft only) The above association suggests assignment to the late Pliocene or Quaternary. The occurrence of robust Neogloboquadrina sp, cf. N. pachyderma form 3 of Keller (1978) and Globorotalia sp. cf G. punticulata in sample 3,460-3,490 ft suggests a Pliocene assignment. Planktic foraminifers in the remaining samples examined are either long-ranging taxa or too poorly preserved for accurate identification.

Table 3.--Benthic foraminifers in the 9940-10570 ft interval, Pt. Conception OCS-Cal 78-164 No. 1 well.

	9940-9970	10000-10030	10360-10390	10480-10570
Arenaceous, no identification	C	C	-	-
Baggina robusta	R	-	-	-
Bolivina cf. B. advena striatella	F	F	F	F
Bulimina montereyana	C	F	F	F
Lenticulina sp.	F	-	-	-
Valvulineria californica var.	A	A	C	C
Bathysiphon sp.		F	-	-
Uvigerina joaquinensis		C	F	-
Lagena costata			R	-
Nodosaria sp.			R	R
Siphogenerina branneri			F	-
Bolivina tumida				F
Vernuilina sp.				F
Planktic foraminifers		F	-	-

PALEOECOLOGY

Benthic foraminiferal assemblages of the Point Conception well suggest water depths of middle to lower bathyal during the Pliocene, lower bathyal or deeper for the nondiagnostic interval, and upper bathyal during the Luisian. These interpretations are based on the abundant to common species and specimens of the superfamilies Cassidulinacea and Buliminacea and abundant agglutinated specimens. The diverse, well-preserved assemblages of the Pliocene interval (samples 2,030-2,060 to 3,970-4,000) contain common to abundant Bolivina argentea, Bolivina sinuata, Bolivina seminuda, costated buliminids, Cassidulina cushmani, epistominellids, and costated and hispid uvigerinids which are indicative of the middle and lower bathyal biofacies of Natland (1957) and Ingle (1967, 1973), Near the base of the Pliocene interval, the appearance of Melonis pompilioides and Bulimina rostrata suggest increased water depths. Although not conclusive, the presence of ?Karreriella milleri, abundant fine-grained agglutinated foraminifers and common planktic foraminifers in the nondiagnostic interval (samples 4,150-4,180 to 7,900-7,930) support a lower bathyal or deeper water depth interpretation. Valvulineria californica s.l. and common Bolvinia advena striatalla, costated uvigerinids and bagginids indicate upper bathyal water depths (Bandy and Arnal, 1969; Ingle, 1973) in the middle Miocene (samples 8,350-8,380 to 10,450-10,480).

REFERENCES CITED

Bandy, O. L., and Arnal, R. E., 1969, Middle Tertiary basin development, San Joaquin Valley, California Geological Society of America Bulletin, v. 80, p. 783-820.

Ingle, J. C., Jr., 1967, Foraminiferal biofacies variation and the Miocene-Pliocene boundary in southern California: Bulletins of American Paleontology, v. 52, no. 236, p 210-394.

_____ 1973, Biostratigraphy and paleoecology of early Miocene through early Pleistocene benthonic and planktonic Foraminifera, San Joaquin Hills-Newport Bay-Dana Point area, Orange County, California, in Miocene sedimentary environments and biofacies, southeastern Los Angeles Basin, SEPM Field Trip No. 1: American Association of Petroleum Geologists-Society of Economic Paleontologists and Mineralogists-Society of Economic Geologists, Annual Meeting, 1973, p. 18-38.

Keller, Gerta, 1978, Late Neogene planktonic foraminiferal biostratigraphy and paleoceanography of the northeastern Pacific: evidence from DSDP Sites 173 and 310 at the North Pacific Front: Journal of Foraminiferal Research, v. 8, p. 332-349.

Kling, S. A., 1973, Radiolaria from the eastern North Pacific, Deep Sea Drilling Project, Leg 18: Deep Sea Drilling Projects Initial Reports, U.S. Government Printing Office, Washington, D.C., v. 18, p. 1069-1117.

Koizumi, I., 1975, Diatom events in the late Cenozoic deep-sea sequences in the North Pacific: Geological Society of Japan Journal, v. 81, no. 9, p. 567-578

Martin Lewis, 1952, Some Pliocene Foraminifera from a portion of the Los Angeles Basin, California: Cushman Foundation for Foraminiferal Research Contributions, v. 3, pt. 3-4, p 107-140.

Natland, M. L., 1933, The temperature and depth-distribution of some Recent and fossil Foraminifera in the southern California region: Scripps Institution of Oceanography Bulletin, Technical Series, v. 3, no. 10, p. 225-230

_____ 1957, Paleoecology of West Coast Tertiary sediments, in Ladd, H. S., ed., Treatise on marine paleoecology: Geological Society of America Memoir 67, v, 2, p 543-572.

Natland, M. L., and Rothwell, W. T., 1954, Fossil Foraminifera of the Los Angeles and Ventura regions, California, [Pt. 5], in Chap. 3 of Jahns, R. H. ed., Geology of southern California: California Division of Mines Bulletin 170, p. 33-42.

COCCOLITH STRATIGRAPHY

David Bukry
U.S. Geological Survey
Scripps Institute of Oceanography
La Jolla, California

INTRODUCTION

Quaternary, Pliocene, Miocene, and Lower Cretaceous or uppermost Jurssic coccoliths occur at variable abundances, in sequence, through the 10,571-ft Pt. Conception well located 19 mi southwest of Pt. Arguello, California (see McCulloch et al., this report). Of the total of 126 samples examined, 73 are barren. Zonally diagnostic coccolith assemblages occur in the Quaternary and Pliocene section from 2,210 to 4,270 ft and in the lower middle Miocene section from 8,200 to 9,820 ft. The bulk of the section from 4,270 to 8,110 ft is barren or contains nondiagnostic traces of coccoliths. The consistent Lower Cretaceous or uppermost Jurassic assemblage of the interval from 9,970 to 10,571 ft has a low-diversity, long-ranged species array that is not zonally diagnostic. All depths and sample numbers in Figure 1 and the text represent drilled depths beginning at the derrick floor. Thus, the sea floor is at a drilled depth of 1,465 ft (derrick floor 37 ft above sea level plus water depth of 1,428 ft).

COCCOLITH STRATIGRAPHY

This study is based on light-microscope examination of smear slides prepared at Menlo Park from washed well cuttings. Each well-cutting sample represents a 30-ft stratal increment within the well. Therefore, biostratigraphic conclusions concerning a 30-ft increment are usually based on a random chip. An oil immersion 100X magnification objective was used for species identification of small Quaternary and Mesozoic species, where possible. In some cases, however, slide preparations for Mesozoic samples were too thick, leading to indefinite species identifications. Samples are assigned to coccolith zones or zonal intervals using the definitions of Bukry (1973a, 1975). Separate slides made for several different lithologic chips were studied for the intervals of the lowest Miocene and Cretaceous part of the section (9,820 to 10,571 ft). These multiple slides permitted the identification of both Miocene and Mesozoic assemblages within only one interval (9,970 to 10,000 ft) which, therefore, includes the contact between the Miocene section and the underlying Mesozoic section (Fig. 1).

QUATERNARY 2,210 to 3,550 ft

Coccoliths and siliceous phytoplankton are common in sample 2210-2240. The overlap of *Emiliania ovata* Bukry and *Gephyrocapsa* sp. aff. *G. caribbeanica* Boudreaux and Hay indicate the Quaternary *Emiliania ovata* Subzone or *Gephyrocapsa caribbeanica* Subzone. Several underlying samples

AGE	ZONE	SUBZONE	COST WELL 78-164-1
Quaternary	*Emiliania huxleyi*		
	Gephyrocapsa oceanica	*Ceratolithus cristatus*	
		Emiliania ovata	2210-2630
	Crenalithus doronicoides	*Gephyrocapsa caribbeanica*	
		Emiliania annula	2870-3550
Pliocene	*Discoaster brouweri*	*Cyclococcolithina macintyrei*	3610-3640
		Discoaster pentaradiatus	
		Discoaster surculus	3700-3880
		Discoaster tamalis	4030-4060 / 4120-4270
	Reticulofenestra pseudoumbilica	*Discoaster asymmetricus*	
		Sphenolithus neoabies	
	Amaurolithus tricorniculatus	*Ceratolithus rugosus*	
		Ceratolithus acutus	
		Triquetrorhabdulus rugosus	
Miocene	*Discoaster quinqueramus*	*Amaurolithus primus*	
		Discoaster berggrenii	
	Discoaster neohamatus	*Discoaster neorectus*	
		Discoaster bellus	
	Discoaster hamatus	*Catinaster calyculus*	
		Helicosphaera carteri	
	Catinaster coalitus		
	Discoaster exilis	*Discoaster kugleri*	
		Coccolithus miopelagicus	
	Sphenolithus heteromorphus		8200-9820
	Helicosphaera ampliaperta		
	Sphenolithus belemnos		9970-10000
	Triquetrorhabdulus carinatus	*Discoaster druggii*	
		Discoaster deflandrei	
Mesozoic	[Lower Cretaceous or uppermost Jurassic]		9970-10571

Figure 1.--Correlation of coccoliths from COST Well 78-164-1 sample intervals. Numbers represent upper and lower limits of individual sample intervals or sequences of samples that are assigned to a biostratigraphic unit. Miocene to Quaternary zonation from Bukry (1973, 1975). An unconformity between Mesozoic and Miocene is indicated in sample interval 9970-10,000.

are barren or have poor nondiagnostic coccoliths, but the occurrence of the silicoflagellates Distephanus octonarius Deflandre of Ling (1973) and D. speculum (Ehrenberg) indicate a cool-water mid Quaternary assemblage in sample 2300-2330. The highest Helicosphaera sellii (Bukry and Bramlette) is noted in sample 2600-2630 overlapping with G. caribbeanica indicating mid or lower Quaternary. The low diversity of these cool-water assemblages prevents detailed zonation.

Coccoliths are more common in samples 2870-2900 and 2990-3015 which contain the highest specimens of Cyclococcolithina macintyrei (Bukry and Bramlette). In the absence of Gephyrocapsa, the sparse C. macintyrei, without Pliocene discoasters, suggest the basal Quaternary Emiliania annula Subzone. But the presence of reworked Eocene and middle Miocene coccoliths means that C. macintyrei might also be reworked. Coccoliths present in 2990-3015 include: Coccolithus pelagicus (Wallich), Crenalithus doronicoides (Black and Barnes), Cyclococcolithina leptopora (Murray and Blackman), C. macintyrei, Emiliania ovata, Helicosphaera carteri (Wallich), H. sellii, and reworked Cyclicargolithus floridanus (Roth and Hay), Discoaster deflandrei Bramlette and Riedel, Helicosphaera seminulum Bramlette and Sullivan, and Sphenolithus heteromorphus Deflandre.

Identifiable coccoliths are sparse or absent in samples 3070-3100, 3160-3190, and 3430-3460. Only general Cenozoic or Neogene to Quaternary determinations are possible.

The deepest sample assigned to the Quaternary, 3520-3550, has no Gephyrocapsa, but Cyclococcolithina macintyrei is significantly sparser relative to underlying sample 3610-3730. The usual criteria employing Discoaster, C. macintyrei or Gephyrocapsa, for identifying the Pliocene-Quaternary boundary that have been proposed by various authors are unsatisfactory at well 78-164-1 because of the scarcity of these three fossils, the reworking, and the low-diversity of th assemblages.

PLIOCENE 3,610-4,270 ft

The coccolith assemblage of sample 3610-3640 is similar to the 3520-3550 but the more abundant Cyclococcolithina macintyrei, slightly more abundant discoasters (in place?), and the lack of Miocene and Eocene reworking, are used for a Pliocene assignment. Three underlying samples 3700-3730, 3790-3820, and 3850-3880, are assigned to the upper Pliocene Discoaster surculus Subzone on the basis of Ceratolithus rugosus Bukry and Bramlette, Discoaster brouweri Tan, D. intercalaris Bukry D. pentaradiatus Tan, D. surculus Martini and Bramlette, and the absence of Reticulofenestra pseudoumbilica (Gartner). Coccoliths are moderately preserved and common to abundant. Reworked taxa, including Cenozoic Discoaster deflandrei and Cretaceous Cretarhabdus crenulatus Bramlette and Martini and Biscutum sp., are sparse.

Abundant coccoliths in sample 4030-4060 belong to the lower upper Pliocene Discoaster tamalis Subzone. Discoaster asymmetricus Gartner and D. tamalis Kamptner occur with D. brouweri and D. surculus. Reticulofenestra

pseudoumbilica is too sparse, in veiw of the Miocene reworking suggested by the silicoflagellate Dictyocha pseudofibula, to assign the sample to the subjacent lower Pliocene Discoaster asymmetricus Subzone Coccoliths are gradationally less abundant and diagnostic in the two underlying samples, 4120-4180 and 4240-4270, but both contain D. asymmetricus indicating correlation with the D. tamalis Subzone or D. asymmetricus Subzone.

NEOGENE, UNDIFFERENTIATED 4,270-8,110 ft

Very sparse, irregular and fragmented Reticulofenestra sp. or Coccolithus sp. in samples -5590, -6280, and -6820, and Helicosphaera carteri? in -5680 may be contaminants. They provide no stratigraphic resolution for the interval of 4,270 to 8,110 ft. The Pliocene, above, and middle or lower Miocene, below established the Neogene correlation of the interval.

MIOCENE 8,200-10,000 ft

Coccoliths in samples from the interval 8200-9820 correlate with assemblages near the internationally recognized lower Miocene to middle Miocene boundary (Bukry, 1978) on the basis of the presence of Sphenolithus heteromorphus. This species ranges from about 14 to 17.5 Ma and has been reported from dart cores in the California Continental Borderland that contain benthic foraminifers indicative of the Saucesian, Relizian, and Luisian provincial benthic stages (Crouch and Bukry, 1979). Coccoliths are rare to meager through this interval and low-diversity and dissolution prevent specific assignment of the assemblages to the Helicosphaera ampliaperta Zone or Sphenolithus heteromorphus Zone which, together, encompass the range of S. heteromorphus. Typical assemblages include only Coccolithus pelagicus, Cyclicargolithus floridanus, Discoaster deflandrei, D. sp., Helicosphaera carteri, Reticulofenestra sp. (small), Sphenolithus heteromorphus, and S. moriformis Bronnimann and Stradner.

Of 39 samples examined from the interval of 8,200 to 10,000 ft (including all 14 from the rotary-cut core 9529-9549), 25 are barren, and 7 of the 14 coccolith-bearing samples contain Sphenolithus heteromorphus. Sample 9970-10,000B occurs below three barren samples from 9,880-9,910 ft and below the deepest S. hetermorphus in sample 9790-9820. Coccoliths of 9970-10,000B are assigned to the lower or middle Miocene because of the overlap of Cyclicargolithus floridanus with Helicosphaera carteria. Other species present include Coccolithus miopelagicus Bukry C. pelagicus, Discoaster deflandrei, and Sphenolithus sp. Two other samples from 9,970-10,000 ft contain unmixed Cretaceous coccoliths (sample 9970-10,000A) and a mixture of Cretaceous and Neogene coccoliths (sample 9970-10,000).

CRETACEOUS OR JURASSIC 9,970-10,571 ft

Low-diversity Lower Cretaceous or uppermost Jurassic coccolith assemblages characterize the lower 600 ft of this well. Preservation is moderate to good with slight to moderate dissolution. Abundance is variable, even for chips from the same coring interval. For example, cocco-

liths are abundant in 10,330-10,360A (medium grey claystone) but sparse in 10,330-10,360B (medium grey siltstone). Two easily identified species, Cyclagelosphaera margerelii Noel and Watznaueria barnesae (Black), dominte these and the other assemblages through the section. Zonation is not possible because of the absence of any short-ranging guide species.

The highest Mesozoic assemblages from 9,970-10,000 ft contain Cyclagelosphaera margerelii, Watznaueria barnesae, and W. sp aff. W. britannica (Stradner). The underlying sample 10,000-10,030 is more diverse, containing Biscutum testudinarium Black, Cretarhabdus crenulatus, Micrantholithus sp., Parhabdolithus embergeri (Noel), P. sp. aff. P. granulatus Stover, and Zygodiscus sp. aff. Z. spiralis Bramlette and Martini, in addition to the more ubiquitous Cyclagelosphaera margerelli and Watznaueria barnesae.

There is little change in the character of the assemblages through the section, most being sparse and containing only two or three species. Of the 34 samples examined from 9,970-10,571 ft, only 6 are barren, but only 5 contain abundant or common coccoliths. Although no differentiation of the Lower Cretaceous or uppermost Jurassic asignment is proposed in this report, the presence of compared or questionable specimens of Diazomatolithus lehmannii Noel, Micula infracretacea Thierstein?, and Watznaueria britannica in some samples is suggestive of Lower Cretaceous. Further, the lack of any of the many readily-preserved, diagnostic Upper Cretaceous taxa would make assignment to Upper Cretaceous difficult. Cyclagelosphaera margerelii is most common in the Oxfordian to Albian (Hill, 1976) and was not recognized in detailed studies of Cenomanian and Turonian assemblages (Amedro et al., 1978a, b).

Although an Upper Jurassic correlation is unlikely, the possibility is suggested by the presence of sparse Watznaueria sp. cf. W. manivitae Bukry in samples 10,240-10,270 and 10,330-10,360. This species is common in low-diversity, placolith-rich Upper Jurassic assemblages from DSDP Sites 167 and 261 in the Indo-Pacific (Bukry, 1973b, 1974). Watznaueria barnesae and W. britannica dominate those assemblages however, instead of W. barnesae and Cyclagelosphaera margerelii, as at well 78-164-1. The lack of any definitive Jurassic guide species and the presence of a few long-ranged taxa believed to be restricted to the Cretaceous makes a Lower Cretaceous assignment more likely. The similarities of Upper Jurassic and Lower Cretaceous placolith assemblages can be seen in Grun and Allemann (1975), Keupp (1977), and Hamilton (1978).

Four of the most diverse uppermost Jurassic or Lower Cretaceous assemblages are listed below:

78-164-1, 10,330-10,360A (medium grey claystone):

> Cretarhabdus sp. aff. C. crenulatus, Cyclagelosphaera margerelii, Watznaueria barnesae, W. sp. cf. W. ovata Bukry?.

78-164-1, 10,360-10,390 (lithology undesignated):

Biscutum testudinarium, Cyclagelosphaera margelii, Micula infracretacea?, Parhabdolithus sp. aff. P. granulatus, Watznaueria barnesae, W. ovata?, and Zygodiscus spp.

78-164-1, 10,420-10,450 (medium grey siltstone):

Cyclagelosphaera margerelii (including one coccosphere), Diazomatolithus sp. aff. D. lehmannii, Micula infracretacea?, Parhabdolithus sp. aff. P. granulatus, Watznaueria barnesae, W. ovata?

78-164-1, 10,540-10 571 (lithology undesignated):

Biscutum testudinarium, Cretarhabdus sp. aff. C. crenulatus, Cyclagelosphaera margerelii, Parhabdolithus embergeri (Noel), Watznaueria barnesae, W. biporta Bukry, W. britannica, and W. ovata?

CONCLUSION

Quaternary and Neogene coccolith assemblages in this well show the same low-diversity temperate aspect as the assemblages at concurrently drilled DSDP Site 467, approximately 50 km farther south at San Miguel Gap. At both sites, Coccolithus pelagicus is common and placoliths prdominate discoasters. The major distinction between the two wells is the lack of a coccolith record for the upper Miocene and lower Pliocene at the Pt. Conception well.

The lower middle Miocene section is similar in the presence of inter spersed barren and low-diversity horizons. Sphenolithus heteromorphus is sparse at both localities, but discoasters and coccoliths as a group are more abundant at DSDP Site 467, signifying warmer waters. However, the diversity and relative abundance of coccoliths at both sites is less than that observed in dart cores from more southerly areas of the California continental borderland. A comparison to coeval assemblages from more northerly DSDP Site 173, at the northern end of the California Current shows that the sparse Sphenolithus heteromorphus in seven samples at the Pt. Conception well is one of the northernmost known occurrences of this warm-water taxon off California At DSDP Site 173 it was reported missing (Bukry, 1973c) and as a trace (Wise, 1973). On land it is known as far north as the Ano Nuevo area of the Santa Cruz Mountains (Poore and Bukry, in press). Therefore, coccoliths of the Pt. Conception well indicate a temperate marine depositional situation from Miocene through Quaternary with a major departure from normal marine sedimentation for upper Miocene and lower Pliocene sediments of the interval 4,270 to 8,110 ft.

The very low-diversity of the Mesozoic coccolith assemblages recovered between 9,970 and 10 751 ft, precludes detailed correlation. But if the Lower Cretaceous or uppermost Jurassic assignment is correct, then these rocks are older than any previously dated by coccoliths from offshore or onshore southern California (Bukry and Kennedy, 1969; Paul et al., 1976; Vedder et al., 1976a, b).

ACKNOWLEDGMENTS

I thank John Barron, U.S. Geological Survey, and Helene Manivit, Bureau de Recherches Geologiques et Minieres, France, for helpful discussion on biostratigraphy during this study. I also thank Harry Cook, U.S. Geological Survey, for arranging extra sample coverage from critical stratigraphic intervals. Richard Z. Poore and John A. Barron, U.S. Geological Survey, helped improve the manuscript by constructive reviews.

REFERENCES CITED

Amedro, F., Bidar, A., Damotte, R., Manivit, H., Robaszynski, F., and Sornay J., 1978a, Échelles biostratigraphiques dans le Turonien du Cap Blanc-New (Pas-de-Calais, F.): Bulletin d' Information des Geologues du Bassin de Paris, v 15, no. 2, p. 3-20

Amedro, F., Damotte, R., Manivit, H., Robaszynski, F., and Sornary, J., 1978b, Echelles biostratigraphiques dans le Cenomanien du Boulonnais: Géologie Méditerranéenne, v. 5, no. 1, p. 5-18.

Bukry D., 1973a, Low-latitude coccolith biostratigraphic zonation: Deep Sea Drilling Project Initial Reports, v. 15, p. 685-703.

_____ 1973b, Phytoplankton stratigraphy, central Pacific Ocean, Deep Sea Drilling Project Leg 17: Deep Sea Drilling Project Initial Reports, v. 17, p. 871-889.

_____ 1973c, Coccolith and silicoflagellate stratigraphy, Deep Sea Drilling Project Leg 18, eastern North Pacific: Deep Sea Drilling Project Initial Reports, v. 18, p. 817-831.

_____ 1974, Coccolith stratigraphy, offshore western Australia, D[illegible] Drilling Project Leg 27: Deep Sea Drilling Project Initial v. 27, p. 623-630.

_____ 1975, Coccolith and silicoflagellate stratigraphy, northwestern Pacific Ocean, Deep Sea Drilling Project Leg 32: Deep Sea Drilling Project Initial Reports, v. 32, p. 677-701.

_____ 1978, Cenozoic coccolith, silicoflagellate, and diatom stratigraphy, Deep Sea Drilling Project Leg 44: Deep Sea Drilling Project Initial Reports, v. 44,, p. 807-863.

Bukry, D., and Kennedy, M. P., 1969, Cretaceous and Eocene coccoliths at San Diego, California: California Division of Mines and Geology Special Report 100, p. 33-43.

Crouch J. K., and Bukry, D., 1979, Comparison of Miocene provincial foraminiferal stages to coccolith zones in the California continental borderland: Geology, v 7, p. 211-215.

Grün, W., and Allemann, A., 1975, The Lower Cretaceous of Carvaca (Spain) Berriasian Calcareous Nannoplankton of the Miravetes Section (Subbetic Zone, Prov. of Murcia): Eclogae Geologicae Helvetiae, v. 68, no. 1, p. 147-211.

Hamilton, G., 1978, Calcareous nannofossils from the Upper Callovian and Lower Oxfordian (Jurassic) of Staffin Bay, Isle of Skye, Scotland: Yorkshire Geological Society Proceedings, v. 42, pt. 1, no. 3, p. 29-39.

Hill, M E., III, 1976, Lower Cretaceous calcareous nannofossils from Texas and Oklahoma: Palaeontographica, v. 156B, p. 103-179.

Keupp, H., 1977, Ultrafazies and Genese der Solnhofener Plattenkalke (Oberer Malm, Sudliche Frankenalb): Adhandlung der Naturhistorischen Gesellschaft Nurnberg e.V , v. 37, p. 1-128.

Ling, H. Y., 1973, Silicoflagellates and ebridians from Leg 19: Deep Sea Drilling Project Initial Reports, v. 19, p. 751-775.

Paul, R. G., Arnal, R. E., Baysinger, J. P., Claypool, G. E., Holte, J. L., Lubeck, C. M., Patterson, J. M., Poore, R. Z., Slettene, R L., Sliter, W. V., Taylor, J. C., Tudor, R. B., and Webster, F. L., 1976, Geological and operational summary, southern California deep stratigraphic test OCS-CAL 75-70 No. 1, Cortes Bank area offshore southern California: U.S. Geological Survey Open-File Report 76-232, 65 p.

Poore, R. Z., and Bukry, D., Eocene to Miocene calcareous plankton from the Santa Cruz Mountains and adjacent areas, California: U.S Geological Survey Bulletin, in press.

Vedder, J. G., Arnal, R. E., Bukry, D., and Barron, J. A., 1976a, Preliminary descriptions of pre-Quaternary samples, R/V LEE, March 1976, offshore southern California: U.S. Geological Survey Open-File Report 76-629, 15 p.

Vedder, J. G., Taylor, J. C., Arnal, R. E., and Bukry D., 1976b, Maps showing location of selected pre-Quaternary rock samples from the California continental borderland: U.S. Geological Survey Miscellaneous Field Studies Maps MF-737, 3 maps.

Wise, S. W., Jr., 1973, Calcareous nannofossils from cores recovered during Leg 18, Deep Sea Drilling Project: Biostratigraphy and observations of diagenesis: Deep Sea Drilling Project Initial Reports v. 18 p. 569-615.